Antioxidative and Anti-inflammatory Activities of the Active Compounds from the Fern *Cyclosorus terminans*

Suriya Chaiwong

A Thesis Submitted in Partial Fulfillment of the Requirements for the Degree of Doctor of Philosophy in Pharmaceutical Sciences

Prince of Songkla University

2019

Antioxidative and Anti-inflammatory Activities of the Active Compounds from the Fern *Cyclosorus terminans*

Suriya Chaiwong

A Thesis Submitted in Partial Fulfillment of the Requirements for the Degree of Doctor of Philosophy in Pharmaceutical Sciences

Prince of Songkla University

2019

Thesis Title	Antioxidative and Anti-inflammatory Activities of the Active Compounds from the Fern *Cyclosorus terminans*
Author	Mr. Suriya Chaiwong
Major Program	Pharmaceutical Sciences

Major Advisor

.....

(Asst. Prof. Dr. Sireewan Kaewsuwan)

Co-advisor

.....

(Asst. Prof. Dr. Panupong Puttarak)

Examining Committee:

.....Chairperson

(Assoc. Prof. Dr. Kornkanok Ingkaninan)

.....Committee

(Assoc. Prof. Dr. Supinya Tiwtrakul)

.....Committee

(Asst. Prof. Dr. Sireewan Kaewsuwan)

.....Committee

(Asst. Prof. Dr. Panupong Puttarak)

The Graduate School, Prince of Songkla University, has approved this thesis as partial fulfillment of the requirements for the Doctor of Philosophy Degree in Pharmaceutical Sciences.

.....

(Prof. Dr. Damrongsak Faroongsarng)

Dean of Graduate School

This is to certify that the work here submitted is the result of the candidate's own investigations. Due acknowledgment has been made of any assistance received.

.....Signature
(Asst. Prof. Dr. Sireewan Kaewsuwan)
Major Advisor

.....Signature
(Asst. Prof. Dr. Panupong Puttarak)
Co-advisor

.....Signature
(Mr. Suriya Chaiwong)
Candidate

I hereby certify that this work has not been accepted in substance for any degree, and is not being currently submitted in candidature for any degree.

.....Signature

(Mr. Suriya Chaiwong)

Candidate

ชื่อวิทยานิพนธ์ ฤทธิ์การต้านออกซิเดชั่นและการต้านอักเสบของสารออกฤทธิ์จากเฟิร์น *Cyclosorus terminans*
ผู้เขียน นายสุริยา ชัยวงค์
สาขาวิชา เภสัชศาสตร์
ปีการศึกษา 2561

บทคัดย่อ

การศึกษานี้สามารถแยกอนุพันธุ์คูมารินได้ 3 ชนิดจากเฟิร์นไซโคลซอรัส เทอร์มิแนนส์ ได้แก่ สารอินเตอร์รับตินเอ บีและซีในปริมาณร้อยละ 0.20-0.84 ของน้ำหนักสารสกัด โดยพบว่าสารอินเตอร์รับตินเอและบี มีฤทธิ์ดีในการกำจัดสารประกอบออกซิเจนที่ไม่คงตัวในผิวหนังมนุษย์ชนิดเซลล์ไฟโบรบลาสและเซลล์เคอราติโนไซต์ โดยมีประสิทธิภาพในการกำจัดสูงถึงร้อยละ 76.98 และยังสามารถกระตุ้นการแสดงออกระดับยีนและโปรตีนของเอนไซม์ต้านอนุมูลอิสระ ได้แก่ superoxide dismutase 1 และ 2, catalase และ glutathione peroxidase รวมทั้งยังมีความสามารถในการกำจัดสารประกอบออกซิเจนที่ไม่คงตัวในเซลล์ผิวหนังมนุษย์ที่เกิดจากการกระตุ้นด้วยแสงอัลตราไวโอเลตเอและบี ได้มากถึงร้อยละ 81.52 และเมื่อเปรียบเทียบผลของสารอินเตอร์รับตินทั้ง 3 ชนิด พบว่าสารอินเตอร์รับตินเอมีประสิทธิภาพดีที่สุดในการกำจัดอนุมูลอิสระ DPPH โดยให้ค่าความเข้มข้นที่ยับยั้งร้อยละ 50 เท่ากับ 21.79 ไมโครโมลาร์ และสามารถให้อิเล็กตรอนโดยการรีดิวซ์สารเฟอร์ริกเป็นสารเฟอร์รัสได้ดีที่สุด โดยให้ค่าแอนติออกซิแดนท์เท่ากับ 682.45±16.31 มิลลิโมลาร์ต่อลิตรของกรดแอสคอร์บิก ต่อโมลของอินเตอร์รับติน รวมทั้งยังมีฤทธิ์ในการยับยั้งการเจริญและฆ่าเชื้อแบคทีเรียก่อโรคที่ผิวหนังชนิด *Propionibacterium acnes* ได้ดีโดยให้ความเข้มข้นของสารที่ต่ำสุดที่ยับยั้งและฆ่าเชื้อได้เท่ากับ 1.95 และ 7.81 ไมโครกรัมต่อมิลลิลิตร ตามลำดับ และยังพบว่าสารอินเตอร์รับตินเอและบี มีประสิทธิภาพดีในการต้านอักเสบโดยสารอินเตอร์รับตินบีมีฤทธิ์ดีที่สุดในการกำจัดอนุมูลอิสระไนตริกออกไซด์ในหลอดทดลองและยับยั้งการหลั่งไนตริกออกไซด์จากเซลล์แมโครฟาจหนูที่กระตุ้นด้วยสารไลโปโพลีแซ็คคาไรด์ ซึ่งให้ค่าความเข้มข้นที่ยับยั้งได้ร้อยละ 50 เท่ากับ 67.68 และ 0.81 ไมโครโมลาร์ ตามลำดับ ด้วยกลไกการออกฤทธิ์ผ่านการยับยั้งการแสดงออกของยีน nitric oxide synthase ซึ่งอาจเป็นผลจากการกระตุ้นการแสดงออกของยีน peroxisome proliferation activated

receptor-γ นอกจากนี้สารอินเตอร์ตินเอ บีและซี ในระดับความเข้มข้นต่ำยังช่วยเร่งการหายของแผลได้ดีปานกลาง โดยการกระตุ้นการเคลื่อนที่เซลล์ผิวหนังเข้าปิดบาดแผล

การเตรียมสารสกัดเฟิร์นไซโคลซอรัส เทอร์มิแนนส์ที่มีสารกลุ่มอินเตอร์รับตินเข้มข้นโดยวิธีการตกตะกอนอย่างง่าย พบว่าได้สารสกัดที่ได้มีปริมาณของสารกลุ่มอินเตอร์รับตินเพิ่มขึ้น 2 เท่า และมีประสิทธิภาพในการกำจัดสารประกอบออกซิเจนที่ไม่คงตัวในเซลล์ผิวหนังมนุษย์ได้ดี รวมทั้งสามารถยับยั้งการหลั่งไนตริกออกไซด์จากเซลล์แมโครฟาจหนูได้ถึง 2.37 เท่า เมื่อเทียบกับสารสกัดเริ่มต้น และสารสกัดที่เตรียมได้ดังกล่าวมีความคงตัวดีเมื่อเก็บที่อุณหภูมิห้องภายใต้การป้องกันแสงในระยะเวลาทดสอบ 3 เดือน อย่างไรก็ตามการเก็บในสภาวะเย็นช่วยให้สารสกัดมีความคงตัวมากขึ้น การศึกษานี้ยังได้พัฒนาและตรวจสอบวิธีวิเคราะห์ปริมาณสารอินเตอร์รับตินเอ บีและซีด้วยวิธีไฮเพอร์ฟอร์แมนซ์ ลิควิดโครมาโตกราฟี (เฮชพีแอลซี) ที่ตรวจวัดสัญญาณด้วยเครื่องโฟโตไดโอดแอร์เรย์ โดยใช้คอลัมน์ชนิด reversed phase C18 และชะสารด้วยส่วนผสมระหว่างเมธานอลและร้อยละ 1 ของกรดอะซิติกที่ละลายในน้ำในอัตราส่วน 85:15 โดยปริมาตรต่อปริมาตร ด้วยอัตราการไหลเท่ากับ 1 มิลลิลตรต่อนาที พบว่าวิธีดังกล่าวผ่านการทดสอบความใช้ได้ตามหลักของ International Conference of Hamonization (ICH) ภายใต้ตัวชี้วัด ได้แก่ linearity ($R^2 \geq 0.999$), range (6.25–200 µg/mL), specificity, accuracy (100±10%), precision (intra-day <1%, inter-day <2%), limit of detection (LOD) และ limit of quantitation (LOQ) ดังนั้นจึงเป็นวิธีที่เหมาะสมสำหรับการวิเคราะห์ปริมาณสารอินเตอร์รับตินเอ บีและซี ภายใต้การวิเคราะห์ครั้งเดียวกัน ผลการศึกษาทั้งหมดจึงสนับสนุนการนำสารอินเตอร์รับตินเอ บี และซี ซึ่งเป็นอนุพันธ์คูมารินธรรมชาติที่สกัดแยกได้จากเฟิร์นไซโครซอรัส เทอร์มิแนนส์ รวมทั้งสารสกัดที่มีอินเตอรร์รับตินเข้มข้นไปพัฒนาเป็นยาหรือผลิตภัณฑ์เวชสำอางสำหรับต้านอนุมูลอิสระ ต้านอักเสบ และต้านเชื้อแบคทีเรีย รวมทั้งวิธีการวิเคราะห์ที่ผ่านการทดสอบความใช้ได้ยังสามารถนำไปประยุกต์ใช้ในการวิเคราะห์ปริมาณสารในสารสกัดเฟิร์นสำหรับการพัฒนาผลิตภัณฑ์สำหรับสุขภาพต่อไป

Thesis Title Antioxidative and Anti-inflammatory Activities of the Active Compounds from the Fern *Cyclosorus terminans*
Author Mr. Suriya Chaiwong
Major Program Pharmaceutical Sciences
Academic Year 2018

ABSTRACT

In this study, the three pure coumarin derivatives, interruptins A, B and C were isolated from *Cyclosorus terminans* with 0.20-0.84% w/w of its crude extract. As a result, interruptins A and B not only potentially scavenged intracellular reactive oxygen species (ROS) in human dermal fibroblast and human epidermal keratinocyte with % ROS scavenging as high as 76.98 %, but also induced mRNA and protein expression of antioxidant enzymes, including superoxide dismutase 1 and 2, catalase, and glutathione peroxidase. Likewise, these two coumarin derivatives remarkably suppressed ROS levels in human skin cells under ultraviolet A and B irradiation with % ROS scavenging up to 81.52%. Among the three tested isolated interruptins A-C, interruptin A exhibited the most effective DPPH proton radical scavenging capacity (IC_{50} = 21.79 μM) and acted as the strongest electron transferring compound to reduce ferric to ferrous ion (antioxidant value of 682.45±16.31 mmol/L ascorbic acid/mol interruptin) as well as strongly inhibited and killed a skin pathogen *Propionibacterium acnes* (MIC/MBC = 1.95/7.81 μg/mL). While both interruptins A and B revealed anti-inflammatory activity, interruptin B acted as the greatest anti-inflammatory agent by quenching NO radical and inhibiting NO production in LPS-induced macrophages with IC_{50} values as low as 67.68 μM and 0.81 μM, respectively. The molecular mechanism involved in suppression of inducible nitric oxide synthase (*iNOS*) gene expression which possibly due to activation of peroxisome proliferation activated receptor-γ gene expression. Moreover, low concentrations of interruptins A-C presented moderate wound healing activity by accelerating human skin cell migration. Furthermore, interruptins-rich *C. terminans* extract developed by simple precipitation not only revealed approximately 2-folds interruptin content higher than its initial extract but also

performed powerful ROS scavenging activity in human skin cells and strongly suppressed NO release from murine macrophages with 2.37 folds better than original crude extract. The prepared interruptins-rich *C. terminans* extract that was stored at room temperature with light protection displayed good stability over 3-months; however, extract stored in cold condition provided better stability. Finally, the high performance liquid chromatography (HPLC) with photodiode array detector was successfully validated for simultaneous analysis of interruptins A, B and C. The HPLC condition was achieved by using a reversed-phase C18 analytical column, methanol/1% aqueous acetic acid (85:15, v/v), 1 mL/min flow rate. According to the International Conference of Harmonization (ICH) guidelines, the method was validated on the basis of these parameters: linearity ($R^2 \geq 0.999$), range (typically 6.25–200 µg/mL), specificity, accuracy (100±10%), precision (intra-day <1%, inter-day <2%), limit of detection (LOD) and limit of quantitation (LOQ). Therefore, this model is suitable as a standard method for simultaneous examination of interruptins A, B and C in a single HPLC run. As a result, it was encouraged that the natural occurring coumarin derivatives, interruptins A and B from an edible fern *C. terminans* and interruptins-rich extract could be further developed as therapeutic agents or cosmeceutical products for antioxidative or anti-photooxidative, anti-inflammatory and antibacterial benefits. The validated analysis method could also provide an application for active ingredient analysis of *C. terminans* extract for further health product development.

ACKNOWLEDGEMENT

I would like to extremely express my sincere gratitude to my advisor, Asst. Prof. Dr. Sireewan Kaewsuwan for kindly supervision and suggestion, countless support, worthy encouragement, and completion of my research work. I am also especially grateful to my co-advisor, Asst. Prof. Dr. Panupong Puttaruk for his valuable guidance and contribution throughout my study.

My special thanks are sincerely extended to Miss. Somporn Sritrirutchai, Immunology Unit, Songklanagarind Hospital, and Asst. Prof. Dr. Kanyanatt Kanokwiroon at Department of Biomedical Sciences, Faculty of Medicine, Prince of Songkla University, for their kindly training and underpinnings of flow cytometry and western blot techniques, respectively. Moreover, my deepest appreciation is conveyed to Assoc. Prof. Dr. Jong-Hyuk Sung at College of Pharmacy, Yonsei University, South Korea, for benevolent collaboration and support throughout the research in South Korea.

Additionally, I would also like to acknowledge to Department of Pharmacognosy and Pharmaceutical Botany, Faculty of Pharmaceutical Sciences for great facility support, and PSU-Ph.D. scholarship for financial support of all over the circumstance.

Finally, my recognition also disclosed to my colleagues for their kindness helps, my family and my friends for their unconditional supports and meaningful encouragements.

Suriya Chaiwong

CONTENTS

Page

CONTENTS (continued)

Page

CONTENTS (continued)

Page

CONTENTS (continued)

Page

LIST OF TABLES

Page

LIST OF TABLES (continued)

Page

LIST OF FIGURES

Page

LIST OF FIGURES (continued)

Page

LIST OF SCHEMES

Page

LIST OF ABBREVIATIONS AND SYMBOLS

α	=	alpha
β	=	beta
γ	=	gamma
δ	=	chemical ship (ppm)
λmax	=	maximum wavelength
° C	=	degree Celsius
>, <, ≤	=	greater than, less than, less than or equal to
%	=	percentage
±	=	plus-minus sign
AA	=	arachidonic acid
$ABTS^{\bullet+}$	=	2,2'-azino-bis (3-ethylbenzthiazoline-6-sulphonic acid
APS	=	ammonium persulfate
ASCs	=	human adipose-derived stem cells
AUC	=	area under curve
BHI	=	brain heart infusion media
CAT	=	catalase
cDNA	=	complementary deoxyribonucleotide
CD_3OD	=	deuterated methanol
CDC_{l3}	=	deuterated chloroform
CE	=	isopropanol *C. terminans* crude extract
CFU	=	colony-forming unit
CH_2Cl_2	=	dichloromethane
COX-1, -2	=	cyclooxygenase-1, -2
C_T	=	cycle threshold
DCF-DA	=	2′,7′-dichlorofluorescein diacetate
DMEM	=	Dulbecco's Modified Eagle Medium
DNA	=	deoxyribonucleic acid
DPPH	=	2,2-diphenyl-1-picrylhydrazyl

LIST OF ABBREVIATIONS AND SYMBOLS (continued)

ECM	=	extracellular matrix
eNOS	=	endothelial nitric oxide synthase
EtOAc	=	ethyl acetate
FBS	=	fetal bovine serum
FRAP	=	ferric reduction antioxidant power
GAPDH	=	glyceraldehyde-3-phosphate dehydrogenase
GC	=	gas chromatography
GPx	=	glutathione peroxidase
GSH	=	glutathione
h	=	hour
H^1-NMR	=	proton (1)-nuclear magnetic resonance
HDF	=	human dermal fibroblast
HEK	=	human epidermal keratinocyte
HPLC	=	high performance liquid chromatography
HT-29	=	human colonic adenocarcinoma
Hz	=	hertz
ICH	=	International Conference on Harmonization guideline
IC_{50}	=	half maximal inhibitory concentration
IgG	=	immunoglobulin G
IL	=	interleukin
iNOS	=	inducible nitric oxide synthase
IRCE	=	interruptin-rich *Cyclosorus terminans* extract
KB	=	nasopharyngeal carcinoma cell
LOD	=	limit of detection
LOQ	=	limit of quantitation
LOX	=	lipoxygenase
LPS	=	lipopolysaccharide
LTs	=	leukotrienes

LIST OF ABBREVIATIONS AND SYMBOLS (continued)

LXs	=	lipoxin
MBC	=	minimum bactericidal concentration
MCF-7	=	human breast adenocarcinoma
MeOH	=	methanol
MIC	=	minimum inhibitory concentration
min	=	minute
MMP	=	matrix metalloproteinase
mRNA	=	messenger ribonucleotide
MRSA	=	methicillin-resistant *Staphylococcus aureus*
MS	=	mass spectroscopy
MSSA	=	methicillin-sensitive *S. aureus*
MTT	=	thiazolyl blue tetrazolium bromide
μL, mL, L	=	microliter, milliliter, liter
μM, mM	=	micromolar, millimolar
NF-κB	=	nuclear factor kappa B
ng, μg, mg, g, kg	=	nanogram, microgram, milligram, gram, kilogram
nm	=	nanometer
NO	=	nitric oxide
nNOS	=	neuronal nitric oxide synthase
Nrf2	=	nuclear factor-erythroid 2-related factor 2
NSAIDs	=	nonsteroidal anti-inflammatory drugs
OD	=	optical density
PCR	=	polymerase chain reaction
PDA	=	photo diode array
PGE_2	=	prostaglandin E_2
PPAR	=	peroxisome proliferation activation receptor
ROS	=	reactive oxygen species
RSD	=	relative standard deviation
Rt	=	retention time

LIST OF ABBREVIATIONS AND SYMBOLS (continued)

sec	=	second
SD	=	standard deviation
SDS-PAGE	=	sodium dodecyl sulfate-polyacrylamide gel
S/N	=	signal-to-noise
SNP	=	sodium nitroprusside
Sp1	=	specificity protein 1
SOD1	=	superoxide dismutase 1
SOD2	=	superoxide dismutase 2
TLC	=	thin layer chromatography
TNF-α	=	tumor necrosis factor-α
UCP-1	=	uncoupling protein-1
UV	=	ultraviolet
v/v	=	volume by volume
w/v	=	weight by volume

CHAPTER 1

INTRODUCTION

1.1 Background and rationale

The human skin is daily exposed to environmental stress factors such as chemicals, pollution, pathogens, and ultraviolet (UV) radiation. These factors can easily trigger reactive oxygen species (ROS) formation in the skin cells (1,2). In principle, ROS are oxygen-containing atoms or molecules that reactive oxidizing other molecules, including hydroxyl radical ($OH^{\bullet}$), superoxide anion ($O_2^{\bullet -}$), hydrogen peroxide (H_2O_2), singlet oxygen ($^1O_2$) and nitric oxide (NO) (3). The excessive level of ROS causes cellular oxidative stress, disturbs in a redox system as well as induces genetic regeneration and facilitates cellular dysfunction, which ultimately leads to cell death and progress skin aging (4). To prevent oxidative damage from excessive level of ROS, cells have established a complex antioxidant defense network, including non-enzymatic compounds, for instance, glutathione (GSH), ascorbic acid (vitamin C) as well as α-tocopherol (vitamin E) and enzymatic antioxidants, for example, catalase (CAT), superoxide dismutase (SOD) and glutathione peroxidase (GPx) (5,6). However, overproduction or inadequate removal of ROS results in oxidative stress and affects to cellular antioxidant depletion and imbalance.

Normally, ultraviolet (UV) radiation, UVA (320-400 nm) and UVB (290-320 nm), can cause various biological effects to human skin such as inducing vitamin D synthesis, pigmentation, sunburn and cell damage (7,8). Nevertheless, a common component of their activities is an enhancement of ROS generation and oxidative stress formation (9) which may be the first step of multiple damages induced by UV irradiation. Moreover, UV exposure can subsequently lead to skin inflammation, immunosuppression and skin cancer (10-12).

Bacterial infection is also a source of cellular oxidative stress. *Propionibacterium acnes* (*P. acnes*), a Gram-positive bacteria that normally dwell in the pilosebaceous units of the skin. Over-proliferation of *P. acnes* in the pilosebaceous

follicles is one of the major pathogenesis of acne vulgaris on the skin. Therefore, infection by *P. acnes* is similarly induced oxidative stress and inflammation of skin cells (1,13).

Inflammation is the body response in order to eliminate exogenous agents causing cell damage (14). In the inflammatory process, nitric oxide (NO), an inflammatory mediator, is generated by inducible nitric oxide synthase (iNOS). Although NO acts as a host defense by destroying pathogenic nucleic acid and regulating local blood flow, an excessive level of NO can react with superoxide radicals to form peroxynitrite. The reactive peroxynitrite can directly damage function of normal cells. Hence overproduction of NO could induce cellular oxidative stress and further facilitate inflammation (15,16).

Interruptins A, B and C, coumarin derivatives, had been isolated from a crude extract of *Cyclosorus terminans* (Thelypteridaceae). Interruptins A and B revealed a variety of bioactivities such as antibacterial, anticancer and antidiabetic activities. More interestingly, these active compounds exhibited potent ROS scavenging property in human adipose-derived stem cells (ASCs) determined by 2′,7′-dichlorofluorescein diacetate (DCF-DA) using a flow cytometer (17,18). However, to date, the antioxidative property on human skin cells and anti-inflammatory activity of interruptins have not been studied yet. Since skin cells such as keratinocytes and fibroblasts physically exposed to a variety of challenges that includes oxidative stress involved with the anomalous ROS production, and they are further altered by exposure to chemicals, UV radiation, infection and inflammatory processes (19,20). Therefore, this will be the first report on the antioxidative and anti-inflammatory efficacy of isolated interruptins from *C. terminans* in human skin cells by using UV as ROS stimulator and in murine macrophage cells, respectively. The results of antioxidative and anti-inflammatory efficacies of active interruptins can further be applied in cosmeceutical and pharmaceutical approaches for product development.

In fact, the use of purified natural occurring compounds was limit due to their naturally low amount. Application of the crude extracts that contain high contents of active ingredients or enriched extracts is therefore interested and required. Likewise, isolated interruptins from *C. terminans* are natural agents with a variety of pharmaceutical potentials, wheras its quantity was insufficient for further application.

The usage of interruptin-rich *C. terminans* extract is an alternative advantage. However, the utilization of enriched extract should be controlled the quality by measuring the content of corresponding constituents in the extract prior to use. The appropriate method for analysis of the target substances is also important. The assurance of analytical procedure efficacy such as accuracy and precision is a key issue for the quality control of herbal extracts. Thus, the validation of analytical process performance is necessary to be assessed before applying the analytical application. Although the high performance liquid chromatography (HPLC) method for content analysis of interruptins A-C was reported, its performance had not yet been validated (17). For this reason, the verification of the HPLC method for interruptins content monitoring should be prioritized as the earliest stages of the active constituent-enriched extracts development process.

1.2 Objectives

1. To isolate and identify the compounds possessing antioxidative and anti-inflammatory properties from the fern *C. terminans*
2. To determine the antioxidative efficacy of isolated compounds from *C. terminans* on human skin cells
3. To determine the anti-inflammatory efficacy of isolated compounds from *C. terminans* on murine macrophage cells
4. To investigate the mechanisms of action of isolated active antioxidative and anti-inflammatory compounds
5. To prepare the interruptins-rich *C. terminans* crude extract and verify its bioactivity
6. To validate HPLC method for analysis the interruptin contents in *C. terminans* crude extract

CHAPTER 2

LITERATURE REVIEW

2.1 Human skin

The human skin is the largest part that outer covering of the body to protect damaging of inner organs from the environmental stress. The skin is divided by difference development origins into two distinct layers, the first layer is epidermis that developed from ectoderm of the embryo and the second is dermis layer which grew from mesoderm. The skin plays general functions in the protection of underlying tissues and organs against scraping, impact, pathogen and chemical attack, fluid loss as well as the maintenance of regular body temperature and synthesis of vitamin D (21,22).

Skin epidermis

The epidermis is a superficial layer that consists of keratinocytes, melanocytes, Langerhans cells and Merkel cells. The epithelium of epidermis is subdivided into five layers, including stratum basale that is the deepest layer connected with skin dermis, next up are stratum spinosum, stratum granulosum, stratum lucidum and stratum corneum, respectively. Keratinocytes proliferate in stratum basale and move up to the top. Thus, keratinocytes are the most abundant cell type in skin epidermis and important in skin structural and functional. Keratinocyte cells are not only a mechanical barrier but also play role in acquired immunity to protect pathogen and exogenous toxins (21-24).

Skin dermis

The dermis is the layer of dense irregular connective tissue consists of collagen, elastin and many cell types (fibroblasts, adipocytes, and macrophages),

vessels (blood and lymphatic) and glands (sweat and adipose). Fibroblast cells are, abundant in skin dermis, the basic structure of dermis tissue. The key functions of fibroblast are producing extracellular matrix (ECM) such as collagen, glycosaminoglycan, elastin, fibronectin, matrix metalloproteinase (MMP) as well as secreting cytokines and growth factors. Moreover, fibroblasts also play important role in wound healing. (25,26).

Naturally, the skin dermis and epidermis degenerate throughout the lifetime because of ECM degradation and skin cell death, and eventually occur physiological skin aging. Moreover, skin frequently exposes to extrinsic factors such as chemical, pathogen and UV radiation. These stimuli trigger the generation of reactive oxygen species (ROS) which are molecular intermediates to damage the cells. ROS formation in the skin may cause oxidative stress, skin inflammation and eventually lead to pathological skin aging (1,19,27,28).

2.2 Oxidative stress

Oxidative stress is referred to the resulting stage of unbalanced between oxidant production and antioxidant defense in cells or tissues. This imbalance may due to (i) increase of oxidant both endogenous and exogenous sources; (ii) decrease of low molecular antioxidant level or inactivation of antioxidant enzymes; and (iii) depletion of low molecular antioxidant compounds and antioxidant enzyme production (3,29,30). Oxidative stress causes damage to cellular compositions, for instance, deoxyribonucleic acid (DNA), proteins as well as membrane lipids. Moreover, accumulation of oxidative damage in cells or tissues might cause cell or tissue dysfunction and eventually causes diseases such as aging, Alzheimer, atherosclerosis and cancer (4,31). ROS are well known as molecular intermediates for oxidative stress, thus cells or tissues that exposed to a high amount of ROS tend to be damaged by oxidative stress. Since skin is the outer most organ, it is frequently exposed to stress factors that trigger ROS generation such as ozone, bacterial infection, chemical as well as UV radiation and easily to be oxidative stress (1,20,28).

2.3 Stress factors for skin

2.3.1 Reactive oxygen species (ROS)

ROS are specified as oxygen-containing compounds that highly engender with other molecules. ROS can be free radical, electron uncoupling molecule, and non-radical, oxidizing agent or molecule that can be changed easily to radical. Basically, ROS are referred to superoxide anion ($O_2^{\bullet -}$), hydroxyl radical ($OH^{\bullet}$), hydrogen peroxide (H_2O_2), peroxy radical ($ROO^{\bullet}$) as well as nitric oxide (NO). In aerobic cells, ROS are generated endogenously during metabolic reactions such as mitochondrial oxidative phosphorylation, endoplasmic reticulum stress, fatty acid β-oxidation of peroxisome as well as enzyme activities, including xanthine oxidase, NADPH oxidase, nitric oxide synthase, lipoxygenase, and cytochrome P450 (3,32). The ROS, potent oxidants within the cells, can cause genetic regeneration and physiological dysfunction, which ultimately progress aging of the organism or diseases. Naturally, ROS perform significant roles in cellular signaling to activate or inhibit the expression of transcription factors and a wide range of genes that involve in cell proliferation and apoptosis. However, the high amount of ROS might induce lipid peroxidation, DNA damage and facilitate the extracellular matrix (ECM) degradation and cell death (4,33). Thus, the antioxidant agents which are capable to quench reactive oxygen intermediates are interested to verify their efficacy and safety.

Table 2.1 Major reactive oxygen species (3).

Type of ROS	Formula
Radical	
Superoxide anion radical	$O_2^{\bullet-}$
Hydroxyl radical	$HO^{\bullet}$
Hydroperoxy radical	$HOO^{\bullet}$
Alkoxyl radical	$LO^{\bullet}$
Alkylperoxyl radical	$LOO^{\bullet}$
Nitric oxide	NO
Non-radical	
Singlet oxygen	$^1O_2$
Hydrogen peroxide	H_2O_2
Alkyl hydroperoxide	LOOH
Hypochlorite ion	ClO^-
Ferryl ion	$Fe^{4+}O$
Periferryl ion	$Fe^{5+}O$

2.3.2 Ultraviolet radiation

Ultraviolet (UV) rays can be categorized by the wavelength ranges as UVA (320-400 nm), UVB (290-320 nm) and UVC (200-290 nm). However, only UVA and UVB spectra reach the earth's surface and affect to living organisms. UVA is the major component of UV portion of sunlight (95% of UVA and 5% of UVB). UVA ray can penetrate deeply to skin epidermis. It has been reported that UVA indirectly damaged the skin by triggering ROS production via cellular chromophore. The ROS formation may be the first step of multiple damages induced by UVA exposure (34). UVB almost affects the superficial layer of the skin (epidermis). Although UVB is a minor portion of UV ray, it can induce deleterious damage effects including, sunburn, immunosuppression, inflammation, DNA damage and melanogenesis (7,8).

When skin exposes to UV ray, ROS are formed by UV photon absorption of photosensitizers in the skin such as DNA and amino acids. Photosensitizers are excited from ground stage to exciting stage of electron, then excited molecules interact with oxygen molecule in two pathways, type I and type II, which result in the generation of ROS and singlet oxygen, respectively (35).

The increasing of ROS production altered structures and functions of genes and proteins. A single dose exposure to UV light of human skin cells, fibroblasts and keratinocytes, not only disturbs antioxidant enzymes activities, including superoxide dismutase (SOD), catalase (CAT) as well as glutathione peroxidase (GPx) but also reduces gene expression of these enzymes (36-38) and induce lipid peroxidation (39,40).

2.3.3 Propionibacterium acnes infection

Propionibacterium acnes (*P. acnes*) is a Gram-positive commensal bacterium that commonly inhabits in the skin pilosebaceous units. The over-colonization of *P. acnes* in pilosebaceous follicles is one of the major pathogenesis of acne vulgaris that causes skin oxidative stress and inflammation (1,11). In the inflammatory process of acne vulgaris, coproporphyrin is produced and then further generates $^1O_2$ when exposing to UV light. This phenomenon can lead to inflammatory lesions of acne. Moreover, O_2-produced from *P. acnes*-infected keratinocytes can further stimulate the inflammatory reaction (41,42). Acne vulgaris is the common disease broadly affects individuals mainly adolescents. This disease can be painful and may lead to acne scar, post-inflammatory hyperpigmentation and psychological problems (11,43,44).

Topical agents (retinoids and benzoyl peroxide) and antimicrobial agents (tetracycline, erythromycin and clindamycin) were widely used for acne treatment (45). However, bacterial drug resistance remains the problem in acne remedy (46). Therefore, novel agents which effectively inhibit *P. acnes* growth will be served as new drugs for acne vulgaris regimen.

2.4 Effects of ROS/oxidative stress in the skin

2.4.1 Skin surface oxidation

ROS alter skin condition by oxidized cellular biomolecules including lipids and proteins. The acute response was observed as skin barrier function disruption and the chronic response was skin roughness (47). Furthermore, lipid hydroperoxides and proteins can be oxidized by alkyl aldehydes to yield carbonylated protein, a marker of protein oxidation, in the stratum corneum layer of the epidermis and further causes stratum corneum thickness. The increase of stratum corneum level has been involved with oxidative stress induced by UV-exposure and season change or by some diseases such as inflammation, allergy and atopic dermatitis. Thus, stratum corneum thickness can reflect the level of oxidative damage that initiated by ROS in the skin (48-51).

2.4.2 Melanogenesis

Skin pigmentation can be also enhanced by ROS. Accumulation of ROS may accelerate melanogenesis in melanocytes. Since keratinocytes intensively expose to ROS stimulators such as UV radiation, H_2O_2-generated from keratinocytes easily crosses the cell membrane and is transferred to melanocytes (52). NO generated from keratinocytes can also trigger melanogenesis in melanocytes by raising the level of tyrosinase and tyrosinase-related protein 1 (53,54). Moreover, H_2O_2 can stimulate phenylalanine hydroxylase which is L-tyrosine producing enzyme from L-phenylalanine. Thus, the increasing of L-tyrosine amount, the initial substrate of tyrosinase enzyme, leads to melanogenesis (55).

2.4.3 Skin aging

ROS are one of the factors influencing skin aging that is characterized by wrinkles. Generally, wrinkles occur when dermal matrix as collagen is decreased. The reduction of collagen fibers caused by collagen fibers breakdown and decreased collagen synthesis. ROS such as $^1O_2$, H_2O_2 and hydroperoxide stimulate the expression

of extracellular matrix degradation enzymes such as matrix metalloproteinase (MMP)-1 or collagenase in skin cells. This enzyme acts to degrade collagen fibers which cause wrinkles (56-58). Moreover, ROS also persuade the reduction of collagen synthesis. Thus, ROS are the intermediate molecules that regulate collagen synthesis (59).

2.4.4 Skin inflammation

The skin is easily exposed to UV ray. After the skin exposes to UV radiation, it induces skin erythema or sunburn by triggering ROS formation. ROS particularly NO that produced from nitric oxide synthase (NOS) enzyme stimulate erythema via activation of prostaglandin E2 (PGE_2) synthesis (60). The PGE_2 is synthesis by cyclooxygenase (COX)-2 enzyme and the COX-2 expression is increased by ROS. Thus, the use of NOS inhibitor and COX inhibitor can suppress UV-activated erythema. These reveal that ROS also acts as skin inflammation stimulator (61,62).

2.5 Antioxidant

Antioxidants, present at low concentration relative to oxidizable substrates, are defined as substances that can interact with oxidants to prevent oxidation by significantly inhibit or delay the initiation and/or prolongation of oxidizing chain. Moreover, some antioxidant can repair the damage of cell or tissue (63,64). In the cell, endogenous antioxidant defense system includes both enzymatic system, for instance, superoxide dismutase (SOD), catalase (CAT) and glutathione peroxidase (GPx) and non-enzymatic system, for example, glutathione (GSH), ascorbic acid (vitamin C) as well as α-tocopherol (vitamin E) (5,6). These cellular antioxidants maintain the balance of cellular redox state by controlling the level of oxidants (Figure 2.1) (65).

For the enzymatic antioxidants, SOD, in the mammal, are identified to three isoforms including copper/zinc (CuZn)-SOD or SOD1, manganese (Mn)-SOD or SOD2 and extracellular (EC)-SOD or SOD3. SOD1 locates in cytoplasm and intermembrane space of mitochondrial while SOD2 is predominantly found in mitochondrial matrix. SOD3 is found in an extracellular fluid such as plasma and in extravascular space of tissue. All of SOD isoforms dismutase two molecules of $O_2^{\bullet-}$

into H_2O_2 and oxygen. Therefore, SOD has been considered the most important antioxidant enzyme (5,6,66). However, in the presence of metal, H_2O_2 can be converted to $OH^{\bullet}$ which is the most highly reactive ROS. This reaction is called "Fenton Reaction" (67). CAT is one of antioxidant enzymes that occupies in cytosol and peroxisome. CAT acts to catalyze H_2O_2 into oxygen and water (5,6). GPx is an enzyme family that its action is similar to CAT. GPx converts H_2O_2 into water by utilizing glutathione (GSH) as a substrate. The GSH is catalyzed by oxidative action of GPx and then oxidized-GSH is recycled by further reducing by glutathione reductase enzyme. There are six isoforms of GPx enzyme family, including GPx1-GPx6, whereas GPx1 is the most abundant and ubiquitously expresses in all tissue (5,6,68). In a non-enzymatic antioxidant network, ascorbic acid or vitamin C is oxidized to dehydroascorbate and acts to eliminate most ROS from the cells. Additionally, ascorbic acid also plays a role as an enzyme cofactor in collagen and elastin synthesizing processes (51,69). In the hydrophobic part of the cell as cell membrane, α-tocopherol or vitamin E participates in redox reaction by donating a hydrogen atom of hydroxyl functional group on chromanol ring of its structure to reduce radicals (70). However, overproduction or inadequate removal of ROS leads to oxidative stress and affects cellular antioxidant depletion and imbalance.

Antioxidants have been widely used in medicine, cosmetic and food additive (71-73). Antioxidant compounds can be categorized to natural antioxidants, that from natural resources (e.g. plant and animal), and synthetic antioxidants which commonly are substances with phenolic composition of different degrees of alkyl substitution (74).

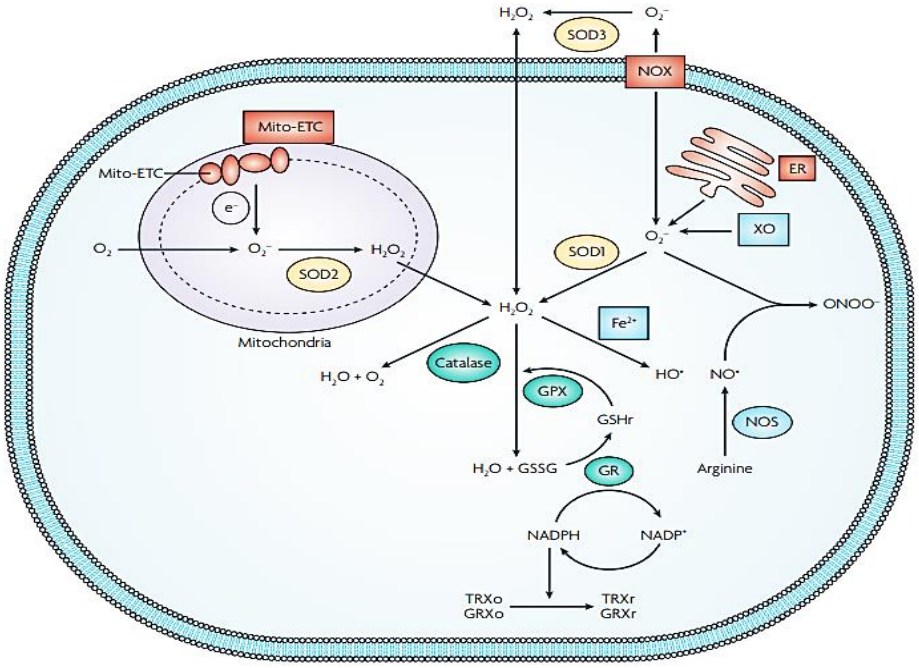

Figure 2.1 The cellular redox reaction in the cell (65).

At present, many natural antioxidants, for example, α-tocopherol, ascorbic acid, carotenoids, flavonoids and other phenolic compounds have commonly utilized as physiological and dietary antioxidants in order to enhance the body's resistance to oxidative damage (75). They usually come from a variety of plants, particularly higher plants. Nevertheless, lower vascular plants such as moss and fern are also the sources of natural antioxidant substances. Currently, it has been reported the antioxidants obtained from the various kinds of ferns (Table 2.2)

Table 2.2 Examples of fern that exhibited antioxidative property.

Plants	Compounds/ extracts	Properties	References
Athyrium multidentatum	Polysaccharide	- $O_2^{\bullet-}$ and $OH^{\bullet}$ scavenging activity - Ferrous ion chelating activity	(76)
Blechum orientale	Methanol extract	- DPPH radical scavenging activity - Ferric ion reducing activity and ferrous ion chelating activity - Beta-carotene bleaching activity	(77)
Cyclosorus acuminatus	Flavonoid-rich extract	- Increase of antioxidant enzyme (SOD, CAT, GPx) levels - Lipid peroxidation inhibition	(78)
Lygodium japonicum	Polysaccharide	- $O_2^{\bullet-}$, H_2O_2 and DPPH radical scavenging activity - Metal chelating activity - Liposome peroxidation inhibition	(79)
Pteris ensiformis	3,5-di-*O*-caffeoylquinic acid and 4,5-di-*O*-caffeoylquinic acid	- DPPH radical scavenging activity - 2,2'-azino-bis (3-ethylbenzthiazoline-6-sulphonic acid ($ABTS^{\bullet+}$) radical scavenging activity	(80)
Stenochlaena palustris	Aqueous extract	- DPPH radical scavenging activity - Ferric ion reducing activity - Metal chelating activity	(81)
Polypodium leucotomos	- Chloroform extract - Crude extract	- $O_2^{\bullet-}$, $OH^{\bullet}$, H_2O_2 and $^1O_2$ scavenging activity -Lipid peroxidation inhibition	(82,83)

2.6 Inflammation

Inflammation is the sophisticated immune responsiveness of the body to molecules or agents that cause cell or tissue injury, in order to eliminate the damaging agents as well as to remove damaged cells or tissues. Inflammation has been categorized into two types including acute inflammation and chronic inflammation (14,84).

Acute inflammation

Acute inflammation, an initial stage of inflammation, rapidly occurs within a minute to days after injury and can remain to 2-3 days. Pathophysiology of acute inflammation is characterized by fluid and plasma protein exudation, tissue edema, and neutrophilic leucocyte accumulation at the injured area (14).

Chronic inflammation

Chronic inflammation occurs after and happens longer than acute inflammation. Pathophysiology of chronic inflammation includes connective tissue formation or fibrosis, angiogenesis, tissue destruction and the influx of lymphocytes and macrophages. However, acute and chronic states of inflammation may co-progression, and other factors may change in histologic appearance (14,85).

The signs of inflammation are clinically characterized by redness, edema or swelling, fever, pain, and loss of function (86). These symptoms happen as consequences of the vascular changes and recruitment and activation of leukocyte. In the inflammatory processes, there are important reactions including vascular change, recruitment of white blood cells to the tissue at injured site and systemic changes (85).

2.6.1 Inflammatory pathways

The pathological pathways of inflammation are classified into two pathways including arachidonic acid-dependent and arachidonic-independent pathways (84).

2.6.1.1 Arachidonic acid-dependent pathway

In arachidonic acid-dependent system, the phospholipase A2, a predominantly isoform of phospholipase enzymes, is stimulated by various stimulators such as microorganism, cytokines or cellular injury to release arachidonic acid (AA). Normally, AA, a basic composition of membrane phospholipid of all cells, is further catalyzed to different lipid mediators or eicosanoids by cyclooxygenase (COX) enzyme and lipoxygenase (LOX) enzyme. The lipid mediators including prostaglandins and leukotrienes involve in development of inflammation (84,87,88).

COX are key enzymes in the process of prostaglandin biosynthesis by catalyzing AA. This enzyme includes two isoforms that are cyclooxygenase (COX)-1 and cyclooxygenase (COX)-2 (89). The COX-1 enzyme exerts constitutive expression in most cells and plays roles in physiological processes of gastrointestinal tract by reduces gastric acid secretion, vasodilates gastric mucosa vessels as well as involves in platelet aggregation (90,91). In contrast, COX-2 activity is commonly undetectable under the normal physiological condition of the body. COX-2 is inducible and rapidly expresses in a response to pro-inflammatory stimulators such as bacterial lipopolysaccharide (LPS) and cytokines, for example, interleukin (IL) and tumor necrosis factor (TNF) (89,92). Both COX-1 and COX-2 are responsible to release prostaglandins (PGs). PGs produced by COX-1 are involved in cytoprotecting of gastric mucosal cells. On the hand, prostaglandins secreted from COX-2 act as inflammatory activators that activate other inflammatory substances and alter the activity of many immune cells. Thus, PGs, particularly prostaglandin E_2 (PGE_2) has been considered to be one of inflammatory mediators (91,93).

LOX enzyme is principally found in inflammatory-involving cells, for example, leukocytes, macrophages, platelets as well as endothelial cells. In mammalian, LOX exists three isoforms, including 5-LOX, 12-LOX and 15-LOX (87).

LOX enzyme plays important role in synthesis process of leukotrienes (LTs) and lipoxin (LXs) from arachidonate via 5-LOX and 15-LOX pathways. LTs such as LTC_4, LTD_4, LTE_4 and LTB_4 activate the response of immune and inflammation by induce vascular dilation and microvascular permeability and trigger the pro-inflammatory mediator release. Moreover, LTB_4 is potent chemoattractant on leukocytes and has been involved in the pathogenesis of various inflammatory-related disorders (84,85,94).

2.6.1.2 Arachidonic acid-independent pathway

In arachidonic acid-independent network, nuclear factor kappa B (NF-κB) and nitric oxide (NO) play role in response to inflammation (84).

NF-κB is a nuclear transcriptional factor that locates in cell cytosol and translocates into nucleus after activated. The stimulation of NF-κB has been implicated in inflammatory response to stimulate gene expression of proinflammatory components, for instance, tumor necrosis factor (TNF)-α, interleukin (IL)-6, IL-8, iNOS, COX-2 and other cytokines (95,96).

NO, a free radical gas, is an inflammatory mediator which involves in normal physiological condition and pathological disorder of the body including vasodilation, innate immunity and inflammation. NO is produced from an activity of NO producing enzyme, nitric oxide synthase (NOS), in the oxidative reaction of L-arginine amino acid. The NOS enzyme family consists of endothelial NOS (eNOS), neuronal NOS (nNOS) and inducible NOS (iNOS) (97). In the physiological status, NO is constitutively released in low level by constitutive NO-producing enzymes, eNOS and nNOS. In contrast, in the inflammatory process, NO is predominantly produced by iNOS in response to pro-inflammatory stimulators, for example, IL-1β, TNF-α as well as lipopolysaccharide (LPS) of bacteria. NO not only regulates vascular blood flow but also acts as a host defense by damaging pathogenic DNA and as antimicrobial armament of macrophage cells. However, an excessive level of NO can further react with superoxide radicals to generate peroxynitrite, a reactive radical, and directly damages the function of cells. Thus, overproduction of NO by iNOS causes the cellular

oxidative stress and conducts to the higher severity level of inflammation as well as may further induce carcinogenesis (98-100).

2.7 Anti-inflammation

Since inflammation is progressed through overproduction of proinflammatory mediators such as PGs, LTs, NF-κB as well as NO, therefore reduction of these mediators could be considered as molecular targets for inflammation treatment. (94,95,99).

At present, nonsteroidal anti- inflammatory drugs (NSAIDs), for example, aspirin, diclofenac, ibuprofen and indomethacin are widely used for anti-inflammation due to their fast onset and curative effect (101,102). These agents share similar therapeutic mechanism by preventing the synthesis of prostaglandins from arachidonic acid by inhibition of COX enzyme (94). However, they may cause some side-effects on gastrointestinal tract when using long-term, due to non-specific action on COX enzymes. The adverse reaction of NSAIDs ranging from mild symptom such as dyspepsia to severe complications, for example, bleeding or gastroduodenal ulceration. Moreover, it can induce some adverse effects on the brain such as convulsion, hallucination and loss of consciousness (103,104). Although glucocorticoids are also alternatively used as anti-inflammatory drugs, the prolonged usage with high doses may cause some undesirable effects. For these reasons, these two categories of medicines are not the ideal for inflammatory treatment (101). Therefore the development of novel pharmaceuticals with no adverse reactions for treatment of inflammation is challenging. At present, a variety of plants both higher and lower vascular plants have been evaluated their anti-inflammatory property. The examples of natural products possessing anti-inflammatory activity are shown in Table 2.3.

Table 2.3 Natural products that exhibited anti-inflammatory property.

Plants/microorganisms	Compounds/ extracts	Mechanism of action	References
Blechnum occidentale	Methanolic extract	- Reduce rat paw edema and neutrophil migration	(105)
Curcuma mangga	Demethoxycurcumin, Bisdemethoxy curcumin	- Inhibit NO and PGE_2 release	(106)
Drynaria quercifolia	Ethanolic extract	- Reduce rat paw oedema and granuloma formation	(107)
Kaempferia parviflora	5-hydroxy-3,7,3′,4′-tetramethoxyflavone	- Inhibit NO and PGE_2 release	(108)
Spaganium stoloniferum	Sparstolonin B	- Inhibit Toll-like receptor (TLR2- and TLR4) signaling - Decrease TNF-α, IL-6 level - Inhibit Erk1/2, p38a, IκBα and JNK phosphorylation - Suppressed NF-κB activity	(109)
Terminalia catappa	Ethanolic extract	- Inhibit IL-1β and nitrite production - Suppress *iNOS* and pro-inflammatory mediator gene expression *(TNF-α, IL-23*, *IL-6* and *CINC-1*)	(110)

2.8 *Cyclosorus terminans* (J.Sm. ex Hook.) Panigrahi

Figure 2.2 Morphological character of *Cyclosorus terminans*

2.8.1 Plant characteristic

Description: *Cyclosorus terminans* is a vascular lower plant that is belonging to genus *Cyclosorus* of Thelypteridaceae family. It is a terrestrial fern with long creeping rhizomes that including brown linear-lanceolate scales on bases of stripes. The stalks are dark stramineous color and its lengths are 20–55 cm. The fronds are laminae oblong-lanceolate compound leaves with non-narrowed bases, apices are caudate with an apical pinna. The fern leaves comprise of 10-15 pairs of subsessile lateral pinnae and a linear-lanceolate middle pinna with rounded-truncate bases. The pinnae are lobed 1/2-1/3 toward costae with long-acuminate apices. There are 20-35 pairs of triangular segments with subacute or obtuse apices on the pinnae. The proximal pair of veinlets is anastomosing. The laminae are brownish green papery with adaxially short hairs along costae and veins. Sori are hairy and confined to upper part of segments of lower surface of laminae, often hollowed indusial persistent (111).

Ecology and distribution: It is common on rather on dry mountain slopes in the forests at low or medium altitudes up to 1,200 m altitudes. This plant usually distributes all over of Thailand and tropics of Asia to Australia (Queensland) (111).

Use: It has been reported that *C. terminans* can be vegetable (17).

2.8.2 Phytochemical study of *C. terminans*

At present, there are three coumarin derivative compounds including interruptins A, B and C (Figure 2.3) isolated from *C. terminans* (0.001-0.002% w/w of powder). These isolated interruptins were implicated as the main ingredients found from *C. terminans* (17). However, they were first elucidated from cogenetically ferns *C. interruptus* (112). The physical characteristics and chemical formulas of interruptins A-C are shown in Tables 2.4.

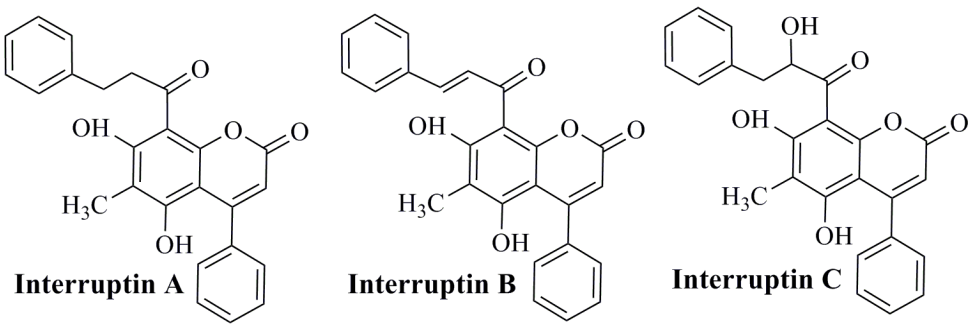

Figure 2.3 Chemical structure of interruptins A-C.

Coumarin compound is a group of secondary metabolites that widely distributes in natural sources such as plants, microorganisms and some animal species (113). The general structure of coumarin is benzo-α-pyrone that synthesized from cinnamic acid. The substitution on the coumarin nucleus makes their structural diversified structures and exhibits various bioactivities (114-116).

So far, a variety of bioactivities of coumarin compounds from natural resources had been reported including antibacterial, antifungal, antioxidative, anticancer, antidiabetic, anti-inflammation activities (17,114,115,117).

Interestingly, the isolated coumarin derivative interruptins and *C. terminans* extract also carried various biological properties such as antibacterial, anticancer, antidiabetic, antiobesity and antioxidative activities (17,112).

Table 2.4 The physical characteristic and chemical formula of interruptins A-C (112).

Compounds	IUPAC name	Chemical formula	Molecular weight (g/mol)	Physical appearance
Interruptin A	5,7-dihydroxy-6-methyl-4-phenyl-8-(3-phenylpropanoyl) chromen-2-one	$C_{25}H_{20}O_5$	400.43	Yellow-white powder
Interruptin B	5,7-dihydroxy-6-methyl-4-phenyl-8-[(E)-3-phenylprop-2-enoyl]chromen-2-one	$C_{25}H_{18}O_5$	398.414	Yellow powder
Interruptin C	5,7-dihydroxy-8-(2-hydroxy-3-phenylpropanoyl)-6-methyl-4-phenylchromen-2-one	$C_{25}H_{20}O_6$	416.429	Pale yellow-white powder

2.8.3 Bioactivity study of C. terminans extracts and its isolated compounds

2.8.3.1 Antibacterial

Ethyl acetate and dichloromethane extracts of *C. terminans* exhibited good antibacterial activity against Methicillin-sensitive *Staphylococcus aureus* (MSSA), methicillin-resistant *S. aureus* (MRSA), *S. epidermidis and Bacillus subtilis* as shown in Table 2.5. Additionally, the isolated interruptin A was identified as the active ingredient showing antibacterial property against above-mentioned microorganisms as well as *B. cereus* and *Micrococcus luteus* (17,112).

Table 2.5 The antibacterial activities of crude extracts of *C. terminans*, interruptins A-C and standard antibiotics (17,112).

Extracts/ Compounds	**MIC/MBC (μg/mL)**					
	MSSA	MRSA	*S. epidermidis*	*B. subtilis*	*B. cereus*	*M. luteus*
Hexane extract	512/1024	256/512	256/>1024	256/>1024	-	-
Dichloromethane extract	256/512	128/>1024	64/128	256/>1024	-	-
Ethyl acetate extract	128/128	128/512	128/128	64/>1024	-	-
Methanol extract	1024/>1024	1024/>1024	256/256	>1024/>1024	-	-
Interruptin A	4/32	4/8	2/16	16/64	2/-	2/-
Interruptin B	>256/>256	>256/>256	>256/>256	>256/>256	>64/-	>64/-
Interruptin C	>256/>256	>256/>256	>256/>256	>256/>256		
Vancomycin	1/4	1/4	2/4	1/4		
Chloramphenicol	-	-	8/-	-	4/-	2/-

- : not test

2.8.3.2 Anticancer/cytotoxicity

The isolated interruptins A and B demonstrated anticancer activity by reducing the viability of cancer cells (Table 2.6). Interruptins A and B exhibited stronger potency of cytotoxic effect against human breast adenocarcinoma (MCF-7) cells and colonic adenocarcinoma (HT-29) cells than standard camptothecin. Additionally, these compounds also carried a good cytotoxic activity on nasopharyngeal carcinoma (KB) cells (17,112).

Table 2.6 Cytotoxic activity of isolated interruptins against cancer cells (17,112).

Compounds	**IC_{50}** (μM)		
	KB	MCF-7	HT-29
Interruptin A	12.73	8.47×10^{-4}	3.75×10^{-4}
Interruptin B	9.54	4.02×10^{-4}	3.26×10^{-4}
Interruptin C	nt	-	-
Camptothecin	nt	3.33×10^{-3}	7.46×10^{-4}
Podophyllotoxin	14.49×10^{-3}	nt	nt

nt : not test

- : no activity

2.8.3.3 Anti-obesity

Interruptin B purified from *C. terminans* exhibited anti-obesity property in adipose-derived stem cells (ASCs). It not only induced cell proliferation and adipogenic differentiation, particularly brown adipocytes which are energy expenditure cells but also enhanced the lipid accumulation in a concentration-dependent fashion at 5-20 μg/ml (121.9-167.2% increase), while the increase with rosiglitazone at 17.87 μg/ml was only 127.7%. Interruptin B also up-regulated the mRNA expression of normal adipogenic markers, *PPAR-α* and *PPAR-γ*, together with triggered markers of brown adipocytes, uncoupling protein-1 (*UCP-1*) and mitochondrial carnitine palmitoyltransferase 1B (*CPT1B*). In addition, interruptin B enhanced the

mitochondrial membrane potential of differentiated adipocyte cells. A computational molecular docking analysis predicted interruptin B as a ligand of PPAR-α and PPAR-γ receptors. The binding affinity of this compound was more selective to PPAR-γ than PPAR-α (18,118).

2.8.3.4 Antidiabetic

The previous studies revealed that interruptin B from *C. terminans* markedly affected glucose metabolism. Interrutpin B at 10 and 20 µg/ml dramatically increased the insulin-stimulated glucose consumption (357-640%) in adopocytes differentiated from ASCs which was 2.3-4.1 times greater than treatment with 17.84 µg/ml of rosiglitazone (157%). Moreover, interruptin B at 20 µg/ml significantly up-regulated the levels of glucose transporter (GLUT) -1 and glucose transporter (GLUT)-4 mRNA compared to the control without treatment (18,118).

2.8.3.5 Antioxidation

Interestingly, interruptins A and B (10 µg/ml) that purified from *C. terminans* showed strong antioxidative property by acted as intracellular ROS scavengers in ASCs (74.5% and 95.4% inhibition, respectively) determined by oxidized 2',7'-dichlorofluorescein diacetate (DCF-DA) using flow cytometry (17).

2.9 The active constituent-enrich extract

Nowadays, the development of substances derived from natural resources to be health care products such as pharmaceutical, cosmeceutical as well as nutraceutical is very popular. However, the use of purified natural substances was limited owing to its amount was inadequate. Moreover, purification procedures were also laborious, high cost and time-consuming. Of these limitations, the crude extracts containing a high content of active constituents or enriched extracts were, accordingly, established as an alternative application (119,120). Nevertheless, employment of enriched extracts must be consistently quality controlled by monitoring the content of corresponding ingredients in the extract prior its utilization. The suitable procedure for analyzing the target compounds is therefore essential for quality control of the extract in batch-to-batch preparation (121).

2.9.1 Enrich extract preparation

For enrichment of active constituents in herbal extracts, the extraction method and fractionation technique that reliably yield products in batch-to-batch are important in the preparation process (120,122). Different methods are applied for the enrichment of target compounds from various medicinal plants extracts as demonstrated in Table 2.7.

Table 2.7 Example of methods for preparation of enriched plant extracts.

Enriched extracts	Enrichment methods	References
Anthraquinone rich extract of *Senna alata*	- Silica gel vacuum chromatography - Anion exchange resin (Amberlite® IRA-67	(123)
Brazilin-rich extract of *Caesalpinia sappan* heartwood	- Diaion®HP-20 chromatography	(124)
Chlorogenic acid-rich extract of *Eupatorium adenophorum*	- Macroporous NKA-II resin	(125)
Ellagic acid-rich extract of *Punica granatum* fruit peel	- Partition	(126)
Flavonoid-rich extract of *Hypericum perforatum*	- Nonionic polystyrene resin LSA	(127)
Pentacyclic triterpene-rich extracts of *Centella asiatica*	- Microwave-assisted extraction - Diaion®HP-20 chromatography - Activated charcoal	(128)
Phenylbutanoid-rich extracts of *Zingiber cassumunar*	- Solvent determination for extraction - Silica gel vacuum chromatography	(122)
Plumbagin derivative-rich extracts of *Plumbago indica* root	- Solvent determination for extraction - Silica gel vacuum chromatography	(129)
Rhinacantin-rich extract of *Rhinacanthus nasutus*	- Solvent determination for extraction - Anion exchange resin (Amberlite IRA-67)	(121)

2.9.2 Method Validation

The application of medicinal plant extracts with an adequate amount of active ingredients is essential in phytomedicine. The standardization of herbal extracts is very important to control the quality of extracts in batch-to-batch. Nowadays, analytical procedures, for instance, high performance liquid chromatography (HPLC)-photodiode array (PDA), HPLC-mass spectroscopy (MS) as well as gas chromatography (GC)-MS have been developed and validated to quantitate the active compounds in medicinal herb extracts (121,130-132). The novel methods used in the analytical application are required performance determination to ensure that they are reliable and reproducible. For method validation, based on the International Conference on Harmonization (ICH) guideline, Validation of Analytical procedures: text and methodology Q2 (R1), the typical validation parameters as the following list are required (119,133,134):

I. Specificity
II. Linearity and range
III. Accuracy
IV. Precision
V. Limit of detection (LOD) and limit of quantitation (LOQ)

I. Specificity

Specificity determination is used to specify whether an analytical procedure can clearly measure the analyte in the sample matrix. Specificity can be accessed by checking the peak purity and the variation of retention time.

Linearity and range

The linearity is generally referred to the linear relationship between analyte signals and analyte levels in the test sample. The linearity of an analytical protocol reflects its capability (within a given range) to give test results which are directly relative to the level of an analyte in the sample. Linearity is expressed as correlation coefficient (R^2) that obtained from linear regression calculation of the graphical plot of detected results versus analyte concentrations. The R^2 value typically should be ≥0.999.

The range of an analytical methodology is obtained from the interval between the lowest and highest concentrations of an analyte that have been evaluated with a suitable value of linearity.

II. Accuracy

The analytical method accuracy indicates the closeness of the acquired value of analyte by a validating procedure to the true value. The standard addition method or spiking technique is wildly used by adding a known amount of analyte into test sample prior to measure the analyte level. If there is analyte in the test sample, its actual amount should be detected before spiking. The accuracy is expressed in percentage of recovery (% recovery) of the test results.

III. Precision

The precision of the analytical procedure reflects the degree of scattering between a series of analysis resulted from multiple determinations of the identical homogeneous sample under the specified circumstances. Precision is used to assess the reproducibility of the procedure. This character may be regarded to three levels: repeatability, intermediate precision and reproducibility. Precision is normally shown as relative standard deviation or % RSD which obtained by measuring a sample in adequate replicates using the analytical method. The typical acceptable values of all levels of precision are ≤2%.

IV. Limit of detection (LOD) and limit of quantitation (LOQ)

LOD of an analytical procedure is achieved from the lowest level of the target substance in the sample that can be monitored under validating condition. This level is not necessarily to be quantitated as a certain value. LOQ is not only the lowest level of an analyte in a sample but also necessary to be quantitated with sufficient accuracy and precision. LOD and LOD are commonly referred to the concentration of target compound that gives a ratio of signal-to-noise of 3:1 and 10:1, respectively.

CHAPTER 3

METHODOLOGY

3.1 Plant material

Aerial parts of *Cyclosorus terminans* (J. Sm. ex Hook.) Panigrahi. were collected from Nakhon Si Thammarat province, Thailand and identified by Professor Dr. Thaweesakdi Boonkard at Department of Botany, Faculty of Science, Chulalongkorn University. The voucher specimen (identification no. SKP 208 03 20 001) was deposited at the herbarum of Faculty of Pharmaceutical Sciences, Prince of Songkla University, Thailand. Plant materials were dried in the oven at 50°C. The dried materials were blended to a powder and kept in well-closed plastic bag until used..

3.2 Chemicals and materials

Authentic interruptin standards, interruptins A, B, and C, were obtained from Asst. Prof. Dr. Sireewan Kaewsuwan's laboratory (17).

Chemicals and materials used in plant extraction and isolation, interruptins-rich *C. terninans* extract preparation, and HPLC method validation sections are shown in Table 3.1.

For antioxidative property determination of isolated interruptins and interruptins-rich *C. terminans* extract, two types of human skin cells, including human dermal fibroblast (HDF) and human epidermal keratinocyte (HEK) which are the representatives of skin dermis and epidermis, respectively, were used in experiments. Moreover, murine macrophage (RAW 264.7) was used in anti-inflammatory evaluation. The detail of cell lines used in this study is given in Table 3.2. And chemicals and materials used in the part of bioactivity evaluation are shown in Table 3.3.

Table 3.1 List of chemicals and materials used in plant extraction and isolation, interruptins-rich extract preparation, and method validation.

Chemicals/ materials	**Company, Country**
Glacial acetic acid	RCI Labscan, Thailand
Dichloromethane (CH_2Cl_2) (commercial grade)	ZEN POINT, Thailand
Ethanol (EtOH) (analytical grade)	RCI Labscan Ltd., Thailand
Ethyl acetate (EtOAc) (commercial grade)	ZEN POINT, Thailand
Hexane (commercial grade)	ZEN POINT, Thailand
Isopropanol (analytical grade)	RCI Labscan, Thailand
Methanol (MeOH) (commercial grade)	ZEN POINT, Thailand
Methanol (HPLC grade)	RCI Labscan, Thailand
Nylon syringe filter (0.45µm)	Fortune Scientific, Thailand
Pre-coated TLC-sheets (DC-Fertigfolien ALUGRAM® Xtra SIL G/UV245), 0.20 mm	MACHEREY-NAGEL, Germany.
Silica gel, 40-60 µm	Silicycle Inc, Canada

Table 3.2 List of cell lines.

Equipment/ instruments	**Cat. number**	**Company, Country**
Human dermal fibroblast (HDF)	PCS-201-012	ATCC, USA
Human epidermal keratinocyte (HEK)	CRL-2404	ATCC, USA
Murine macrophage RAW264.7	TIB-71	ATCC, USA

Table 3.3 List of chemicals and materials used in bioactivities determination.

Chemicals/ materials	Company, Country
2,2-diphenyl-1-picrylhydrazyl (DPPH)	Sigma-Aldrich, USA
2,4,6-tripyridyl-s-triazine (TPTZ)	Sigma-Aldrich, USA
2′,7′-dichlorofluorescein diacetate (DCFDA)	Sigma-Aldrich, USA
5x HOT FIREPol® EvaGreen® qPCR Mix Plus (ROX)	Solis BioDyne, Estonia
Ammonium persulfate (APS)	Bio-Rad, USA
Anaerocult® A (anaerobic milieu producer)	MARK, Germany.
Anti-β-actin (cat no #8457)	Cell Signaling Technology, USA
Anti-CAT antibody (cat no #3286)	Cell Signaling Technology, USA
Anti-GPx antibody	Cell Signaling Technology, USA
Anti-SOD1 antibody (cat no #2770)	Cell Signaling Technology, USA
Anti-SOD2 antibody (cat no #13194)	Cell Signaling Technology, USA
Ascorbic acid	Sigma-Aldrich, USA
Brain Heart infusion (BHI) broth	HiMedia, India
Coomassie (Bradford) protein assay kit	Thermo SCIENTIFIC, USA
Dimethyl sulfoxide (DMSO)	Sigma-Aldrich, USA
Dulbecco's Modified Eagle Medium (DMEM) low glucose	Gibco, USA
Dulbecco's Modified Eagle Medium (DMEM) high glucose	Gibco, USA
FavorPrep™ Blood/Cultured Cell Total RNA Purification Mini Kit	FAVORGEN Biotech Corp, Taiwan
Fetal bovine serum (FBS)	Gibco, USA
FIREScript RT cDNA Synthesis KIT	Solis BioDyne, Estonia
Glycine	Bio-Rad, USA

Table 3.3 List of chemicals and materials used in bioactivities determination (continued).

Chemicals/ materials	**Company, Country**
Goat Anti-Rabbit IgG Antibody, Peroxidase Conjugated (cat no #AP132P)	MARK, Germany
Hydrochloric acid	RCI Labscan, Thailand
Immun-Blot PVDF membranes for protein blotting	Bio-Rad, Germany
Iron III) chloride hexahydrate ($FeCl_3.6H_2O$)	POCH, Poland
Keratinocyte-serum free medium (SFM)	Gibco, USA
Lipopolysaccharide (LPS)	Sigma-Aldrich, USA
N-(1-Naphthyl) ethylenediamine dihydrochloride	Sigma-Aldrich, USA
Sodium chloride (analytical grade)	RCI Lab-scan, Thailand
Sodium lauryl sulfate	Ajax Finechem, New Zealand
sodium nitroprusside	Sigma-Aldrich, USA
Spectra™ Multicolor Broad Range Protein Ladder	Thermo SCIENTIFIC, USA
Sulfanilamide	Sigma-Aldrich, USA
SYBR DNA gel stain	Invitrogen, USA
Thiazolyl blue tetrazolium bromide (MTT)	Sigma-Aldrich, USA
Tris hydrochloride (Tris-HCl)	Bio Basic Inc, Canada
Tris (hydroxymethyl) aminomethane	Research Organics Inc, USA
Trypsin-EDTA	Gibco, USA

3.3 Equipment and instruments

The general laboratory equipment and instruments employed in this project are shown in Table 3.4.

Table 3.4 List of general laboratory equipment and instruments.

Equipment/ instruments	**Model**	**Company, Country**
Biosafety cabinet class II	11232BBC 86	BIOBASE, China
CCD camera	Fusion FX5XT	Vilber lourmat, France
Centrifuge	LMC-3000	Grni-bio, UK
Centrifuge	ROTINA 380 R	Hettich, Germany
CO_2 incubator	NB-203	N-BIOTEK, India
Flow cytometer	BD FACSCalibur	Becton Dickinson, USA
Fluorescent light	FL 18W Daylight	Lamptan, Thailand
Horizontal electrophoresis system	MJ-105-S	Major Science, USA
HPLC binary pump	Water 1500 series	Water Corporation, USA
HPLC C18 column	TSKgel ODS-100V	TOSHO Bioscience, Japan
HPLC quaternary pump	Chromaster 5000 series	Hitachi, Japan
Humidity chamber	Allen-Bradley PanelView C400	Newtronic Lifecare Equipment, India
Incubator	SL incubator	SHEL LAB, USA)
Inverted microscope	Nikon ECLIPSE TS100	Nikon, Japan
LED transilluminator	BLooK	GeneDireX, Taiwan
Microplate reader	SPECTROstar nano	BMG LABTECH, Australia
Microplate reader	Varioskan Lux	Thermo Scientific, Finland
pH meter	Mettler LE409	METTLER TOLEDO, USA

Table 3.4 List of general laboratory equipment and instruments (continued).

Equipment/ instruments	Model	Company, Country
Protein blotting system	Mini Trans-Blot Electrophoretic	BIO-RAD, USA
Protein electrophoresis system	Mini-PROREAN Tetra Cell	BIO-RAD, USA
Real-time PCR	ABI 7300	Applied Biosystems, USA
Rotary evaporator	G3 heidolph	Heidolph, Germany
Ultrasonic bath	S 100H	Elma, Germany
Spectrophotometer	GENESYS 6	Thermo Scientific, USA
Thermal cycler	Gene Q Thermal Cycler	BIOER, China
Ultrasonic bath	S 100 H Elmasonic	Elma, Germany
UV lamp (18W)	UVA (λmax = 365 nm) UVB (λmax = 316 nm),	PHILIPS, Holland
UV light meter	UV340B	China

3.4 General techniques of chromatography

3.4.1 Thin layer chromatography

Thin layer chromatography or TLC was used in separation processes for monitoring the target compounds in the crude extracts. Pre-coated TLC-sheets, 0.20 mm, was used as absorbent or stationary phase. The solvent system or mobile phase was the mixture between hexane and EtOAc in the ratio of 8:2. The samples were dissolved in organic solvent and spotted on TLC plate. Then TLC plate was put in TLC tank containing the mobile phase by leaving the sample spots over the solvent level and allowed the solvent ascending move until reached upper solvent front. TLC patterns were assessed by spraying with the mixture of ethanol and sulfuric acid (1:1 v/v) and heating on a hot plate. Then the spots of compounds were detected under UV lights at wavelengths of 254 nm and 365 nm.

3.4.2 Quick column chromatography

The quick column chromatography technique was utilized as the first step of separation process. Silica gel was used as an absorbent. Organic solvents including hexane, CH_2Cl_2, EtOAc, and MeOH were used as eluents. The eluents were prepared in a step gradient of hexane with an increasing percentage of CH_2Cl_2 and CH_2Cl_2 with an increasing percentage of EtOAc and EtOAc with an increasing percentage of MeOH, respectively. For column packing, silica gel was dryly packed into the sintered grass. The crude extract was dispersed in a small volume of solvent, mixed with a small quantity of silica gel and dried, and further loaded over the packed silica gel. The eluent was then poured down on the sample and vacuumed through the column to receiving flask by using suction. Each fraction was evaluated by TLC. The fractions that showed similar TLC pattern were then combined and dried using rotary evaporator.

3.4.3 Open column chromatography

Open column chromatography was mainly used in compound isolation method. The stationary phase and the mobile phase used in this technique were similar to a quick column technique. The stationary phase was silica gel. The mobile phase consisted of hexane, CH_2Cl_2, EtOAc, and MeOH. Wet packing technique was used for column packing by put silica gel in the solvent, stirred and loaded into the column. While dry packing was used for sample loading by dissolving the extract with a small volume of solvent, mixing with a small amount of silica gel and drying, and then loading on the top of silica gel. The loaded sample was allowed to descending move through the stationary phase with mobile phase that performed in an increasing step gradient of solvents. TLC was carried out to check the similarity of each fraction before combination and drying.

3.5 Plant extraction

The four organic solvents including hexane, CH_2Cl_2, EtOAc and MeOH were used for *C. terminans* extraction combined with reflux method. The solvent providing the best interruptins extraction efficacy determined by TLC was then selected for further plant extract preparation. In brief, the plant powder (500 g) was extracted for 1 h by serial reflux extraction at 80-90°C with hexane, CH_2Cl_2, EtOAc and MeOH (3 L), respectively (three times each). The resulting extracts were filtered through filter paper and dried at 45-50°C under reduced pressure condition using rotary evaporator (Scheme 3.1). All extracts were chromatographed by using TLC with hexane: EtOAc (8:2) as a solvent system to identify interruptins-containing extract. Interruptins A, B and C were used as markers.

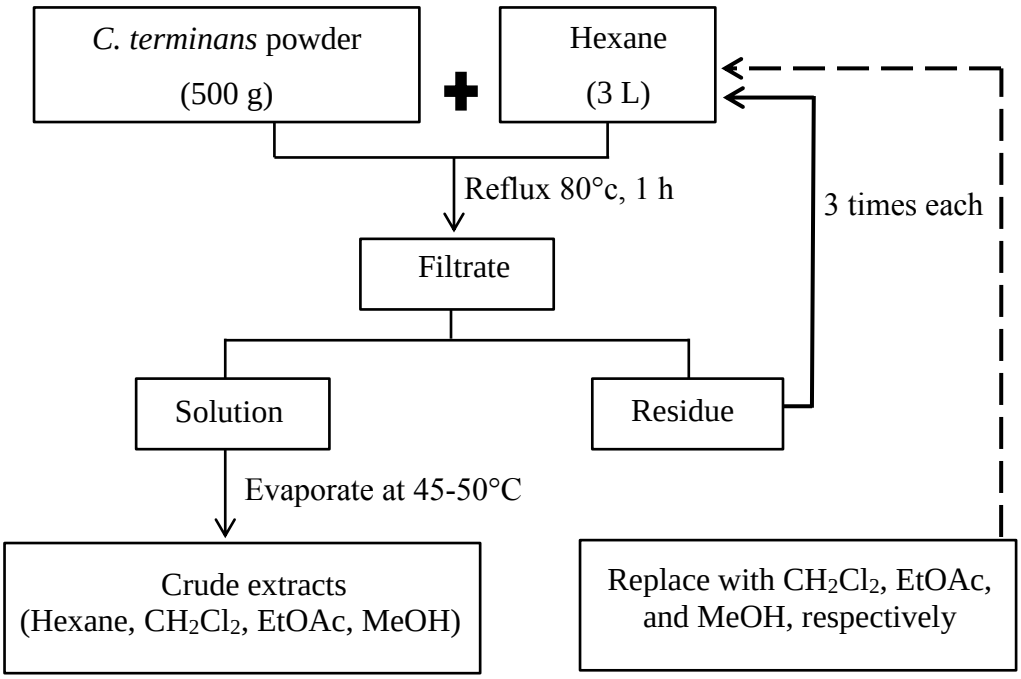

Scheme 3.1 The steps of plant extraction.

3.6 Isolation and identification

Among four solvents (hexane CH_2Cl_2, EtOAc, and MeOH) used for plant extract preparation in section 3.5, hexane exhibited the best efficacy of interruptins extraction by providing highest interruptin contents in the extract. Therefore, hexane extract was then further prepared and applied for interruptins isolation by using column chromatography. The quick chromatography (13 cm in diameter) was firstly used to fractionate the crude extract. Briefly, hexane extract (50 g) was dispersed in a small volume of solvent, mixed with a small quantity of silica gel and dried. The extract was applied over stationary phase and eluted with a step gradient of hexane with an increasing percentage of CH_2Cl_2 and CH_2Cl_2 with an increasing percentage of EtOAc and EtOAc with an increasing percentage of MeOH, respectively. The fractions that had similar TLC pattern were combined to yield 8 fractions of A-H (Scheme 3.2).

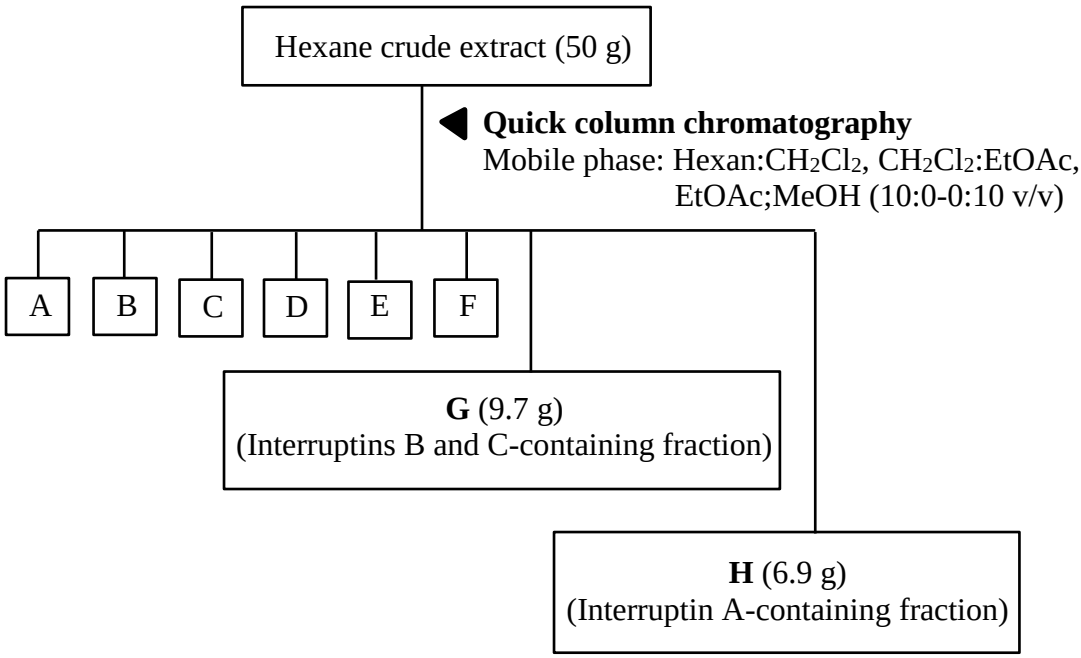

Scheme 3.2 The steps of fractionation of hexane crude extract with quick column chromatography.

3.6.1 Isolation of interruptin A

The 6.9 g of interruptin A-containing fraction (fraction H) was subjected to quick column chromatography (7.5 cm in diameter) using dry-packing method. An eluent was the mixture between hexane and EtOAc in the ratio of 8:2 to 7:3. The elution was checked with TLC. The fractions that showed similar TLC pattern were combined to obtain 4 subfractions of H1-H4. The 3.8 g of interruptin A-containing fraction (fraction H2) was crystallized by dissolved in small volume of EtOAc then slowly dropped with hexane in the ratio of 3:1 v/v. The solution was removed and interruptin A crystals were recrystallized with the same solvent system until obtained pure interruptin A (Scheme 3.3).

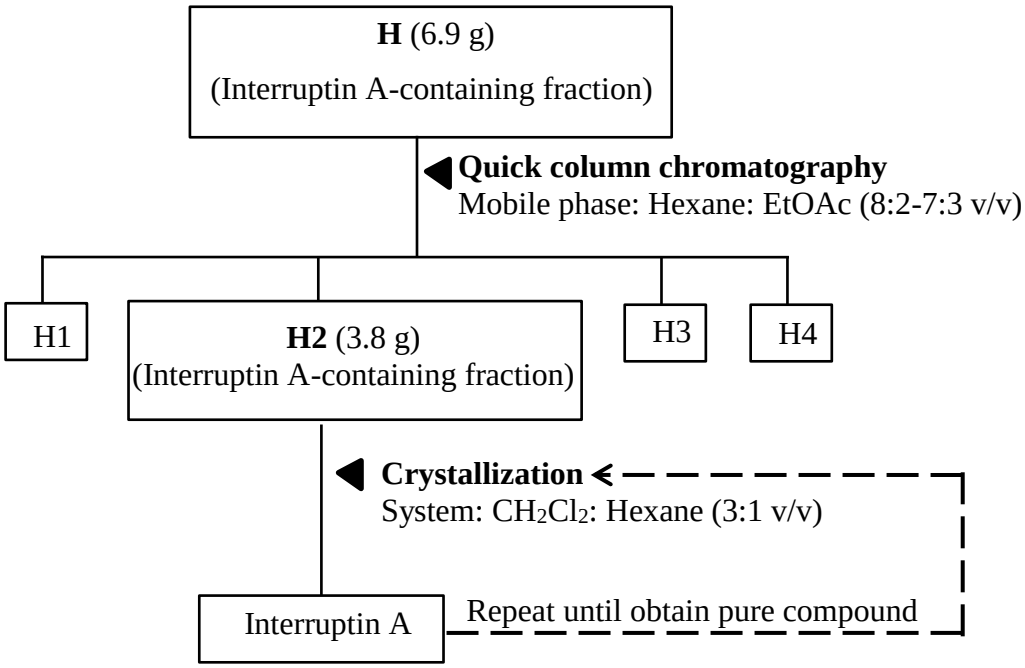

Scheme 3.3 The steps of isolation of interruptin A.

3.6.2 Isolation of interruptins B and C

The interruptins B and C-containing fraction (fraction G) was further purified by open column chromatography (1-5 cm in diameter). The extract (9.7g) was dispersed in a small volume of CH_2Cl_2, mixed with a small amount of silica gel and dried. The extract was loaded over the stationary phase and eluted with a step gradient of hexane with an increasing percentage of CH_2Cl_2 and CH_2Cl_2 with an increasing percentage of EtOAc and EtOAc with an increasing percentage of MeOH, respectively. The TLC with interruptins markers was applied to monitor interruptins B and C. The processes were repeated until obtained the pure compounds (Scheme 3.4).

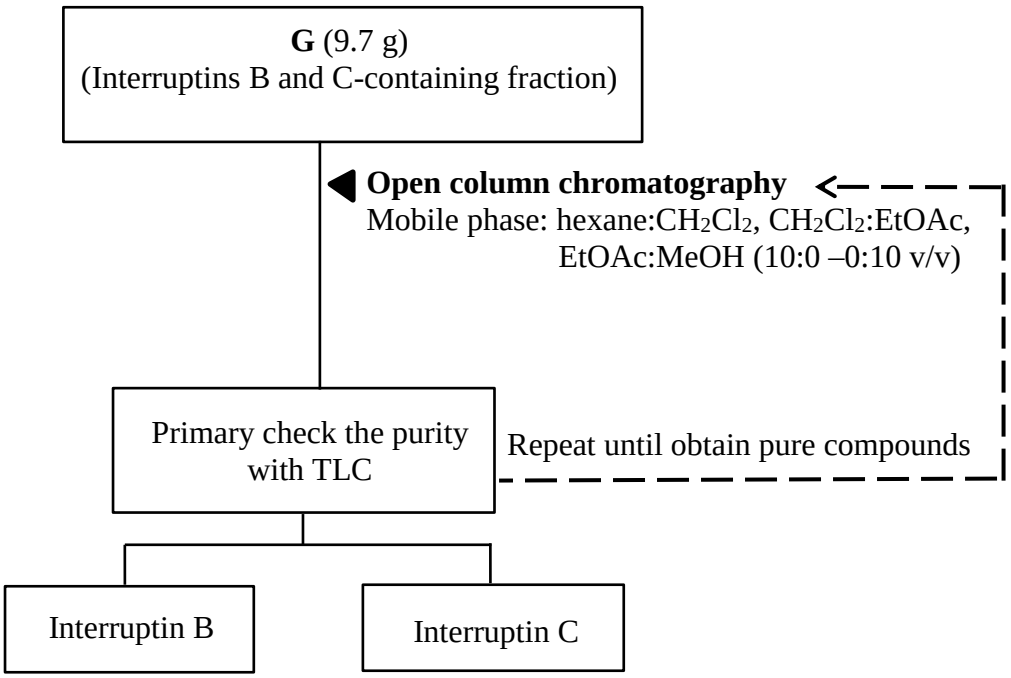

Scheme 3.4 The steps of isolation of interruptins B and C.

3.6.3 Structure identification and purity assessment

For structure identification, proton-1 nuclear magnetic resonance (^{1}H-NMR) was used to preliminary investigate the compound structures and their purity. ^{1}H spectra were obtained by a Fourier Transform NMR Spectrometer (^{1}H-NMR 500 MHz), model UNITY INNOVA Varian (Scientific Equipment Center, Prince of Songkla University) and compared with a previous report (112).

Furthermore, the validated HPLC method for analysis of interruprins (see in section 3.16 HPLC method validation) was applied to specify the compounds by checking the retention time together with the UV absorption pattern compared with each interruptin standards and to measure their purity by assessing area under curve (AUC) of each compound. The purity of compounds was obtained from % of peak area (AUC). The compound with high purity normally expresses a high of % of AUC (close to 100%).

3.6.4 Stock sample solution preparation

The sample stock solutions were prepared by accurate weighting isolated interruptins A-C in desired amount and then dissolving in DMSO. The stock sample solutions were kept in -20° C until used. Standard drug stock solutions including ascorbic acid, indomethacin and clindamycin were prepared and kept with a similar procedure of interruptins.

3.7 Cell culture

Human skin cells, including HDF and HEK cells, and murine macrophage RAW 264.7 cells (Figure 3.1) that used in this study were cultured in different culture media. HDF were cultured in 1% (v/v) antibiotics (penicillin/streptomycin)-added DMEM-low glucose containing 10% fetal bovine serum (FBS). While the mixture between keratinocyte-SFM medium containing 5 ng/ml human recombinant EGF and MEM-high glucose supplied with 10% FBS and 1% (v/v) antibiotics in the ratio of 2: 3 was used as HEK culture medium. RAW264.7 cells were maintained in 10% serum-containing RPMI-1640 medium supplemented with 1% (v/v) antibiotics. All cell types were normally incubated under a humidified 5% CO_2 atmosphere at 37°C in CO_2 incubator. The medium was typically changed in three days interval until reaching 80% confluency. The confluent cells were routinely sub-cultured by trypsinization with trypsin-EDTA.

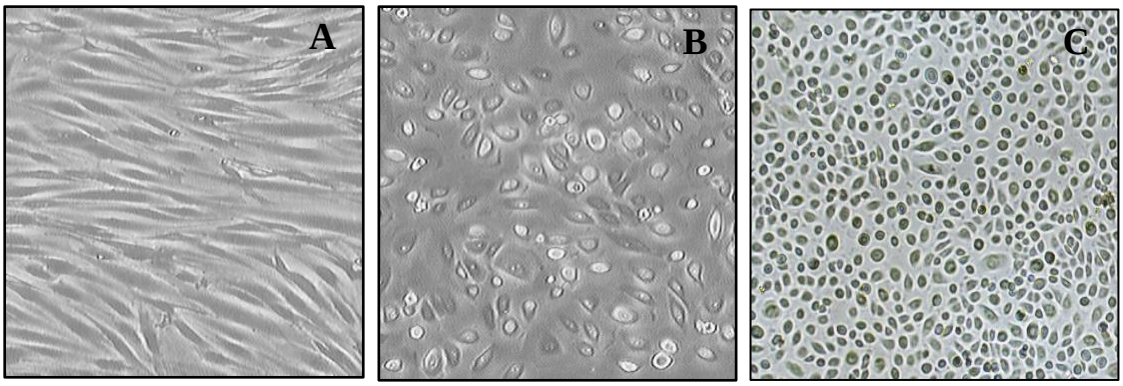

Figure 3.1 Human dermal fibroblast (A), human epidermal keratinocyte (B), and murine macrophage RAW 264.7 (C).

3.8 Cell viability assay

The survival of cell was assayed by using thiazolyl blue tetrazolium bromide (MTT) reagent. The viable cells normally metabolize yellow tetrazolium salts into purple formazan crystals by mitochondrial reductase enzyme (Figure 3.2). HDF (8×10^3 cells) and HEK (1.8×10^4 cells) were plated into 96-well plate and grown in their complete medium at 37°C under humidified 5% CO_2 atmosphere for 24 h. The cells were treated with various dosages of interruptins A-C (1, 5, 10, 20 µM) in 100 µL complete medium. Non-treated cells were used as control. After being incubation for 24 h, the incubated cells were washed once with PBS and substituted with 100 µL of fresh medium. Then, 10 µl of 5 mg/ml MTT reagent was added into each well and further kept at 37°C in CO_2 incubator for 2 h. The mixture of culture medium and MTT solution was then discarded and DMSO (100 µl) was added to dissolve formazan crystals. The formazan solution was recorded an optical density (OD) at 570 nm with a microplate reader. The experiment was done in triplicate. The viability of living cells was calculated and presented as % cell viability using the following equation 1:

$$\% \text{ Cell viability} = \frac{\text{OD of sample}}{\text{OD of control}} \times 100 \qquad [1]$$

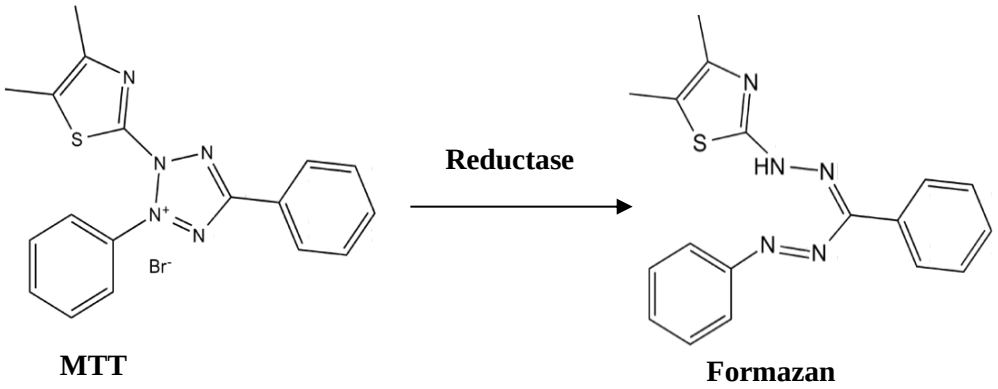

Figure 3.2 MTT assay (modified from Bahuguna *et al*, 2017) (135).

3.9 The study of antioxidative property of interruptins

3.9.1 Intracellular reactive oxygen species scavenging assay

The intracellular ROS scavenging efficacy of interruptins was examined using 2′,7′-dichlorofluorescein diacetate (DCF-DA). Basically, intracellular ROS generally oxidize non-fluorescence DCF-DA to highly fluorescence DCF which can be detected by a flow cytometer (Figure 3.3). Based on previous reported method (17) with some modification, HDF (4×10^5 cells) and HEK (9×10^5 cells) were plated in 60 mm culture dish with their complete media for 24h, then starved overnight with serum-free medium. The cells were treated with interruptins A-C in various concentrations (1, 5, 10, 20 µM) and DCF-DA (20 µM) in 0.5% FBS-containing medium for 30 min at 37°C in the dark condition. Non-treated cells were performed as a negative control. All cells were harvested by trypsinization using tryptin-EDTA. The cell pellets were washed twice, resuspended in PBS and then detected the fluorescence signals using a flow cytometer. Ascorbic acid was used as an antioxidant standard. The observation was done in triplicate. Percentages of fluorescence intensity (% FI) which stand for the levels of ROS in the cells were calculated according to the following equation 2. Additionally, percentages of ROS scavenging of tested samples were evaluated by using equation 3.

$$\% \text{ Fluorescence intensity (\% FI)} = \frac{\text{Fluorescence intensity of sample}}{\text{Fluorescence intensity of control}} \times 100 \qquad [2]$$

$$\% \text{ ROS scavenging} = \frac{\text{\% FI of control - \% FI of sample}}{\text{\% FI of control}} \times 100 \qquad [3]$$

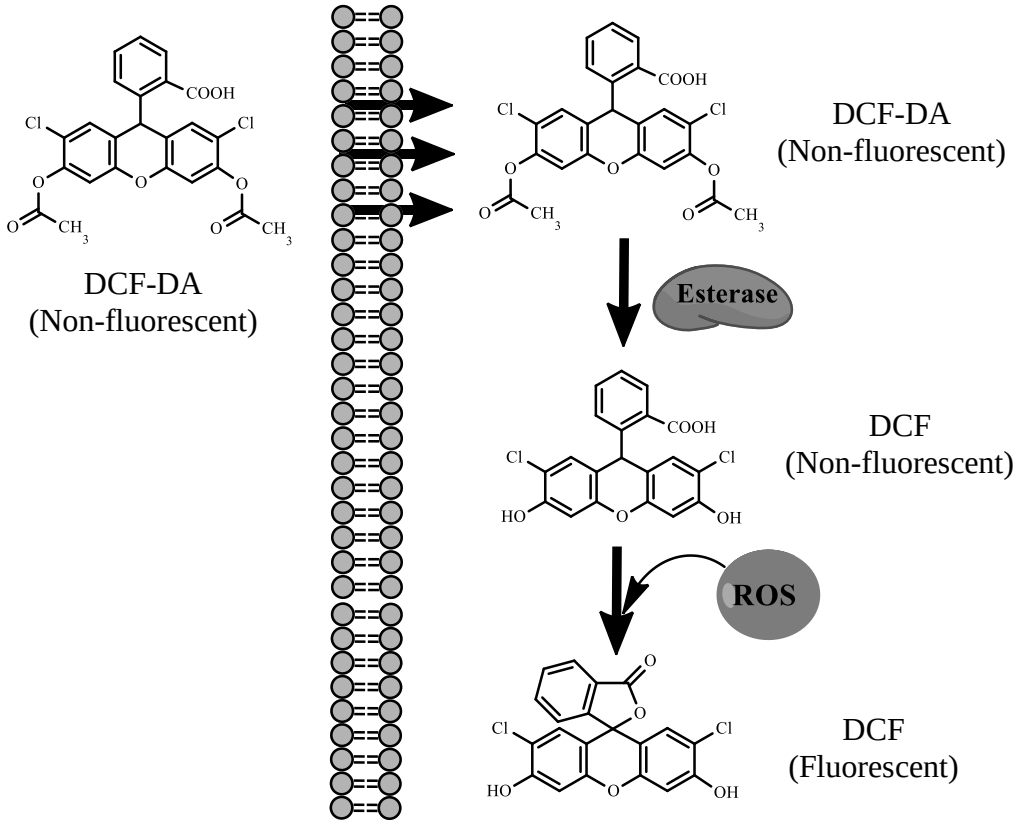

Figure 3.3 Fluorescent DCF formation by ROS. DCF-DA, dichlorofluorescein diacetate; DCF, dichlorofluorescein. (modified from Eruslanov and Krusmartsev, 2010) (136).

3.9.2 DPPH free radical scavenging assay

The 2,2-diphenyl-1-picrylhydrazyl (DPPH) radical quenching capacity of interruptins was examined followed a previous report (137) with slight modification. The DPPH working solution was freshly made by dissolving DPPH in MeOH and measuring an OD at wavelength 515 nm with a UV-visible spectrophotometer to obtain an absorbance unit of 1.1 ± 0.02. Interruptins A-C stock solutions were diluted with methanol into various concentrations in a range of 5-30 µM. The sample solutions (70 µL) and DPPH solution (70 µL) were added into 96-well plate and incubated in the dark condition at ambient temperature. After 30 minutes, the absorbance of reactions was detected at 515 nm with a microplate reader. Ascorbic acid was applied as a positive control. The experiment was done in triplicate. The % inhibition was achieved using the following equation 4. The result was expressed as IC_{50} value that was a sample concentration giving 50% inhibition. The IC_{50} values were extrapolated from linear regression equation of a graph constructed by plotting between % inhibitions and sample concentrations.

$$\% \text{ Inhibition} = \frac{\text{OD control} - \text{OD sample}}{\text{OD control}} \times 100 \qquad [4]$$

OD control = absorbance of DPPH solution without sample.
OD sample = absorbance of DPPH solution with sample.

3.9.3 Ferric reduction antioxidant power (FRAP)

The FRAP method was employed to assess the antioxidant capacity of substances based on the reduction of ferric (Fe^{3+}) to ferrous ion (Fe^{2+}). The ferrous product reacts with 2,4,6-tripyridyl-s-triazine (TPTZ) to form ferrous-TPTZ complex. The intense blue color will be performed when antioxidants exhibit their reducing activities in the reaction. The ferric reducing activity of interruptins was carried out by using a previously reported FRAP method (140) with slightly modified. The FRAP working solution (20 mM $FeCl_3$ and 10 mM TPTZ in 300 mM acetate buffer pH 3.6) was provided newly before use. The 198 µL of FRAP solution and 2 µL of interruptins A-C (20 µM) or ascorbic acid (0.01-0.03 mM) standard were added into 96-well plate and allowed to react 15 min at ambient temperature. The blue color of reactions was detected by measurement an OD at 593 nm with a microplate reader. The experiment was conducted in triplicate. The reducing power was evaluated from the graph of ascorbic acid that plotted between OD value against its concentration and reported as ascorbic acid equivalent (AAE) (mmol/L ascorbic acid/mol interruptin).

3.10 Gene expression of antioxidant enzymes

Gene expression of antioxidant enzymes including, SOD 1 and 2, CAT, and GPx from cells treated with interruptins was monitored. HDF (4×10^5 cells) and HEK (9×10^5 cells) were plated in cell culture dish (60 mm), grown in their complete medium for 24 h, and then starved overnight in serum-free medium. After that, cells were incubated with interruptins A and B (1, 5, 10 µM) in 2 % FBS-containing medium for 6 h. The sole media was done parallel as a control. Subsequently, total RNA was extracted from treated cells using RNA extraction kit (FAVORGEN Biotech, Taiwan). The RNA was subjected to measure its concentration by using spectrophotometer at an optical density of 260 nm and 280 nm. The ratio of OD at 260/280 nm should be in the range of 1.6-2.2. The cDNA was synthesized from 500 ng of RNA template using Oligo(dT)18 primer and a reverse transcription system in accordance with the instruction provided by manufacturer (Solis BioDyne, Estonia).

Real time-polymerase chain reaction (real time-PCR) was employed to monitor the mRNA expression levels of antioxidant enzymes. The ready to use PCR master-mix 5× HOT FIREPol® Evagreen® qPCR Mix Plus (Solis BioDyne, Estonia) was utilized in the PCR condition. The PCR reaction consisted of 2 µL of cDNA template (250 ng), 0.5 µL of forward and reverse primers (10 ng/µL) and 5 µL of PCR master-mix in a final volume of 25 µL. The amplification reaction was operated with activation of polymerase at 95°C for 15 min followed by 40 cycles of denaturation at 95°C for 15 sec, annealing at 54°C for 20 sec, and elongation at 72°C for 30 sec. The primer sequences are shown in Table 3.5. Glyceraldehyde-3-phosphate dehydrogenase (*GAPDH*) was applied as the endogenous gene. The control group was applied as calibrator. The relative gene expression level was quantitated from fluorescence signal emission using the comparative C_T method. A melting point dissociation curve was generated to confirm the presence of a single product (Figure 3.4). All samples were performed in triplicates. The relative gene expression was evaluated from the following equations 5-8.

$$\Delta C_T = [C_T \text{ of target gene} - C_T \text{ of endogenous gene}] \quad [5]$$

$$\Delta\Delta C_T = [\Delta C_T \text{ of target gene} - \Delta C_T \text{ of calibrator}] \quad [6]$$

$$\text{Relative gene expression} = 2^{-\Delta\Delta} \quad [7]$$

$$\text{The fold of expression} = \frac{\text{Relative gene expression of target gene}}{\text{Relative gene expression of calibrator}} \quad [8]$$

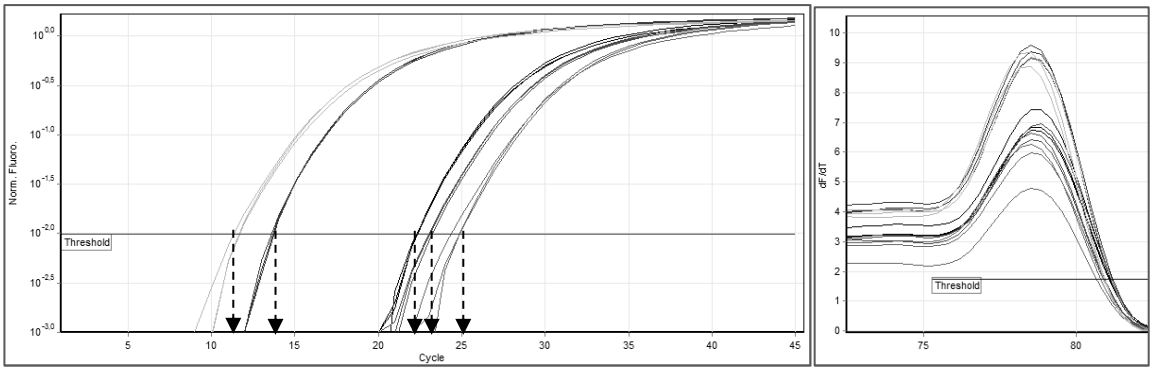

Figure 3.4 Amplification curve and melting curve from real-time PCR (Modified from https://en.wikipedia.org/wiki/Real-time_polymerase_chain_reaction) (139).

Table 3.5 Sequences of primers used for real-time PCR (18).

Gene	**Primer sequence**	**Product size** (bp)
SOD 1	Forward: 5′-TGT GAC TGC TGA CAA AGA TG -3′ Reverse: 5′-TCA TCT GCT TTT TCA TGG AC -3′	117
SOD 2	Forward: 5′-GAG CAC GCT TAC TAC CTT CA -3′ Reverse: 5′-GCA AGC CAT GTA TCT TTC AG -3′	105
CAT	Forward: 5′-TAA CTG GGA TCT CGT TGG AA -3′ Reverse: 5′-AGG ACG TAG GCT CCA GAA GT-3’	148
GPx	Forward: 5′-GAC TAC ACC CAG ATG AAC GA-3′ Reverse: 5′-CGT ACT TGA GGG AAT TCA GA -3′	133
GAPDH	Forward: 5′-CGA GAT CCC TCC AAA ATC AA -3′ Reverse: 5′-TGT GGT CAT GAG TCC TTC CA-3′	294

3.11 Protein expression of antioxidant enzymes

Similarly, proteins of antioxidant enzymes (SOD1, SOD2, CAT and GPx) from interruptins-treated cells were evaluated the expression level by western blotting assay. In brief, HDF and HEK were grown for 24 h and then starved overnight. After 6 h expose of interruptins A and B (1, 5, 10 μM) in 2 % FBS-containing medium, the cells were subjected to protein analysis using western blot. Non-treated cells were performed as a control. Total protein from treated cells was extracted with RIPA protein extraction solution and determined the amount with Coomassie protein assay reagent by following the protocol provided by manufacture (Thermo SCIENTIFIC, USA). Aliquots of 30 μg protein were separated on sodium dodecyl sulfate-12% polyacrylamide gel (SDS-PAGE) and transferred to polyvinylidene difluoride (PVDF) membrane. The membrane was blocked with 5% milk, washed 3 times with 1% milk and further hybridized with rabbit primary antibodies (1:1000) against SOD1, SOD2, CAT, GPx and β-actin control. The membrane was washed again with 1% milk in order to remove the excessive antibodies and subsequently incubated with secondary antibody, goat anti-rabbit IgG conjugated horseradish peroxidase (HRP). The protein bands on the membrane were detected by reacted with Immobilon^{TM} Western Chemiluminescent HRP substrate. The chemiluminescent signals were monitored under a CCD camera.

3.12 The study of anti-photooxidative property of interruptins

On the basis of UV radiation can trigger ROS generation in cells and lead to cell death, in this study, UVA (λ_{max} = 365 nm) and UVB (λ_{max} = 316 nm) lamps were used as alternative UV light sources in order induce ROS production and disturb cells. UV intensity was measured with a UV meter. ROS scavenging effect of interruptins on UV-induced ROS generation in human skin cells was conducted.

HDF (4×10^5 cells) and HEK (9×10^5 cells) were seed in 60 mm culture dish with the complete medium and cultured for 24 h. After cell starvation overnight with serum-free medium, the media was replaced with PBS and the cells were subsequently exposed to UVA 3J (for both cells) or UVB 300 mJ (for HDF) and UVB

20 mJ (for HEK). After UV exposure, PBS was removed and cells were treated with interruptins (5, 10, 20 µM) in 0.5% FBS-containing medium with 20 µM DCF-DA for 30 min in the dark. Non-UV exposed cells and non-treated UV exposed cells were done as the controls. All cells were subjected to measure the intracellular ROS level by using a flow cytometer as described procedure in section 3.9.1.

3.13 Study of anti-inflammatory property of interruptins

3.13.1 Nitric oxide scavenging assay

Base on the production of nitrite ion (NO_2^-) from the reaction between nitric oxide (NO) and oxygen, and NO scavengers compete with oxygen leading to reduce nitrite radical. Hereby NO radical scavenging efficacy of interruptins was determined by following the method in the previous report (140) with slight modification. Sodium nitroprusside (SNP) was used as NO generator and Griess reagent was used to determine the nitrite accumulation. SNP solution (20 mM) was mixed with interruptins A-C (20-100 µM) and kept at ambient temperature for 180 min. The incubated mixtures were reacted with Griess reagent. The color of the reaction was detected at 546 nm using a microplate reader. Gallic acid was applied as a positive control. % NO radical scavenging by tested samples were calculated using equation 9. The IC_{50} values were evaluated from the graphical plot between % NO radical scavenging and sample concentration. The experiment was done in triplicate.

$$\% \text{ NO radical scavenging} = \frac{\text{OD control} - \text{OD sample}}{\text{OD control}} \times 100 \qquad [9]$$

OD control = absorbance of SNP solution without sample.
OD sample = absorbance of SNP solution with sample.

3.13.2 Nitric oxide production inhibition assay

The inhibitory effect of interruptins on NO release was examined using the model of murine macrophage-like RAW 264.7 cells and followed the process from the previous report (141) with slightly modified. The cells (1×10^5 cells/well) were plated into 96-well plate with the complete culture medium and then allowed to adhere the plate for 1 h at 37ºC under humidified 5% CO_2 atmosphere. Then the medium was substituted with 200 µl of 1 µg/ml LPS in fresh medium supplemented with 1-20 µM interruptins A-C and cells were further cultured for 24 h. Indomethacin was used as a standard. NO release by LPS-induced RAW 264.7 cells was evaluated by detecting the accumulation of nitrite in the culture medium using Griess reagent. The OD of reaction was read at 570 nm using a microplate reader. The demonstration was done in triplicate. The percentage of NO production inhibition by tested substances were calculated using equation 10. The IC_{50} values were also evaluated from the graphical plot between % inhibition of NO production and sample concentration. The remaining cells were subjected to determined cell viability using MTT followed the procedure as described in section 3.8

$$\% \text{ Inhibition of NO production} = \frac{\text{OD control} - \text{OD sample}}{\text{OD control}} \times 100 \qquad [10]$$

3.13.3 Gene expression of inflammatory related genes

The molecular mechanism of interruptins on anti-inflammation was investigated by detecting mRNA level of *iNOS*, *COX-2* and *PPAR-γ* genes. The experiment was carried out base on the reported procedure in the previous study (142) with some modification Briefly, RAW264.7 cells (1.5×10^6 cells/well) were added to 6-well plate, incubated for 1 h and further exposed to interruptins A-C (1, 5, 10 µM) in 1 µg/mL LPS-containing medium for 20 h at 37 ◦C under humidified 5% CO_2 atmosphere. The treated cells were subjected to total RNA extraction and cDNA was synthesized using RNA as a template.

PCR was applied to detect the mRNA expression levels of *iNOS, COX-2,* and *PPAR-γ.* The PCR reaction consisted of cDNA (200 ng), forward and reverse primer (5 ng each) and PCR master-mix in a total volume of 25 µL. The amplification reaction was performed with a pre-denaturation step at 95°C for 2 min followed by 30 cycles of denaturation at 98°C, 30 sec; annealing at 60°C, 30 sec; and extension at 74°C, 1 min and a final extention at 75°C for 5 min. The sequences of primers used in this experiment are shown in Table 3.6. *GAPDH* was used as the standard gene. The amplicons were distinguished on 1.2% agarose gel by electrophoresis. SYBR dye was used to stained DNA bands and observed under a blue light boxbox.

Table 3.6 Sequences of primers for PCR (142,143).

Gene	**Primer sequence**	**Product size** (bp)
iNOS	Forward: 5′- ATCTGGATCAGGAACCTGAA-3′ Reverse: 5′-CCTTTTTTGCCCCATAGGAA-3′	580
COX-2	Forward: 5′-GGAGAGACTATCAAGATAGTGATC-3′ Reverse: 5′-GGAGAGACTATCAAGATAGTGATC-3′	680
PPAR-γ	Forward: 5′-CAAAGTAGAACCTGCATC TCC-3′ Reverse: 5′-CCTTCACAAGCATGAACTCC-3′	156
GAPDH	Forward: 5′-AAC ATC ATC CCT GCA TCC AC-3′ Reverse: 5′-AGT GGG AGT TGC TGT TGA AG-3′	262

3.14 *In vitro* wound healing assay

The wound healing effect of interruptins on human skin cells was taken under the cell migration assay. HDF (4×10^5 cells) and HEK (8×10^5 cells) were added into 96-well plate in complete medium and allowed to grow in the condition of 5% CO_2 atmosphere, 37°C until reaching 100% confluency. Then confluence cells were starved in serum-free medium overnight. The cells were wounded with 1000 μL of micropipette tip having a large orifice and washed with PBS to remove debris. The wounded cells were treated with various concentrations of interruptins A-C (1, 5, 10 μM) in complete medium. For the monitoring of cell migration, photographs of wound area were taken every 12 h by inverted microscope. Three randomly determined points by the side of the wound edge were marked, and the transverse lengths of the immigrating cell from the initial wound were recorded. The % wound closure was estimated by equation 11. The experiment was carried out in three replicates.

$$\% \text{ Wound closure} = \frac{\text{Wound distance of time}_0 - \text{Wound distance of time}_n}{\text{Wound distance of time}_0} \times 100 \qquad [11]$$

Time_0 = initial time of migration

Time_n = time of detection

3.15 Antibacterial assay

Since *Propionibacterium acnes* infection causes the cellular oxidative stress by triggering ROS generation and induces inflammation, anti-*P. acnes* activity of interruptins was also assessed in this study by evaluation tion of minimum inhibitory concentration (MIC) and minimum bactericidal concentration (MBC) using broth microdilution method (144). *P. acnes* (DMST 149) was kindly supported by Asst. Prof. Dr. Sukanya Dej-adisai, Department of Pharmacognosy and Pharmaceutical Botany, Faculty of Pharmaceutical Sciences, Prince of Songkla University, Thailand.

For detail, the test agents were serial 2-fold diluted in BHI broth with a starting concentration of 250 μg/mL. The *P. acnes* was suspended in normal saline to obtain

McFarland No 0.5 turbidity that approximate 1.5×10^8 Colony-Forming Unit (CFU)/mL by measuring an OD of 625 nm (OD 0.08-0.11 unit) with a spectrophotometer. The bacterial suspension was then diluted to 1×10^7 CFU/mL. The interruptins-containing medium (200 µL) was added into 96-well plate and 10 µL of diluted bacterial suspension (5×10^4 CFU/well or 5×10^5 CFU/mL) was inoculated. The solely media and media with microbial were used to check sterility and growth condition. The culture plates were kept in anaerobic condition for 72 h at 37°C. The 0.1% sterilized-resazurin solution (10 µL) was dropped in each well and further incubated in the same condition for 2 h. The lowest dosage of sample that inhibits bacterial growth showing the blue color of resazurin was defined as MIC. The MBC was achieved by streaking the broth from the cultured well that showed growth inhibition onto BHI agar and incubated for 72 h in anaerobic condition at 37°C. The lowest concentration of interruptins that exhibited no *P. acnes* colony was evaluated as the MBC. The experiment was operated in triplicate.

3.16 High performance liquid chromatography (HPLC) method validation

Although quantitative analysis HPLC method of interruptins was conducted in the preliminary study (17), it has not yet been validated. In this study, validation of HPLC method was operated following the International Conference on Harmonization (ICH) guideline, validation of analytical procedures: text and methodology Q2 (R1) (133). The validation parameters consisted of linearity, range, specificity, accuracy, precision, limit of detection (LOD), and limit of quantitation (LOQ). HPLC instrument used was the Water 1500 series HPLC model with binary pumps accompanied with a photodiode array detector (PDA) and autosampler. HPLC condition consisted of the following list.

Column	:	Reversed phase C18
Mobile phase	:	1% aqueous acetic acid/methanol (15:85, v/v)
Flow rate	:	1 mL/min
Detection	:	290 nm with PDA detector

3.16.1 Standard and sample solution preparation

The interruptins A, B and C were used as standard compounds. The standard stock solution was prepared by accurately weighed in equal amount, mixed and dissolved in DMSO. After that, it was filtrated through 0.45 µm filter and kept in -20 °C until use. For HPLC analysis, the standard stock solution was diluted in methanol to obtain desired concentrations.

Ethyl acetate extract of *C. terminans* was used as a sample in the validation process. For plant extraction, fern powder was extracted with ethyl acetate using reflux. After filtration, the liquid extract was evaporated under *vacuo* at 50°C to achieve crude extract. Then the ethyl acetate crude extract was accurately weighed, dissolved in methanol by sonication at 30°C for 15 minutes and filtrated through 0.45 µm filter to provide the 20 mg/mL sample solution for HPLC analysis.

3.16.2 Linearity and range

Linearity was determined by using the standard solution at six concentration points for each interruptins, in triplicates. After analysis, standard curves were plotted between the mean of the area under curve (AUC) and concentration. Regression analysis was used to achieve the linear equations and the coefficients of determination (R^2). Range was obtained from the range of standard concentration that gave $R^2 \geq 0.999$.

3.16.3 Specificity

Specificity of procedure was tested by inspecting the variance of retention time and comparing the similarity of UV absorption pattern of standards and interruptins in samples. The absorption pattern was checked on three points of target peak. The analysis was done in nine replications.

3.16.4 Limit of detection (LOD) and limit of quantitation (LOQ)

Standard solutions were diluted in methanol by serial dilution and analyzed in three replicates. LOD and LOQ of analysis method were desired from the minimum concentration required to give a signal-to-noise (S/N) ratio equal to 3 and 10, respectively.

3.16.5 Accuracy

Method accuracy was carried out by using a spiking technique. Three different known concentrations of standard interruptins A, B, and C including low (10 µg/mL), average (50 µg/mL) and high (100 µg/mL)-were added into sample solution in order to evaluate the recovery. The quantities of interruptins in sample solution were elucidated prior to spiking standard for calculating actual recovery. The amounts of spiked interruptins were measured in triplicate for each spiked level and their recoveries were calculated using the equation: % recovery = 100 × measured content/fortified amount.

3.16.6 Precision

Method precision was evaluated to find out repeatability (intra-day precision) and intermediate precision (inter-day precision) by determining a scatter degree of series analysis. For intra-day precision, six replicate injections of one sample solution were analyzed within the same day using the same condition. The intermediate precision was accessed by measuring the interruptin amounts in three different concentrations of sample solution in three-day interval. The analysis was done in triplicate for each concentration in each day. The data was calculated to obtain % RSD for intra-day precision and inter-day precision (less than 2%).

3.17 Interruptins-rich *C. terminans* extract

Due to the limitation of using isolated interruptin compounds, this experiment purposed to prepare the interruptins-rich *C. terminans* extract for an alternative application. In a pilot study, EtOAc, EtOH, and isopropanol were evaluated their interruptins extraction capacity using four different extraction methods, including maceration, microwave-assisted extraction, ultrasonic-assisted extraction, and reflux. Among these three organic solvents, EtOAc has been introduced as the most suitable for extraction of interruptins from *C. terminans* powder followed by isopropanol (data not shown). However, non-polar organic solvents, including hexane, CH_2Cl_2, chloroform, as well as EtOAc were rarely used in pharmaceutical and cosmeceutical industries owing to their inherent toxicities and volatilities. Herein, thus, less toxic solvent isopropanol was selected for preparing interruptins-rich *C. terminans* extract using a combination of ultrasonication and reflux extraction.

3.17.1 Preparation of isopropanol extract of *C. terminans* (CE)

For extraction step, fern powder (1 kg) was soaked in isopropanol (3 L) and then sonicated at 37 kHz for 1 h. After sonication, the plant was subjected to reflux at 70-80° C for 1 h. The resulting extract was filtrated through filter paper. The residue was re-extract by reflux two times. The filtrated was pooled together and evaporated to dryness in *vacuo*. The prepared isopropanol extract of *C. terminans* (CE) was subjected to quantify interruptins content using a validated HPLC method with the mentioned condition in section 3.16.

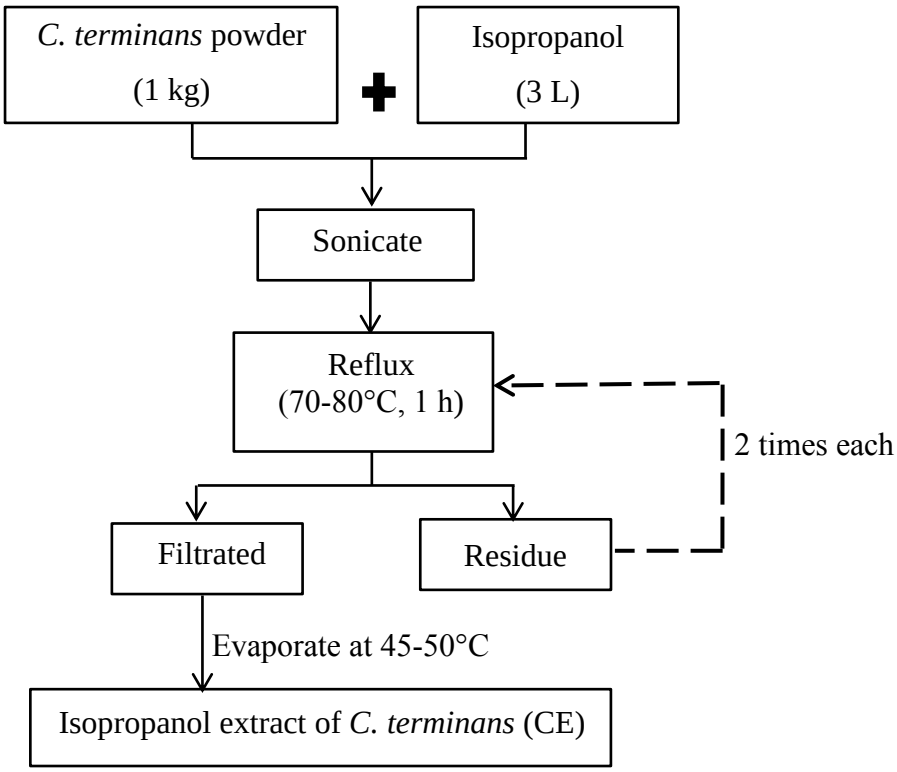

Scheme 3.5 Preparation of isopropanol extract of *C. terminans* (CE).

3.17.2 Preparation of interruptin-rich *C. terminans* extract (IRCE)

Isopropanol extract of *C. terminans* (CE) was subjected to remove impurities by using simple precipitation technique. Briefly, CE (15 g) was dissolved in isopropanol (35 mL) and then distilled water (20 mL) was dropped. The mixture was left for precipitation at ambient temperature for 3 h. The precipitated was filtrated by filter paper. The filtrated solution was re-precipitated again by adding 30 mL of distilled water, left for 3 h and filtrated. The precipitate on filter paper was dissolved in isopropanol and evaporated in *vacuo* to obtain interruptins-rich *C. terminans* extract (IRCE). The IRCE was subjected to quantify interruptin contents using a validated HPLC method as mentioned in section 3.16.

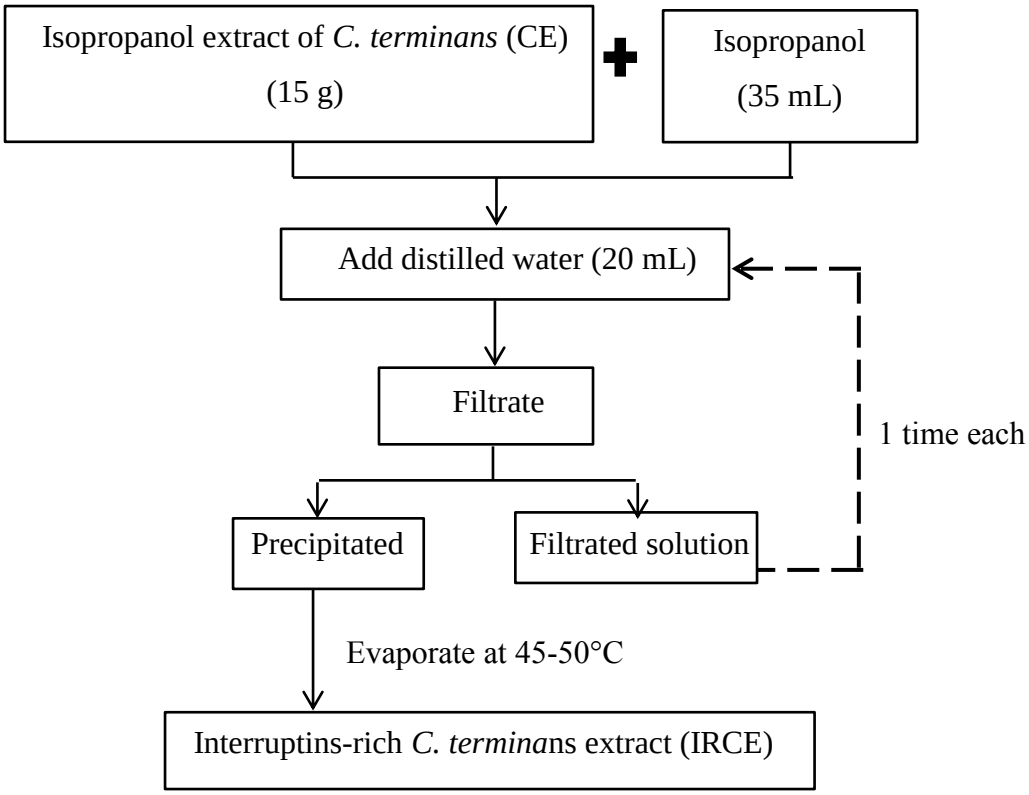

Scheme 3.6 Preparation of interruptins-rich *C. termina*ns extract (IRCE).

3.17.3 Bioactivity study of CE and IRCE

According to the potencies of isolated interruptins on antioxidation and anti-inflammation, both CE and IRCE were subjected to evaluate their bioactivities on cell viability, intracellular ROS scavenging activity, and anti-inflammatory efficacy followed the mentioned protocols in section 3.8, 3.9.1, and 3.13.2, respectively. Crude extracts were dissolved in DMSO and kept in -20°C for use as stock solutions. In the experiments, sample solutions were diluted with test media to various concentrations typically in the range of 5-80 μg/mL. The % DMSO in test media was allowed as 0.05%.

3.17.4 Stability study of CE and IRCE

The CE and IRCE were evaluated their stability by monitoring interruptin contents in extracts in corresponding to various conditions including light protection and light exposure condition, cold and room temperature, as well as accelerated condition based on previous methods (145,146) with some modification.

The aliquots (500 mg) of CE and IRCE were contained in well-closed containers. The samples were preserved in each condition for three months. The actual initial amounts of interruptins in CE and IRCE determining at the beginning of the study (month-0) were defined as 100% remaining. The samples were taken at month-1, -2 and -3 to quantitate interruptins A and B levels in the extracts by validated HPLC method. The experiments were performed in three replicates. The extracts with not less than 80% remaining of interruptin contents were considered as stable extracts.

Effect of light on CE and IRCE stability

The fluorescent lights (18-Watts ×2) were used as light source. CE and IRCE (500 mg each) in well-closed containers were exposed to fluorescent light for 3 months at room temperature. The light-protected samples were done in parallel. The distance between samples and the light source is 40 cm.

Effect of temperature on CE and IRCE stability

Thermostability of extracts was performed in different condition, including cold and normal temperature. CE and IRCE (500 mg each) in well-closed containers were protected from light by covering with foil and maintained for 3 months at 4 ± 2° C and room temperature (30 ± 2° C).

Effect of accelerated condition on CE and IRCE stability

CE and IRCE (500 mg each) in well-closed containers were protected from light by covering with foil and kept in a humidity chamber at 40 ± 2°C with 75% relative humidity for 3 months.

3.18 Statistical analysis

The results were represented as the mean ± standard deviation (SD). The comparisons between control and tested groups were conducted by using one-way ANOVA followed by Duncan test. Microsoft Excel was employed to calculate IC_{50} values. The statistically significant was considered as $p < 0.05$ and $p < 0.01$.

CHAPTER 4

RESULT AND DISCUSSION

4.1 Plant extraction

The four organic solvents, including hexane, CH_2Cl_2, EtOAc, and MeOH were used to preliminary extract the interruptins from *C. terminans* by reflux extraction. The TLC result showed that hexane was the best solvent for interruptin extraction, since hexane extract demonstrated the highest interruptins A-C content compared to other prepared extracts (Figure 4.1).This probably due to the low polarity of interruptins A-C which could be easily extracted by low polarity solvent as hexane. Whereas the % yield of MeOH extract was maximum as 8.8 % w/w of dried powder (Table 4.1), unfortunately, sequential extraction by high polarity MeOH could not extract interruptins A-C as shown in Figure 4.1. Thus, hexane was chosen as a solvent to prepare the *C. terminans* extract for further isolation of the interruptins.

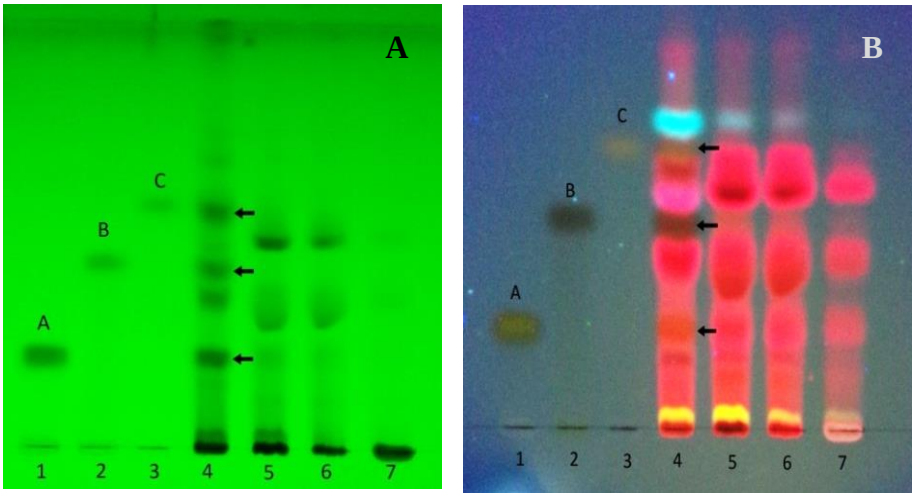

Figure 4.1 The TLC pattern of *C. terminans* crude extracts using hexane: EtOAc (8:2) as the mobile phase detected at UV 254 (A) and 366 (B) nm. Lanes 1-3 were interruptins A-C, respectively. Lanes 4-7 were hexane, CH_2Cl_2, EtOAc and MeOH crude extracts, respectively. The arrows indicated interruptins A, B and C.

Table 4.1 The % yield of *C. terminans* crude extracts.

Crude extract	**% yield of crude** (% w/w of dried powder)
Hexane	0.5
CH_2Cl_2	2.2
EtOAc	0.7
MeOH	8.8

4.2 Isolation and identification

4.2.1 Isolation of interruptins

Fifty grams of hexane extract was fractionated by quick column chromatography to obtain 8 fractions of A-H. After TLC determination, interruptin A was found in fraction H (6.9 g), while interruptins B and C were in fraction G (9.7 g). Interruptin A was recrystallized from fraction H2 to yield 418 mg. Interruptins B and C were purified from fraction G to yield 96 mg and 149 mg, respectively. The % yields of interruptins A-C are shown in Table 4.2.

Table 4.2 The % yield of isolated interruptins from *C. terminans* hexane extract.

Samples	**Weight of extract / pure compounds** (g)	**% yield** (% w/w of crude extract)
Hexane extract	50.02	-
Interruptin A	0.42	0.84
Interruptin B	0.10	0.20
Interruptin C	0.15	0.30

4.2.2 Structure identification and purity assessment

To access the identity of compounds, the proton (^{1}H) NMR spectroscopy was used for primary checking the identical of isolated interruptins. In this study, the ^{1}H NMR spectrums of isolated interruptins A-C (Figures 4.2-4.4) were compared with previously reported information (112) and it was found that all ^{1}H NMR data were almost similar to reference data of interruptins A-C (Tables 4.3-4.5).

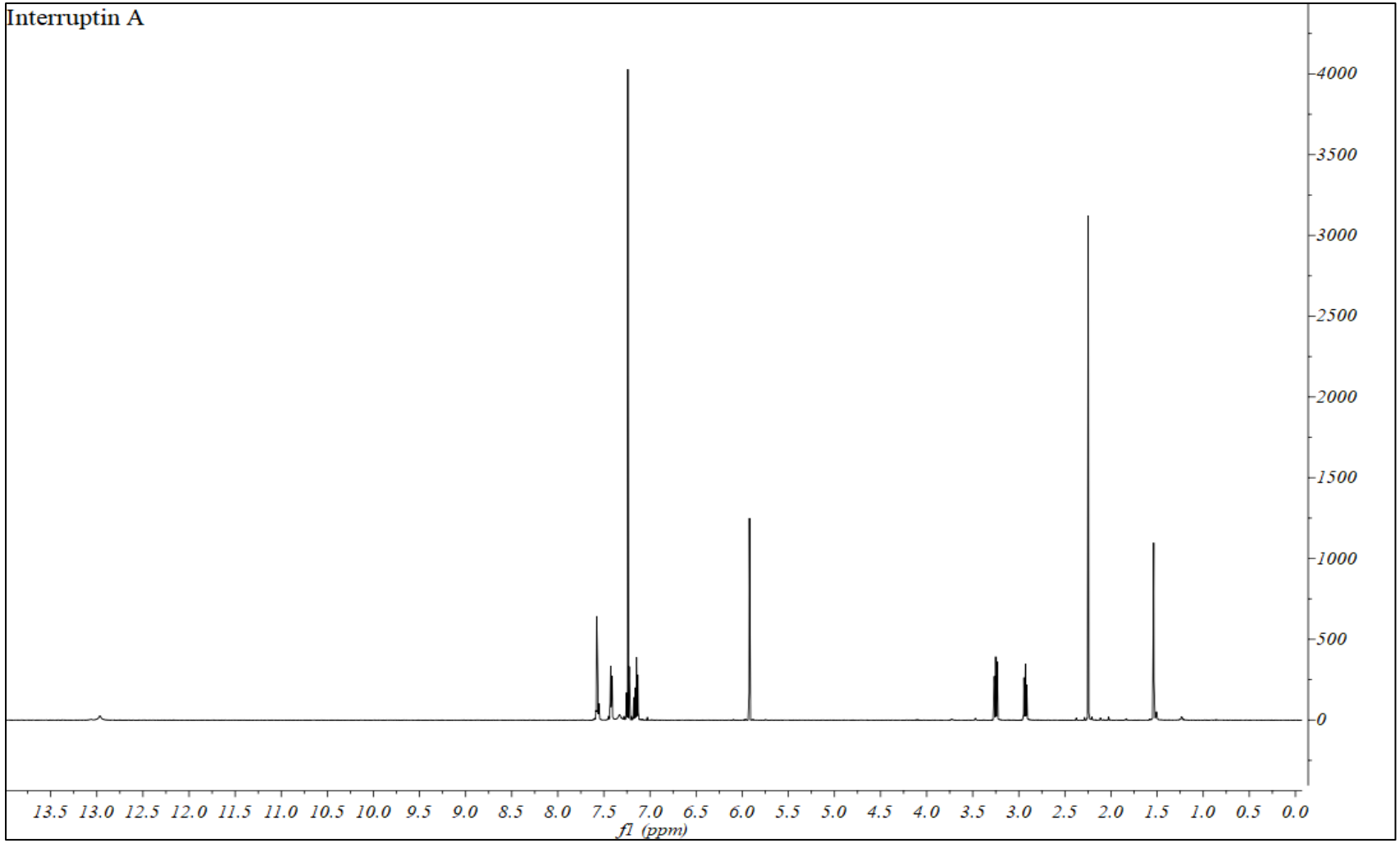

Figure 4.2 H^1 NMR (500 MHz) spectrum of interruptin A.

Table 4.3 H^1 NMR (500 MHz) data of interruptin A in $CDCl_3$.

Positions	δ_H (ppm)**, multiplicity** (coupling constants (Hz))	
	Reference data (112**)**	**This study**
3	5.95 (s)	5.92 (s)
2'	3.29 (t, 7.6)	3.26 (t, 7.0)
3'a	2.96 (t, 7.6)	2.93 (t, 8.5)
3'b	2.96 (t, 7.6)	2.93 (t, 8.5)
5'	7.16-7.29 (m)	7.13-7.25 (m)
6'	7.16-7.29 (m)	7.13-7.25 (m)
7'	7.53-7.61 (m)	7.54-7.58(m)
8'	7.16-7.29 (m)	7.13-7.25 (m)
9'	7.16-7.29 (m)	7.13-7.25 (m)
2''	7.43-7.47 (m)	7.41-7.43(m)
3''	7.53-7.61 (m)	7.54-7.58 (m)
4''	7.16-7.29 (m)	7.13-7.25 (m)
5''	7.53-7.61 (m)	7.54-7.58 (m)
6''	7.43-7.47 (m)	7.41-7.43 (m)
CH_3	2.28 (s)	2.25 (s)
5-OH	-	7.33 (br, s)
7-OH	12.89 (s)	12.96 (s)

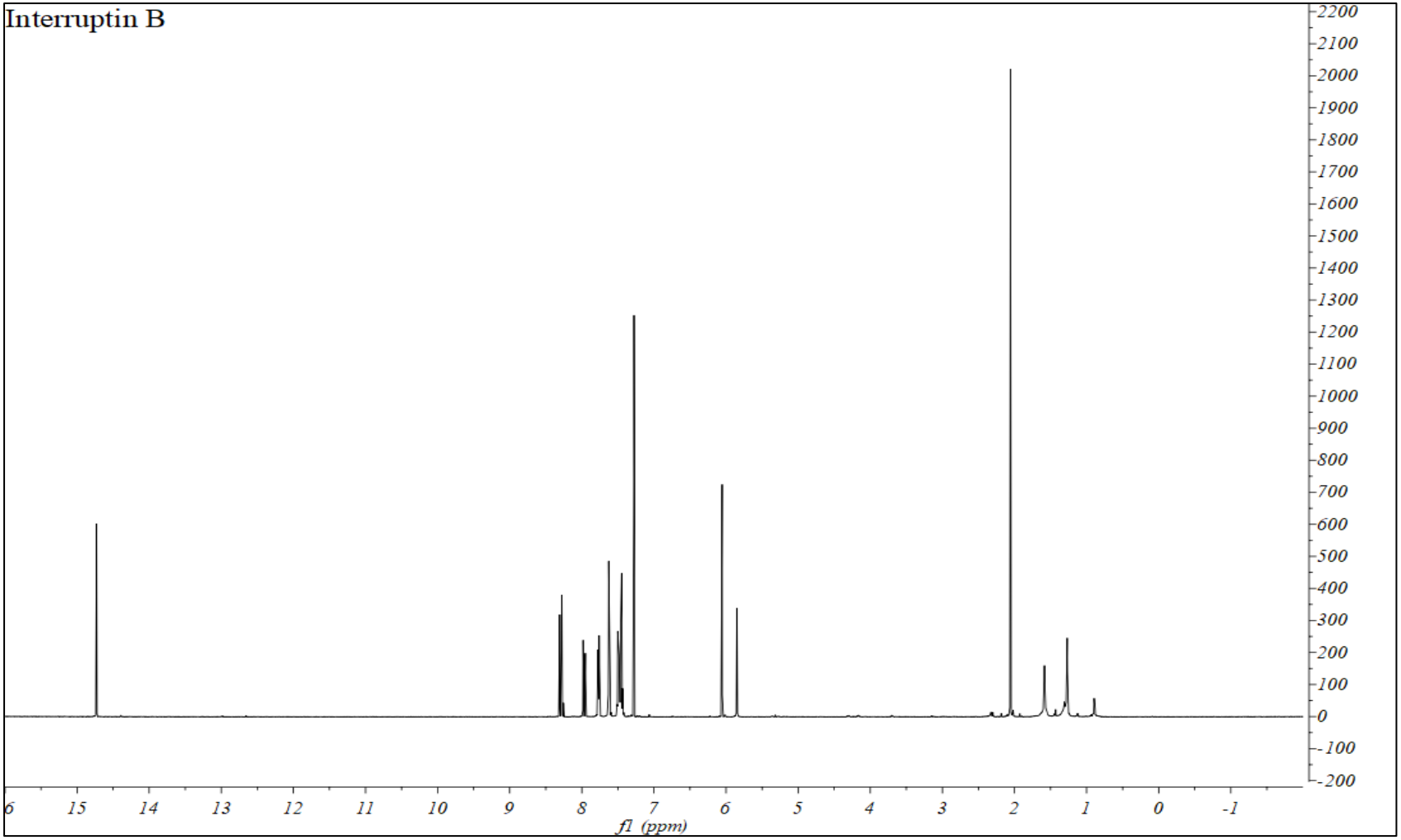

Figure 4.3 H^1 NMR (500 MHz) spectrum of interruptin B.

Table 4.4 H^1 NMR (500 MHz) data of interruptin B in $CDCl_3$.

Positions	δ_H (ppm)**, multiplicity** (coupling constants (Hz))	
	Reference data (112)	**This study**
3	6.04 (s)	6.01 (s)
2'	8.28 (d, 15.5)	8.28 (d, 15.5)
3'	7.95 (d, 15.5)	7.93 (d, 15.0)
5'	7.43-7.50 (m)	7.39 -7.47 (m)
6'	7.74-7.77 (m)	7.72-7.74 (m)
7'	7.43-7.50 (m)	7.39 -7.47 (m)
8'	7.74-7.77 (m)	7.72-7.74 (m)
9'	7.43-7.50 (m)	7.39 -7.47 (m)
2''	7.43-7.50 (m)	7.39 -7.47 (m)
3''	7.59-7.62 (m)	7.57-7.60 (m)
4''	7.43-7.50 (m)	7.39 -7.47 (m)
5''	7.59-7.62 (m)	7.57-7.60 (m)
6''	7.43-7.50 (m)	7.39 -7.47 (m)
CH_3	2.05 (s)	2.02 (s)
5-OH	5.84 (s)	5.81 (s)
7-OH	14.72 (s)	14.69 (s)

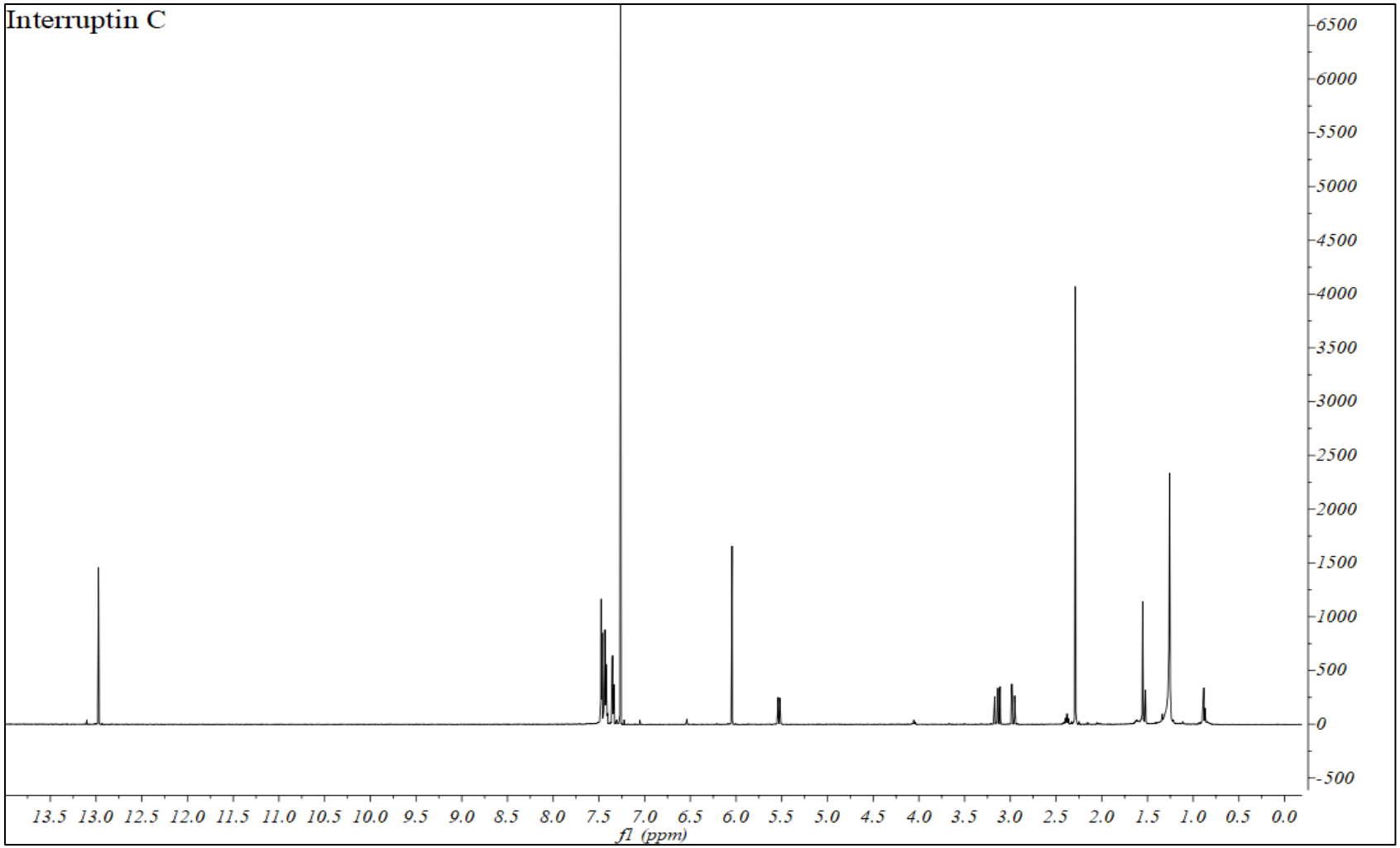

Figure 4.4 H^1 NMR (500 MHz) spectrum of interruptin C.

Table 4.5 H^1 NMR (500 MHz) data of interruptin C in $CDCl_3$.

Positions	δ_H (ppm)**, multiplicity** (coupling constants (Hz))	
	Reference data* (112)	**This study**
3	5.91 (s)	6.01 (s)
2'	5.31 (dd, 3.8; 8.7)	5.50 (dd, 1.5; 6.2)
3'a	3.18 (dd, 3.8; 13.8)	3.11 (dd, 12.4; 17.3)
3'a	2.77 dd, 8.7; 13.8)	2.94, (dd, 3.4; 17.3)
5'	7.24-7.26 (m)	7.38-7.43 (m)
6'	7.07-7.09 (m)	7.31-7.32 (m)
7'	7.24-7.26 (m)	7.38-7.43 (m)
8'	7.07-7.09 (m)	7.31-7.32 (m)
9'	7.24-7.26 (m)	7.38-7.43 (m)
1"		
2"	7.39-7.48 (m)	7.44-7.45(m)
3"	7.28-7.36 (m)	7.44-7.45(m)
4"	7.18-7.23 (m)	7.38-7.43 (m)
5"	7.28-7.36 (m)	7.44-7.45(m)
6"	7.39-7.48 (m)	7.44-7.45(m)
CH_3	2.27 (s)	2.26 (s)
5-OH	-	-
7-OH	-	-
2'-OH	-	12.96 (s)

*H^1 NMR data of interruptin C in CD_3OD.

Although the H^1 NMR data revealed that the isolated substances are interruptins A-C, the confirmation of the exact structure was still important. Thus, the identity of isolated substances should be confirmed with additional technique, moreover, their purity should also be assessed prior to further studies. HPLC method was widely used to analyze substances in terms of identity and purity. Normally, the same substance shows similar characteristic such as retention time (Rt) and UV absorption pattern in the same HPLC condition (17,147-149). Likewise, pure compounds usually display only one peak on the HPLC chromatogram. In this study, isolated interruptins were characterized their structures and analyzed their purity by using a validated HPLC method (see in section 4.9). HPLC chromatograms exhibited that each interruptin shared similar characters to standard interruptins A, B and C (Figure 4.5). The retention time of interruptins A, B and C were 17, 20 and 13 min, respectively. Furthermore, UV absorption patterns of each purified coumarin compound were identical to their standards. Therefore, the results of H^1 NMR and HPLC analysis confirmed that the isolated compounds were interruptins A, B and C. Based on HPLC analysis, they also demonstrated high purity of 99.6 ± 0.1%, 97.7 ± 0.7% and 96.2 ± 0.6% purity, respectively.

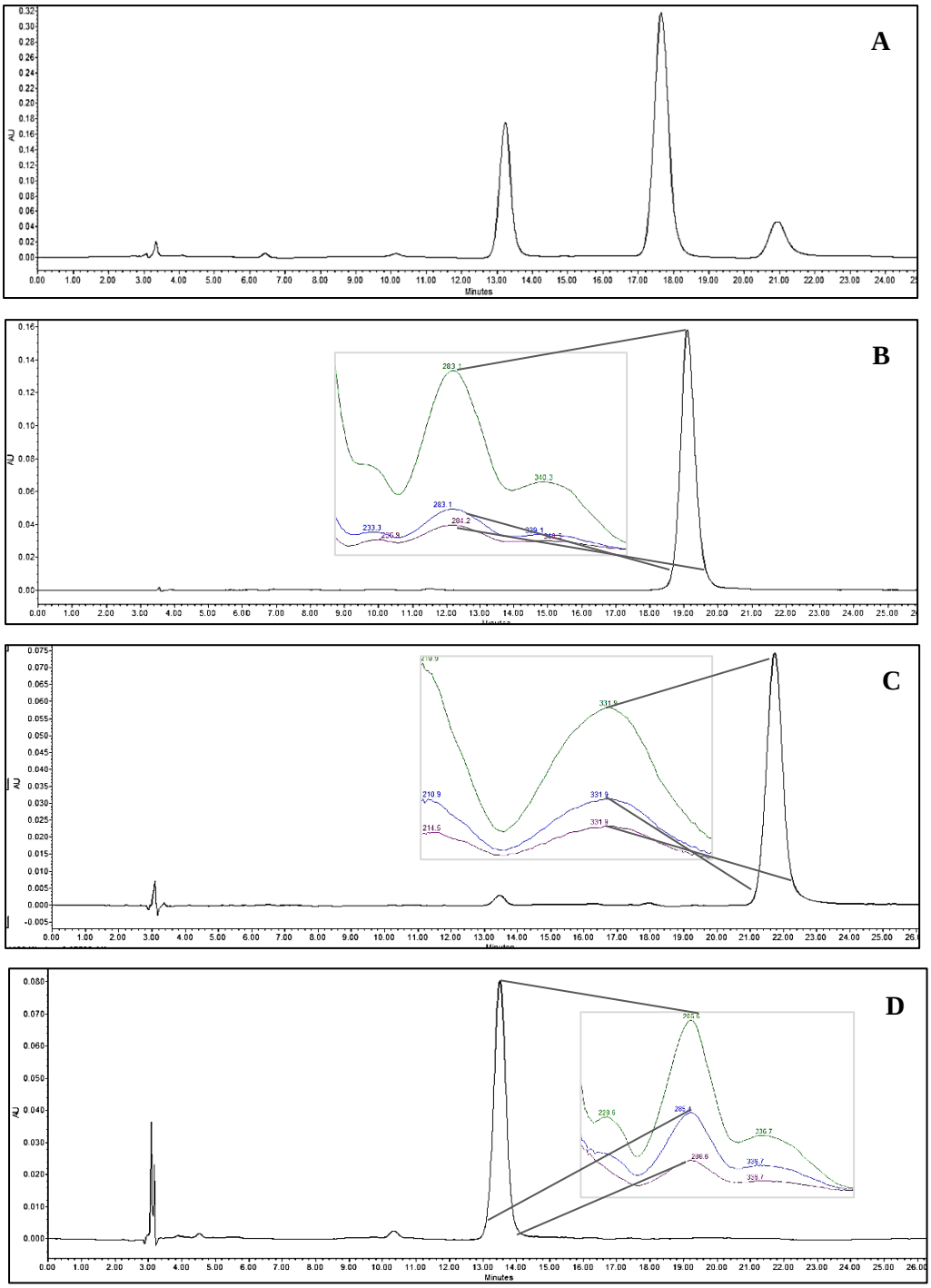

Figure 4.5 The HPLC chromatograms of standard interruptins A-C (A) and isolated interruptins A (B), B (C), C (D). The smaller pictures in each chromatogram represent UV absorption patterns of each interruptin measured at 3 points of the peak.

4.3 Effect of interruptins on cell viability of human skin cells

Nowadays, the efficacy regarding the biological activity of natural isolated compounds is widely interested. However, their safety is still noteworthy concerned before each experiment. MTT assay is one of popular methods for assessing the viability of cells in response to chemical tested compounds. In general, viable cells catalyze yellow tetrazolium salts to purple formazan crystals by the action of mitochondrial reductase enzyme. The intense purple color is directly proportionate to a number of survival cells. The faded purple color is obtained if test substances are toxic to cells. Since this study aimed to evaluate the effect of interruptins A-C on skin cells, their safeties were examined on skin cells, HDF and HEK, by MTT assay. Non-treated cells were counted as 100% of cell viability. The percentages of skin cell viability of interruptins A-C are shown in Tables 4.6 and 4.7. According to ISO 10993-5, the non-cytotoxic agent should demonstrate above 80% of cell viability. Compounds that provide within 80-60%, 60-40% and below 40% of cell viability are considered as weak, moderate and strong cytotoxic substances, respectively (150,151).

In HDF cells, no cytotoxic was observed for all isolated interruptins at all tested concentrations with % cell viability ranges of 95.72-101.49%. Thus, interruptins A-C were innoxious to HDF cells. Additionally, interruptins A and C at all tested concentrations similarly exhibited no toxic to HEK cells with 82.54-106.63% cell viability, whereas interruptin B at high concentrations of 10 and 20 μM decreased cell viability to 42.79-67.80%. From this effect, interruptin B at concentrations of 10-20 μM was considered to modulate cytotoxic to HEK cells. While ascorbic acid was non-toxic to both skin cells with 93.75-107.04% cell viability. These results were similar to the effect of interruptins A-C on macrophage RAW264.7 that almost tested dosages of interruptins were non-toxic, except interruptins A and B at 20 μM demonstrated weak toxicity (section 4.6.2). As a result, cytotoxicity of interruptins A and B was slightly observed at high tested concentration, however, this seemed to depend on cell type. Due to the toxicity of interruptin B to HEK, using this compound at high dosage should therefore be concerned. Although interruptin B revealed minor cytotoxic to HEK cells, the potential effect on intracellular ROS scavenging of this

compound (section 4.4.3) indicted the benefit on antioxidation. Thus, both interruptins A and B were subjected to study on other aspects of antioxidation.

Table 4.6 Effect of interruptins A-C on HDF cell viability.

Concentration	**% Cell viability**			
(µM)	**Interruptin A**	**Interruptin B**	**Interruptin C**	**Ascorbic acid**
Control	100.00±0.58	100.00±0.58	100.00±0.48	100.00±0.48
1	98.14±0.65	97.11±2.50	98.60±1.57	97.90±1.54
5	99.53±0.70	99.44±1.40	99.56±0.30	101.14±0.61
10	99.16±0.74	101.12±1.56	96.56±0.66	101.49±1.82
20	99.35±1.41	95.72±2.99	96.94±0.99	102.80±0.79

Values are expressed as mean ± SD (n=3). No toxicity was observed.

Table 4.7 Effect of interruptins A-C on HEK cell viability.

Concentration	**% Cell viability**			
(µM)	**Interruptin A**	**Interruptin B**	**Interruptin C**	**Ascorbic acid**
Control	100.00±3.09	100.00±3.09	100.00±1.54	100.00±1.54
1	91.02±4.36	98.76±3.81	106.63±2.09	101.45±0.99
5	92.70±3.93	87.78±1.54	103.17±2.02	107.04±1.48
10	103.27±4.65	67.80±3.46*	101.13±3.12	106.63±1.49
20	82.54±1.58	42.79±0.37*	98.90±1.76	93.75±0.70

Values are expressed as mean ± SD (n=3). * defined toxicity of compounds.

4.4 Antioxidative property of interruptins

4.4.1 DPPH free radical scavenging activity

DPPH is an agent that carried proton free radical in the molecule. The proton radical scavenging activity was known to be one of the various actions for antioxidation. In the reaction mixture, the purple color of DPPH will be fade when it was counteracted with antioxidant (152,153). Substances that can eliminate DPPH radical are considered as proton radical scavengers (154,155). The antioxidation of interruptins A-C was performed by DPPH free radical scavenging assay and result is shown in Table 4.8. Interruptin A exerted an obvious highest activity with an IC_{50} value of 21.79 μM, while the others exhibited mild efficacy. Although the antioxidant capacity of all tested substances was ascended with the increase of concentrations (5-30 μM), their activity was 3.3 times lower than the standard antioxidant ascorbic acid (IC_{50} = 8.52 μM). It has been reported that compounds with IC_{50} < 10 μg/mL determined by DPPH radical scavenging was considered to have high or significant antioxidant capacity, while compounds with 10 < IC_{50} < 20 μg/mL and IC_{50} > 20 μg/mL were classified as moderate and low antioxidant capacities, respectively (156). This finding revealed that interruptin A that exhibited IC_{50} of 21.79 μM (equal to 8.75 μg/mL) carries high antioxidant capacity by means of DPPH scavenging assay. Additionally, its antioxidant ability might be due to the hydrogen-donating capability (154,155,157).

Table 4.8 The DPPH radical scavenging activity of interruptins A-C.

Compounds	**IC_{50}** (μM)
Interruptin A	21.79
Interruptin B	> 30
Interruptin C	> 30
Ascorbic acid	8.52

4.4.2 Ferric reduction antioxidant power (FRAP)

FRAP test is based on the redox reaction of electron transfer which indicates the reducing capacity of antioxidant substances (138,152). The antioxidant power of isolated interruptins was also expanded by FRAP assay. Ascorbic acid was used to construct the linear regression of OD 593 nm against the concentration (mmol/L) in order to evaluate reducing efficacies of interruptins A-C (Figure 4.6). A higher ascorbic equivalent value indicates greater reducing power ability. Consistent with DPPH scavenging activity, interruptin A exhibited an emphatic reducing efficiency among tested samples on the reduction of ferric (Fe^{3+}) to ferrous (Fe^{2+}) with an antioxidant value of 682.45±16.31 mmol/L ascorbic acid/mol interruptin A, while the activities of interruptins B and C were 4.3-5.2 times lower than interruptin A (Table 4.9). The antioxidative property of substances have been attributed to various actions, for examples, interception of chain initiation, disintegration of peroxides, protection of extended hydrogen abstraction, reductive reactivity, radical eradication, and binding of transition metal ion catalysts (158). According to the reducing efficacy of interruptins, this action may serve as an important indicator of their antioxidative potential. The results indicated that interruptin A was the best electron transferring compound among tested substances by reacted with Fe^{3+} to convert them into Fe^{2+}.

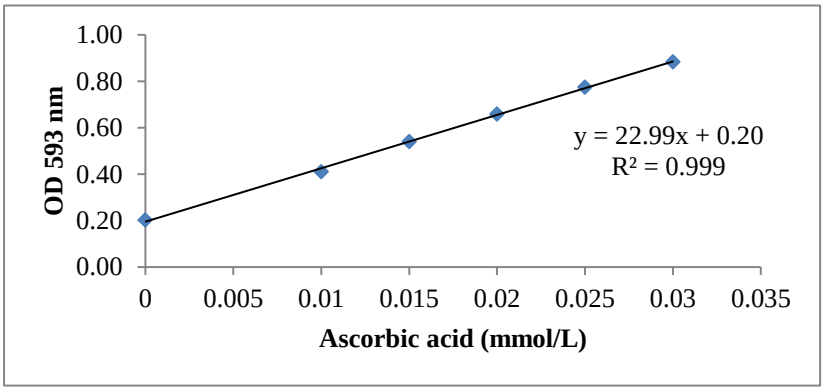

Figure 4.6 Calibration curve of ascorbic acid for determination of ferric reducing antioxidant power.

Table 4.9 The ferric reducing antioxidant power of interruptins A-C.

Compounds	**Ascorbic acid equivalent** (mmol/L ascorbic acid/mol interruptin)
Interruptin A	682.45±16.31
Interruptin B	130.42±12.77
Interruptin C	158.11±16.67

Values are expressed as mean ± SD (n=3).

4.4.3 Intracellular ROS scavenging activity

Although ROS play important roles within the cells by acting as a secondary messenger in cellular signal transduction and microbial killing weapon of immune cells, overproduction of ROS can lead to cellular oxidative stress. Thus, an encounter with excess ROS is essential to protect cells from oxidative damage. The intracellular ROS scavenging efficacy of interruptins in human skin cells is shown as % fluorescence intensity compared with the control vehicle treatment (Figures 4.7 and 4.8). On the basis of ROS detection in the cell using DCF-DA, the fluorescence signal is directly proportionate to the ROS level. Interruptins A and B demonstrated potent ROS scavenging effects on HDF by dramatically reduced fluorescence signal that was counted for 37.76-56.24% and 42.77-76.98% ROS scavenging, respectively, compared with the control, whereas interruptin C had no activity (Table 4.10). Interestingly, interruptins A and B of all tested concentrations established more effective ROS scavenging than 20 μM ascorbic acid standard. The result suggests that interruptins A and B could pass through the cell membrane and act as ROS scavengers in the polar intracellular environment. In contrast, although, interruptin C carries a hydroxy group in the propionyl chain on its structure that should exhibit scavenging activity, this substitution makes higher polarity of interruptin C and might disturb cell membrane penetration. However, intracellular ROS scavenging efficacy of interruptins A and B in another skin cell, HEK, demonstrated minor effect, only at high tested concentrations (Table 4.11). This may be due to keratin produced by HEK that is a barrier to protect

the entry of external compounds (159,160). Since keratinocytes stay in epidermis that is the outer skin layer, the absorption of interruptins through epidermis may be limited.

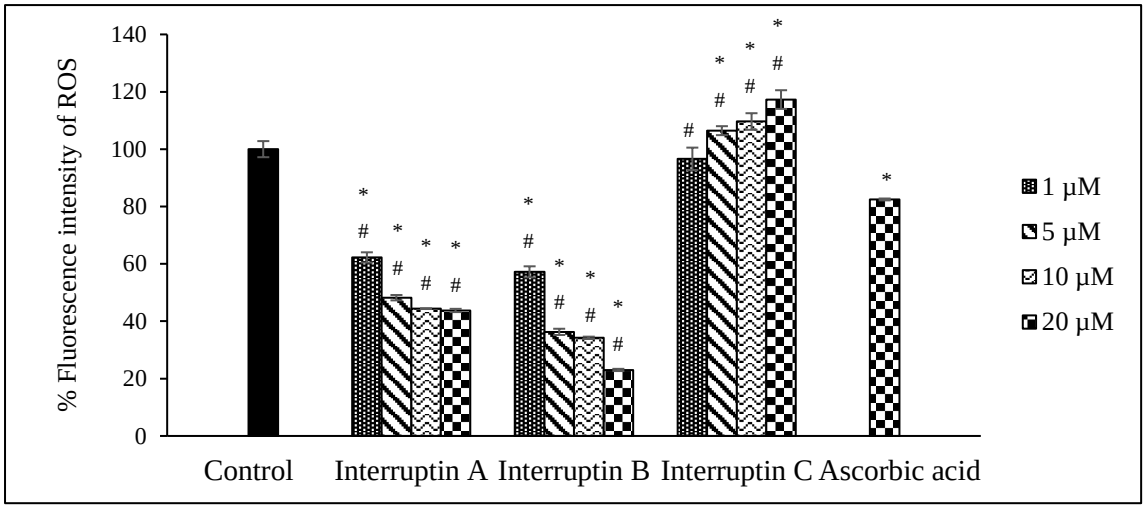

Figure 4.7 Percentage of fluorescence intensity of ROS in interruptins A-C-treated HDF determined by DCF-DA using flow cytometry. Values are expressed as mean ± SD (n=3). *, $^{\#}P < 0.01$ compared to the control (0 µM) and ascorbic acid, respectively.

Table 4.10 Percentage of ROS scavenging of interruptins A-C in HDF cells.

Concentration	**% ROS scavenging**			
(µM)	**Interruptin A**	**Interruptin B**	**Interruptin C**	**Ascorbic acid**
Control	0.00±2.80	0.00±2.80	0.00±2.80	0.00±2.80
1	37.76±1.78$^{*,\#}$	42.77±1.92$^{*,\#}$	3.38±3.92$^{\#}$	
5	51.79±0.94$^{*,\#}$	63.71±1.09$^{*,\#}$	-6.45±1.57$^{*,\#}$	
10	55.62±0.12$^{*,\#}$	65.79±0.41$^{*,\#}$	-9.64±2.89$^{*,\#}$	
20	56.24±0.56$^{*,\#}$	76.98±0.38$^{*,\#}$	-17.29±3.25$^{*,\#}$	17.53±0.33*

Values are expressed as mean ± SD (n=3). *, $^{\#}P < 0.01$ compared to the control (0 µM) and ascorbic acid, respectively.

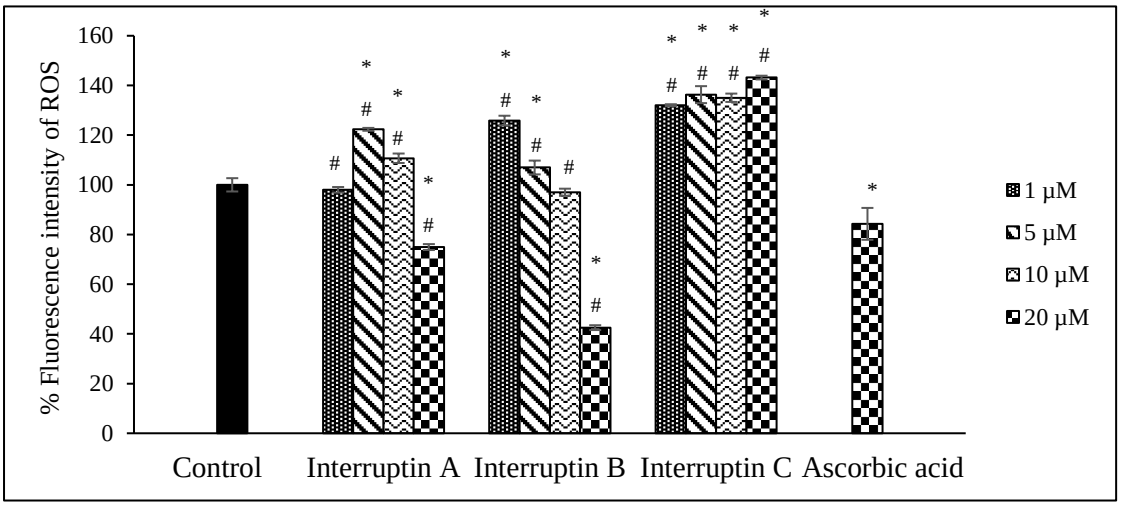

Figure 4.8 Percentage of fluorescence intensity of ROS in interruptins A-C-treated HEK determined by DCF-DA using flow cytometry. Values are expressed as mean ± SD (n=3). *, $^{\#}P < 0.01$ compared to the control (0 µM) and ascorbic acid, respectively.

Table 4.11 Percentage of ROS scavenging of interruptins in HEK cells.

Concentration (µM)	**% ROS scavenging**			
	Interruptin A	**Interruptin B**	**Interruptin C**	**Ascorbic acid**
Control	0.00±2.67	0.00±2.67	0.00±2.67	0.00±2.67
1	2.01±1.11$^{\#}$	-25.86±1.95$^{*,\#}$	-32.05±0.38$^{*,\#}$	
5	-22.34±0.58$^{*,\#}$	-6.98±2.78$^{*,\#}$	-36.3±3.41$^{*,\#}$	
10	-10.7±1.90$^{*,\#}$	2.99±1.44$^{\#}$	-35.04±1.67$^{*,\#}$	
20	25.06±1.20$^{*,\#}$	57.48±0.98$^{*,\#}$	-43.18±0.75$^{*,\#}$	15.71±6.42*

Values are expressed as mean ± SD. (n=3). *, $^{\#}P < 0.01$ compared to the control (0 µM) and ascorbic acid, respectively.

It has been reported that ROS suppression capacity of coumarins involved in the number of hydroxy (OH) functional groups on benzene ring of α-pyrone structure (113). Coumarinoids that carried two OH groups were more preferable to scavenge free radical than single OH group. The oxidative suppression capacity owing to their tapping abilities of unpaired electron via hydrogen atom donating action. Furthermore, the position of two OH substitutions on benzene ring of coumarin nucleus also affected the antioxidant ability. The *ortho*-OH substitution exhibited stronger antioxidation than *meta*-OH system. The great reactivity of *ortho*-dihydroxy phenolic structure maybe toward the smaller dissociation energy of O-H bond (113,115,161). Although interruptins A-C shared similar structure and carried *meta*-dihydroxy system on benzene ring of benzo α-pyrone structure, the obtained results of DPPH radical scavenging and FRAP assays revealed that only interruptin A exerted distinct antioxidant activities. This could possibly relate to the presence of a single bond at C2 carbon on proprionyl chain of interruptin A. However, these results were not exactly consistent with intracellular ROS scavenging activity that interruptin B was the most potent ROS scavenger followed by interruptin A. This might cause by the difference of experimental tested systems. The DPPH and FRAP assays were colorimetric reactions performed in organic MeOH and acidic solution, respectively, while intracellular ROS scavenging by DCF-DA evaluated inside the cells. It has been suggested that overall antioxidant potential of interesting substances should be determined in a variety of assays because the antioxidative efficacy relies on the physical and chemical characteristics of the evaluation system (162,163). In this study, interruptins A and B could act as powerful ROS scavengers within the cells which was more mimic to the human body than in the test tube. As a result, due to the strong intracellular antioxidant activity of interruptins A and B, these two compounds were selected to further evaluate their effect on gene and protein expression of antioxidant enzymes.

4.4.4 Gene expression of antioxidant enzymes

Antioxidant enzymes are the primary defense mechanism of the cells to counteract oxidative damage. The SOD, CAT, and GPx are major cellular antioxidant enzymes which prevent the formation of oxidant as well as eliminate formed radical (65, 164). Thus, increase of antioxidant enzyme levels in the cells is important for controlling cellular oxidant. Since interruptins A and B revealed ROS scavenging effect in HDF and HEK, herein, their induction of antioxidant enzyme expression was expanded. The effects of interruptins A and B on gene expression of antioxidant enzymes, including SOD1, SOD2, CAT, and GPx on human skin cells were monitored using real-time PCR. The transcriptional responses were presented in term of relative mRNA expression. The result in HDF cells showed that both interruptins A and B could up-regulate *SOD1*, *SOD2*, and *GPx* gene expression but did not affect to *CAT* gene (Table 4.12 and Figure 4.9). Similarly, interruptins A and B also acted as transcriptional stimulators in HEK cells by dose-dependent enhancing gene expression of all antioxidant enzymes (Table 4.13 and Figure 4.10). According to the levels of antioxidant in skin, epidermis layer contained much greater antioxidant enzyme levels than dermis. This possibly because epidermis is the outermost layer of skin and directly exposes to various environmental oxidative stress stimulators (165,166). Because HEK are the most abundant cell type in epidermis, it was speculated probably more susceptible to interruptins A and B induced transcriptional response. To the best of our knowledge, the present study suggested that interruptins A and B acted as antioxidant agents not only by scavenging intracellular ROS but also up-regulating antioxidant enzyme genes in skin cells.

The gene expression of antioxidant enzymes has been involved in signal transduction of a variety of transcription factors such as nuclear factor-erythroid 2-related factor 2 (Nrf2), nuclear factor-kappa B (NF-κB), CCAAT/Enhancer binding proteins (C/EBPs), specificity protein (Sp1), tumor suppressor p53, as well as peroxisome proliferator-activated receptors (PPAR) (167-174). It has also been reported that interruptins A and B were PPAR ligands by acting as PPAR-α and PPAR-γ agonists (18). The effects of these two coumarin derivatives on antioxidant enzyme gene expression probably involve PPAR signal transduction. However, the additional studies are still needed to clarify the transcriptional response mechanisms underlying antioxidant enzyme induction by interruptins.

Table 4.12 Relative gene expression of antioxidant enzymes in HDF after treated with interruptins A and B for 6 h determined by real-time PCR.

Gene	**Concentration** (μM)	**Relative mRNA expression** (fold change)	
		Interruptin A	**Interruptin B**
SOD1	Control	1.00±0.05	1.00±0.05
	1	2.34±0.17*	2.71±0.13*
	5	2.64±0.06*	3.09±0.09*
	10	2.53±0.15*	3.05±0.13*
SOD2	Control	1.00±0.09	1.00±0.09
	1	1.74±0.28*	1.25±0.17
	5	1.45±0.02*	1.93±0.23*
	10	1.88±0.12*	2.59±0.25*
CAT	Control	1.00±0.04	1.00±0.04
	1	1.01±0.06	1.04±0.03
	5	1.04±0.02	1.24±0.07*
	10	0.98±0.04	1.05±0.07
GPx	Control	1.00±0.03	1.00±0.03
	1	1.02±0.03	1.19±0.03*
	5	1.13±0.07*	1.40±0.09*
	10	1.22±0.03*	1.36±0.04*

Values are expressed as mean ± SD (n=3). *$P < 0.01$ compared to the control (0 μM) of each gene. SOD1, superoxide dismutase 1; SOD2, superoxide dismutase 2; CAT, catalase; GPx, glutathione peroxidase.

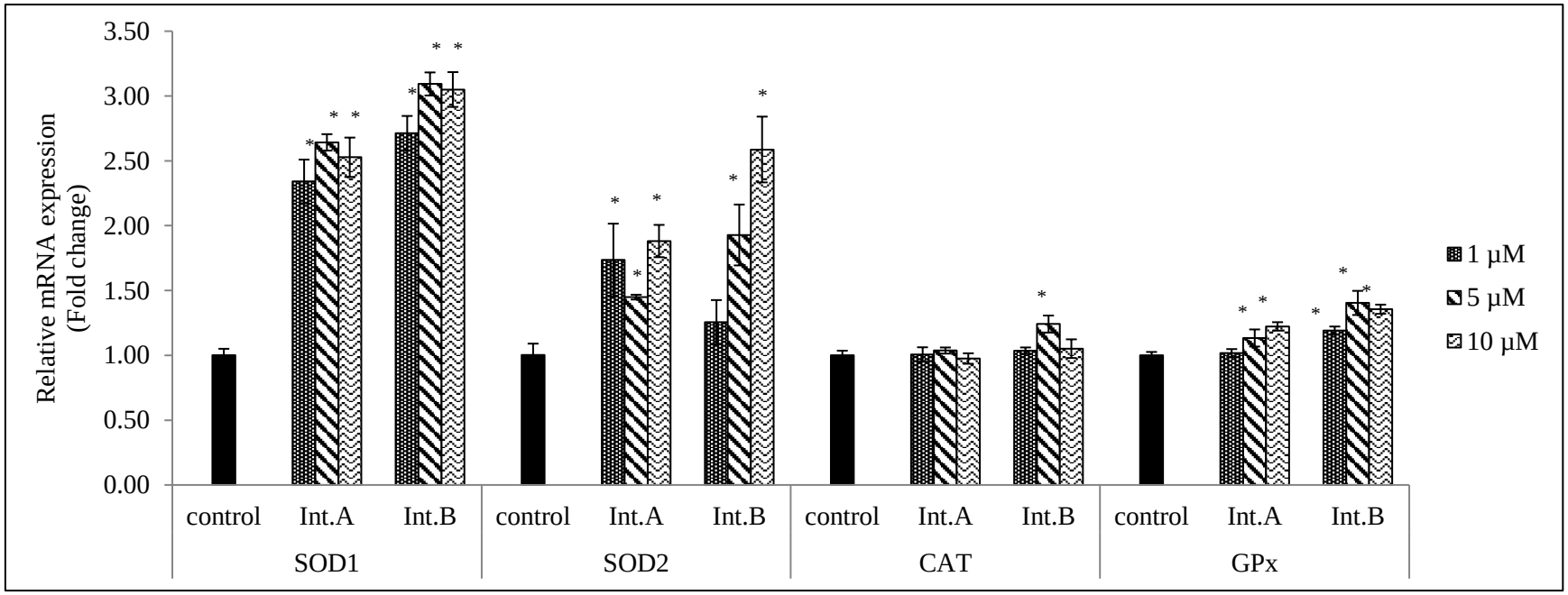

Figure 4.9 Gene expression levels of antioxidant enzymes in HDF after treated with interruptins A and B for 6 h determined by real-time PCR. $^{*}P < 0.01$ compared to the control of each gene. Int.A, interruptin A; Int.B, interruptin B; SOD1, superoxide dismutase 1; SOD2, superoxide dismutase 2; CAT, catalase; GPx, glutathione peroxidase.

Table 4.13 Relative gene expression of antioxidant enzyme in HEK after treated with interruptins A and B for 6h determined by real-time PCR.

Gene	**Concentration** (μM)	**Relative mRNA expression** (fold change)	
		Interruptin A	**Interruptin B**
SOD1	Control	1.00±0.04	1.00±0.04
	1	1.25±0.06*	1.42±0.06*
	5	1.19±0.17	1.77±0.12*
	10	1.21±0.02*	2.36±0.10*
SOD2	Control	1.00±0.05	1.00±0.05
	1	1.26±0.03*	1.39±0.06*
	5	1.27±0.06*	1.82±0.04*
	10	1.55±0.07*	1.83±0.06*
CAT	Control	1.00±0.06	1.00±0.06
	1	1.24±0.14	1.43±0.08*
	5	1.40±0.09*	1.68±0.09*
	10	1.46±0.31*	1.80±0.03*
GPx1	Control	1.00±0.10	1.00±0.10
	1	1.43±0.13*	1.68±0.25*
	5	1.64±0.09*	1.90±0.17*
	10	1.64±0.14*	1.92±0.15*

Values are expressed as mean ± SD (n=3). *$P < 0.01$ compared to the control (0 μM) of each gene. SOD1, superoxide dismutase 1; SOD2, superoxide dismutase 2; CAT, catalase; GPx, glutathione peroxidase.

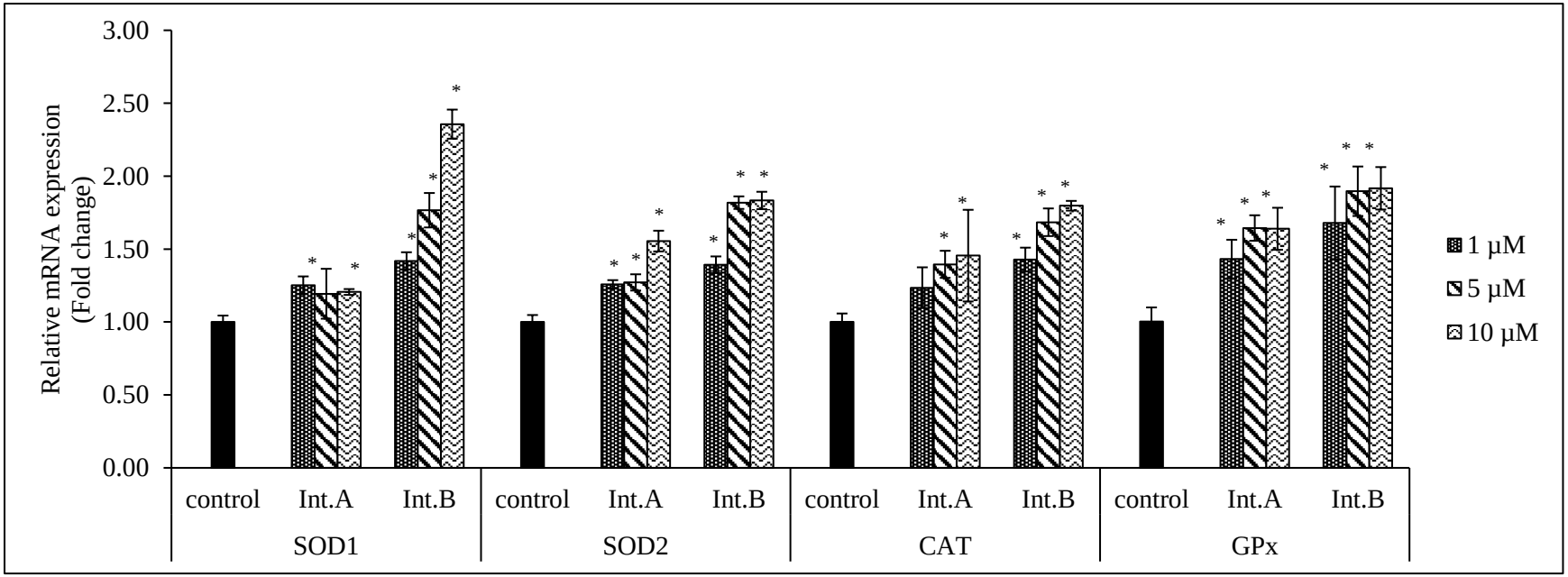

Figure 4.10 Gene expression levels of antioxidant enzymes in HEK after treated with interruptins A and B for 6h determined by real-time PCR. $^{*}P < 0.01$ compared to the control of each gene. Int.A, interruptin A; Int.B, interruptin B; SOD1, superoxide dismutase 1; SOD2, superoxide dismutase 2; CAT, catalase; GPx, glutathione peroxidase.

4.4.5 Protein expression of antioxidant enzymes

According to the gene expression results of antioxidant enzymes, interruptins A and B performed as transcription stimulators of cellular antioxidant enzymes. Subsequently, the translational responses of SOD1, SOD2, CAT and GPx to interruptins A and B in HDF and HEK were evaluated by western blotting. Actin, constitutively expressed structural protein, was used as a protein calibrator. In HDF, the effects of interruptins on antioxidant enzyme proteins are illustrated in Figure 4.11. Interruptins A and B undoubtedly elevated SOD1 and GPx protein level up to 1.78-5.87 folds and 1.50-2.04 folds, respectively, compared to the control and slightly induced SOD2 protein level but did not influence on CAT protein. Furthermore, in HEK, both interruptins A and B obviously upregulated the protein expression of SOD1 (1.24-4.37 folds), SOD2 (1.61-2.4 folds), and GPx (1.10-1.30 folds), while slightly induction of CAT protein level was found (Figure 4.12). The results revealed that interruptins A and B could elevate antioxidant enzyme proteins in HEK better than in HDF. The difference in antioxidant enzyme expression in different cells might cause by the characteristic of each cell. Dermal keratinocytes locate in epidermis that directly faces to various environmental oxidative stress challenges, therefore higher antioxidant levels were speculated (162,166). The obtained results in this study showed that interruptins A and B concurrently induced transcriptional and translational responses of antioxidant enzyme in both of HDF and HEK. Although the mRNA expression of CAT in interruptins-treated HEK was obviously upregulated, the translational response of this enzyme was slightly induced. This might involve in complex phenomena after RNA transcription. In post-transcriptional and post-translational regulatory processes, unidentified factors may stabilize or unstabilize CAT mRNA (172). For instance, binding of unidentified redox-sensitive proteins on 5′ untranslated region (UTR) or 3′ UTR of catalase mRNA expedited its translational rate and enhanced protein translation (175,176) and suppressing of protein 14-3-3, inhibitor of catalase transcription factor, by micro-RNA miR-451 led to enhance of CAT expression. In contrary, binding of 3′ UTR by miR-30b drastically decreased CAT protein. In addition, the CAT protein itself possibly affect its levels and activity. The phosphorylated CAT enzyme is subjected to ubiquitination and degraded by proteasome (177,178). Of the possible reasons, the

inconsistency of CAT mRNA and protein expression in HEK cells might rely on the effect of post-transcriptional and post-translational regulation.

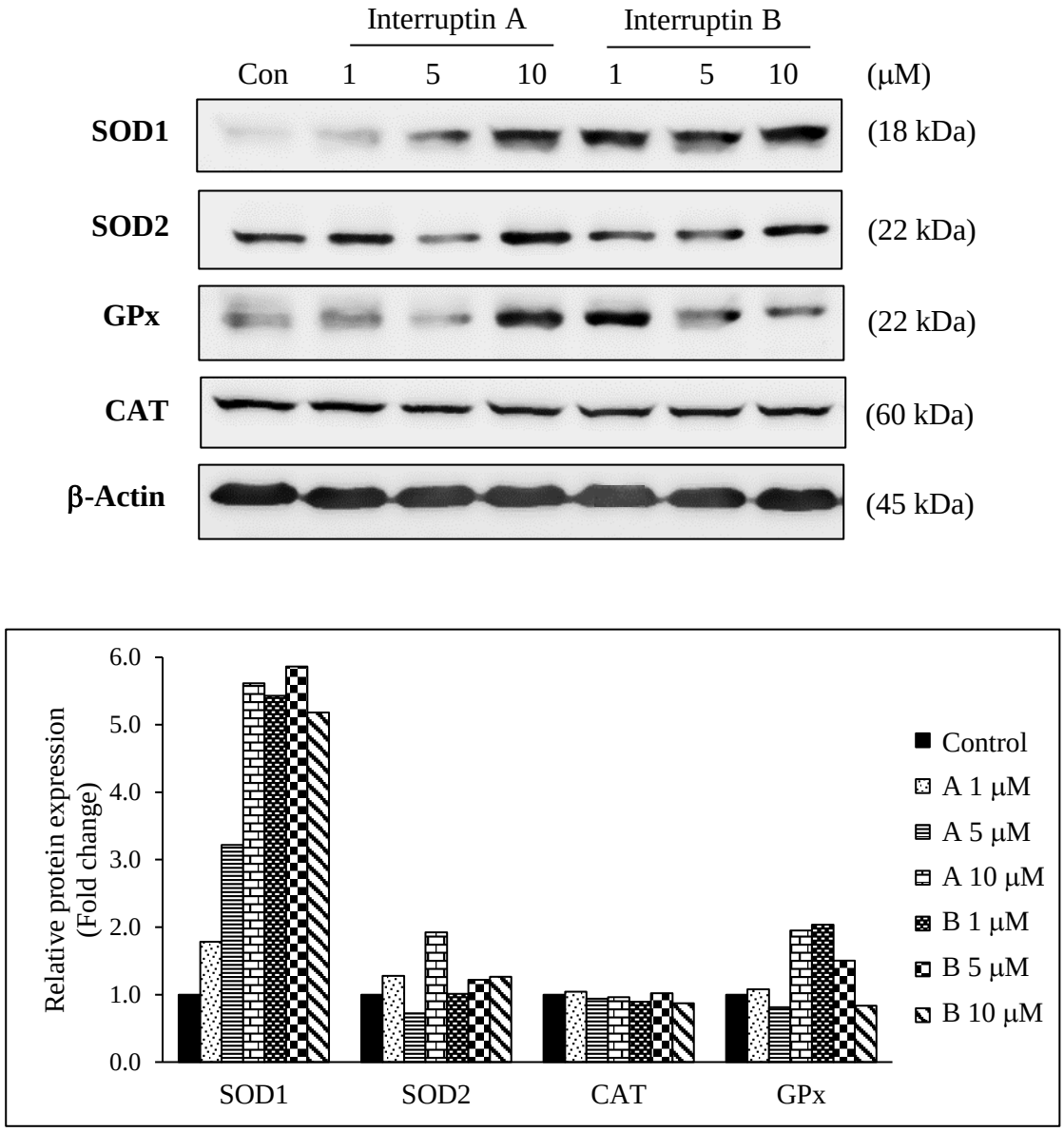

Figure 4.11 Protein expression levels of antioxidant enzymes in HDF after treated with interruptins A and B for 6 h determined by western blotting. Con, control (0 μM); Int.A, interruptin A; Int.B, interruptin B; SOD1, superoxide dismutase 1; SOD2, superoxide dismutase 2; CAT, catalase; GPx, glutathione peroxidase.

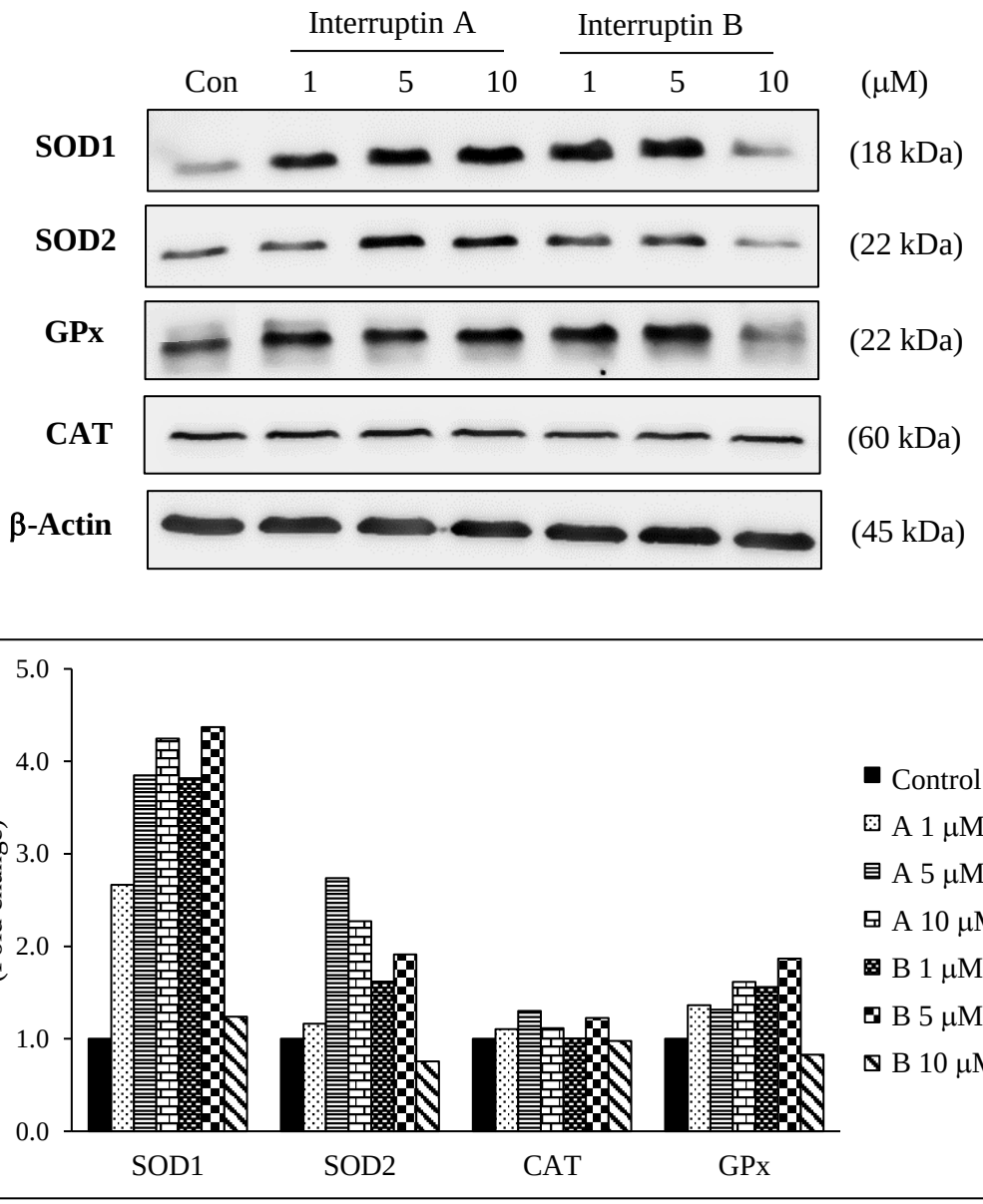

Figure 4.12 Protein expression levels of antioxidant enzymes in HEK after treated with interruptins A and B for 6 h determined by (A) western blotting. Con, control (0 μM); Int.A, interruptin A; Int.B, interruptin B; SOD1, superoxide dismutase 1; SOD2, superoxide dismutase 2; CAT, catalase; GPx, glutathione peroxidase.

4.5 Anti-photooxidative activity of interruptins

ROS in cells could be generated by endogenous and exogenous stimulators. UV radiation is one of exogenous factors that can trigger ROS formation in skin cells. A single dose of UV radiation could induce ROS formation via excitation of photosensitizers such as nucleic acid and amino acid (35). The UV-induced ROS would further damage cellular components and lead to cell death. The anti-photooxidation efficacies of interruptins A and B on human skin cells under UV exposure conditions were evaluated using DCF-DA probe. The antioxidants neutralize UV-induced ROS, leading to reduce fluorescence signal (Figures 4.14 and 4.15). In HDF cells, interruptin A and B could suppress UVA-induced ROS formation in the cells with % ROS scavenging ranging from 20.72-53.74% and 44.80-79.26%, respectively. In case of UVB exposure, these two compounds also acted as effective ROS quenchers with % ROS scavenging of 10.29-56.89% and 52.73-81.52%, respectively (Table 4.14). Moreover, interruptins A and B exhibited potent anti-photooxidative effect in HEK cells by scavenging intracellular ROS under UVA radiation that counted for 37.65-62.47% and 40.37-78.40% ROS scavenging, respectively. Likewise, these coumarin derivatives eliminated UVB-generated ROS in HEK with 16.66-50.40% and 12.39-68.90 % ROS scavenging, respectively (Table 4.15). The ROS suppression activity of interruptins A and B in both cells were dose-dependent manner. As a result, intracellular ROS scavenging capacity of interruptins A and B in HEK under UV radiation was better than scavenging efficacy without ROS stimulator, this may cause by UV radiation effect that help pore forming on the cell membrane (179,180) which enhance penetration of interruptins A and B into the cells.

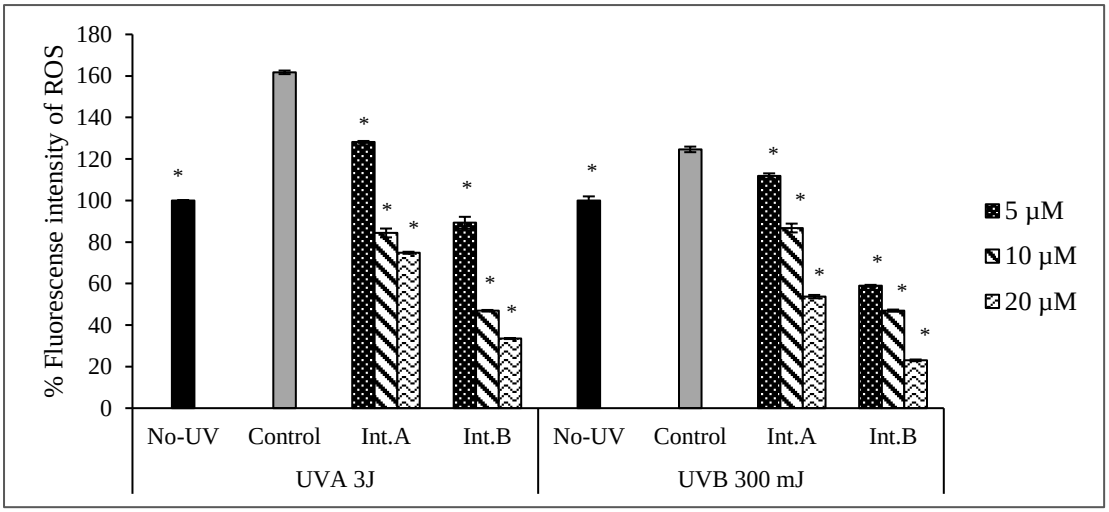

Figure 4.13 Percentage of fluorescence intensity of UV-stimulated ROS in interruptins A and B-treated HDF determined by DCF-DA using flow cytometry. $^{*}P < 0.01$ compared to the control (0 µM). Int.A, interruptin A; Int.B, interruptin B.

Table 4.14 Percentage of UV-stimulated ROS scavenging of interruptins A-C in HDF cells.

Concentration	**% ROS scavenging**	
(µM)	**Interruptin A**	**Interruptin B**
No-UVA	0.00±0.25*	0.00±0.25*
UVA 3J		
Control	-61.74±0.86	-61.74±0.86
5	20.72±0.28*	44.80±1.77*
10	47.83±1.32*	71.00±0.24*
20	53.74±0.30*	79.26±0.16*
No-UVB	0.00±1.99*	0.00±1.99*
UVB 300 mJ		
Control	-24.62±1.34	-24.62±1.34
5	10.29±1.03*	52.73±0.42*
10	30.39±1.70*	62.31±0.34*
20	56.89±0.65*	81.52±0.34*

Values are expressed as mean ± SD (n=3). * $P < 0.01$ compared to the control (0 µM).

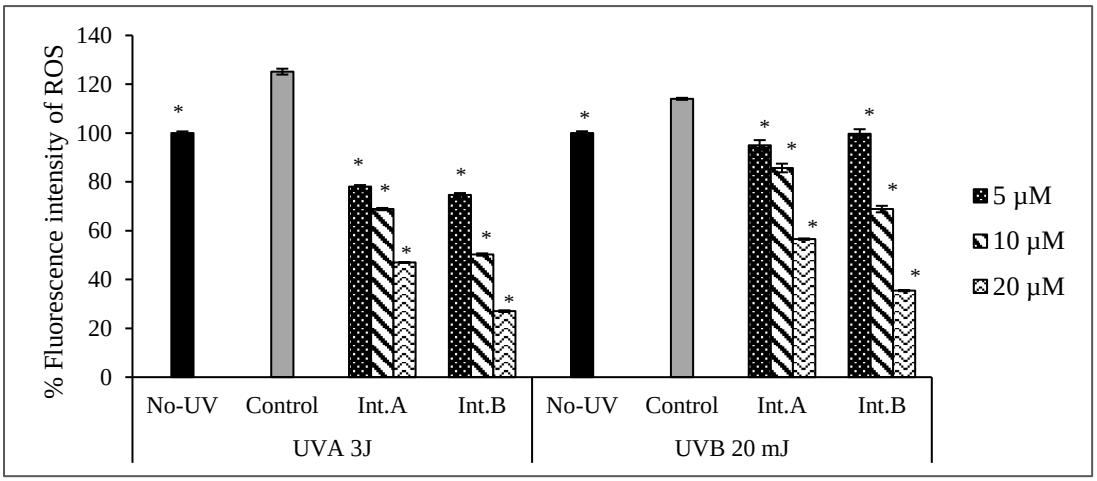

Figure 4.14 Percentage of fluorescence intensity of UV-stimulated ROS in interruptins A and B-treated HEK determined by DCF-DA using flow cytometry. $^{*}P < 0.01$ compared to the control (0 µM). Int.A, interruptin A; Int.B, interruptin B.

Table 4.15 Percentage of UV-stimulated ROS scavenging of interruptins A-C in HEK cells.

Concentration	**% ROS scavenging**	
(µM)	**Interruptin A**	**Interruptin B**
No-UVA	0.00±0.67*	0.00±0.67*
UVA 3 J		
Control	-25.16±1.21	-25.16±1.21
5	37.65±0.51*	40.37±0.62*
10	44.99±0.37*	59.87±0.38*
20	62.47±0.09*	78.40±0.28*
No-UVB	0.00±0.73*	0.00±0.73*
UVB 20 mJ		
Control	-14.01±0.41	-14.02±0.41
5	16.66±1.83*	12.39±1.68*
10	24.84±1.56*	39.61±1.17*
20	50.40±0.25*	68.90±0.57*

Values are expressed as mean ± SD (n=3). * $P < 0.01$ compared to the control (0 µM)

4.6 Anti-inflammatory property of interruptins

4.6.1 Nitric oxide scavenging activity of interruptins

The excessive level of NO is implicated as inflammation, suppression of NO formation is therefore one of methods for inflammation treatment (95,99). The NO radical scavenging ability of interruptins A, B and C were tested by monitoring nitrite ion formation from the reaction of NO and oxygen. NO scavengers compete with oxygen to interact with NO and lead to a reduction of nitrite formation. The NO scavenging ability of interruptins A-C is shown in Table 4.16. Among tested compounds, interruptin B showed the best capacity to directly scavenge NO with an IC_{50} value of 67.68 μM followed by interruptin A with an IC_{50} value of 90.07 μM, while interruptin C was not active within the tested concentrations. The NO quenching ability of interruptins A and B was concentration-dependent manner. Interestingly, the NO scavenging ability of interruptins A and B was 1.2-1.6 folds more effective than gallic acid standard (IC_{50} = 107.92 μM). Indeed, NO is one of oxidants, substances with antioxidative property may exhibit NO controlling. Previous studies had reported that antioxidative coumarins that possessed NO scavenging might attribute to the electron donating character of the substitution group like -Cl, $-CH_3$, and -OH on benzopyrone scaffold (181). Since interruptins A-C contain OH and CH_3 functional groups on the coumarin nucleus, their NO scavenging activity might be due to these substitutions. Additionally, regarding the similarity of structure of interruptins, interruptins A and B that carry single bond and double bond on the C2-C3 of propionyl chain, respectively, presented effective NO scavenging capacity, while interruptin C that presents OH at the same carbon position of the structure possessed no activity on NO scavenging. Therefore, the presence of single bond or double bond on the C2-C3 of propionyl substitution was necessarily for NO scavenging capacity of interruptins.

Table 4.16 NO radical scavenging activity of interruptins A-C.

Compounds	**IC_{50}** (μM)
Interruptin A	90.07
Interruptin B	67.68
Interruptin C	> 100
Gallic acid	107.76

4.6.2 Nitric oxide production inhibitory activity of interruptins

The stimulation of LPS on receptors of macrophage cells leads to the production of pro-inflammatory mediators such as NO and PGE_2. Overproduction of NO can cause oxidative stress and potentiate the higher severity level of inflammation (98-100). As the previous experimental result indicated anti-inflammatory potential of interruptins A and B by suppression of NO radical. Herein, the anti-inflammatory property of interruptins was expanded by assessing their NO production inhibitory efficacy in LPS-induced macrophage cells. The NO production inhibition activity of all tested interruptins was concentration-dependent manner. Among tested compounds, interruptin B exhibited the most potent inhibitory activity with IC_{50} values of 0.81 μM which was 16.3-folds more effective than standard indomethacin (IC_{50} = 13.23 μM). While interruptin A (IC_{50} = 12.18 μM) revealed comparable NO inhibition effect to indomethacin. On the other hand, interruptin C did not show the inhibitory activity against NO production in LPS-stimulated macrophages (Table 4.17). More interestingly, interruptin B demonstrated 15.03 folds higher ability on inhibition of NO production in murine macrophage than interruptin A. This implied that the presence of the olefinic character of C2-C3 of propionyl substitution seems to be more important for NO inhibitory activity of interruptins.

Of note, all tested concentrations of tested samples as well as indomethacin did not toxic to RAW 264.7 cells (Table 4.18), except only interruptin B at 20 μM demonstrated weak cytotoxic to the cells by giving 75.68% cell viability (compounds providing cell viability not less than 80% are considered as innoxious substances (150,151). Therefore, it was clearly that interruptins A and B could be applied as potent innoxious anti-inflammatory agents.

Table 4.17 NO production inhibitory activity of interruptins A-C in RAW264.7 cells.

Compounds	**IC_{50}** (μM)
Interruptin A	12.18
Interruptin B	0.81
Interruptin C	> 50
Indomethacin	13.23

Table 4.18 Effect of interruptins A-C on RAW264.7 cell viability.

Concentration	**% Cell viability**			
(μM)	**Interruptin A**	**Interruptin B**	**Interruptin C**	**Indomethacin**
0	100.00±2.36	100.00±2.69	100.00±2.36	100.00±2.36
1	95.22±2.36	93.13±1.13	87.13±0.92	99.58±2.68
5	84.04±4.26	85.14±1.10	92.41±0.61	96.61±2.86
10	86.06±4.52	83.62±1.71	94.50±1.29	96.89±1.89
20	81.77±4.84	75.68±1.65*	94.29±0.41	94.44±3.53

Values are expressed as mean ± SD (n=3). * defined weak cytotoxicity (150,151).

4.6.3 *iNOS, COX2* and *PPAR-γ* gene expression

In the inflammatory response of the organisms, inflammatory enzymes such as COX-2 and iNOS are stimulated in order to produce inflammatory mediators, for example, PGE_2 and NO, respectively (91, 99). In the other hand, the activation of PPAR-γ by its ligand agonists resulted in downregulating the expression of pro-inflammatory genes. Therefore, PPAR-γ agonists have been considered as anti-inflammatory agents In order to determine the anti-inflammatory mechanism of interruptins, the transcriptional responses of iNOS, COX-2, and PPAR-γ were monitored using PCR. As shown in Figures 4.15A and 4.15E, interruptin A moderately suppressed *iNOS* gene expression and strongly induced *PPAR-γ* gene expression. Furthermore, interruptin B dramatically reduced *iNOS* mRNA level and increased *PPAR-γ* mRNA expression in a concentration-dependent character (Figures 4.15B and 4.15F), while interruptin C did not affect any tested genes (Figures 4.15C and 4.15G). The *iNOS* gene suppression capacity of interruptin B was greater than the reference drug indomethacin (Figures 4.15D and 4.15H). However, all tested compounds did not affect *COX-2* gene expression. The effect at the transcriptional level of interruptins was consistent with NO inhibition production activity that interruptin B was the most powerful NO production inhibitor followed by interruptin A. Since the activation of PPAR-γ has been reported to reduce inflammation. The simulation of PPAR-γ expression by its ligands such as rosiglitazone, prostaglandin D_2 metabolite 15-deoxy-$\Delta^{12,14}$ prostaglandin J_2 (15d-PDJ_2), apigenin, kaempferol, as well as chrysin led to inhibit *iNOS* gene expression and activity (182-185). Additionally, interruptins A and B were indicated as PPAR-α and -γ agonists (17). These results suggested that interruptins A and B could inhibit NO production through the mechanism of *iNOS* mRNA down-regulation which probably due to up-regulation of *PPAR-γ* mRNA expression.

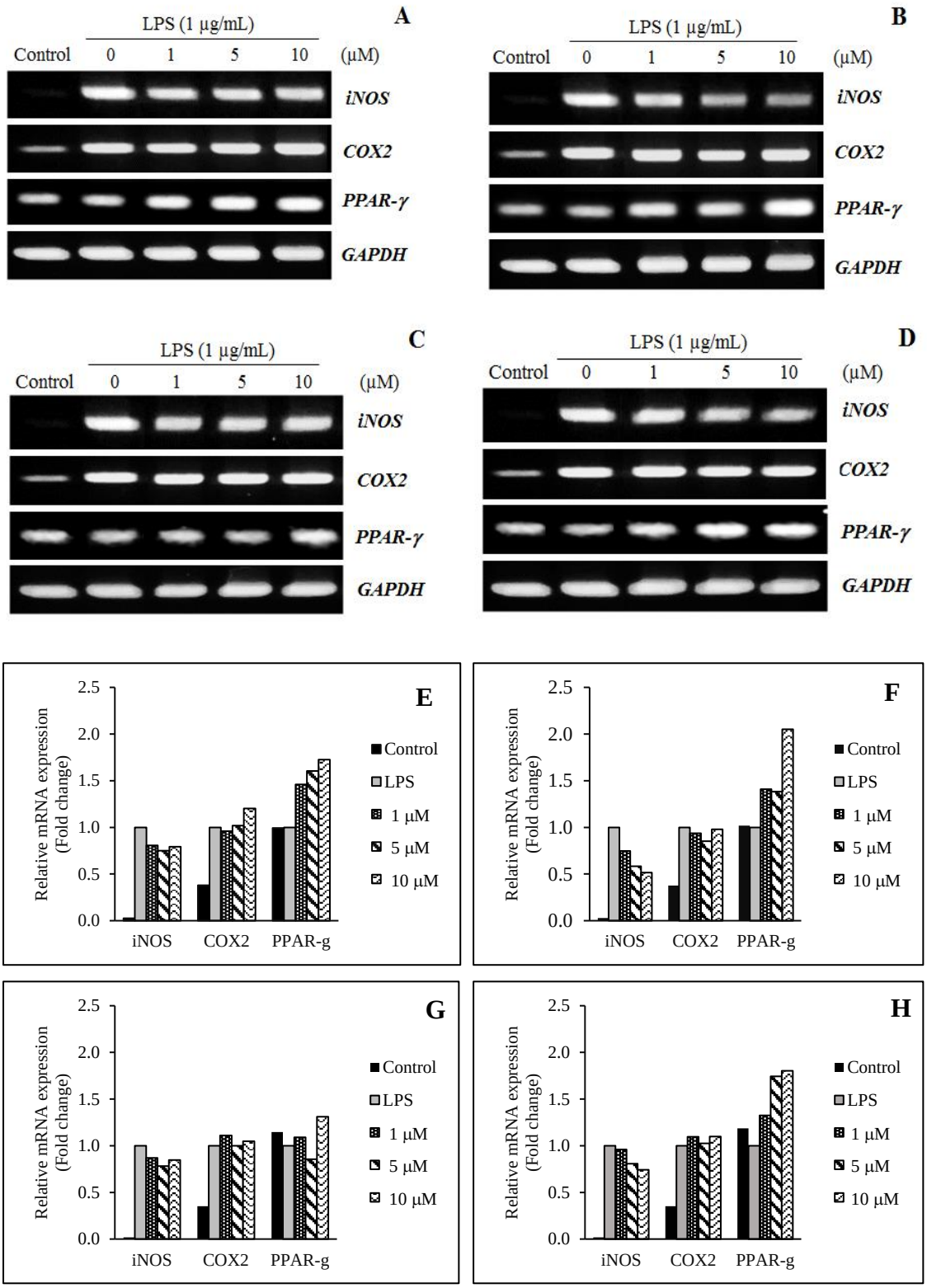

Figure 4.15 The transcriptional response of interruptins A (A and E), B (B and F), C (C and G) and indomethacin (D and H) on *iNOS*, *COX-2*, and *PPAR-γ* gene in RAW264.7 cells determined by PCR.

4.7 Effect of interruptins on cell migration

As oxidative stress and inflammation could retard wound healing process, substances demonstrating antioxidant and anti-inflammatory properties may improve wound healing. Herein, wound healing property of interruptins was evaluated by monitoring the migration capacity of human skin cells, HDF and HEK. In HDF, the migration ability of interruptins-treated cells was observed over 36 h. The overall cell migration effects of interruptins A-C on HDF were comparable to the control (Table 4.19 and Figures 4.16 and 4.17). Although at 36 h from initial time (0 h), cell migration efficacy of all tested compounds and control revealed equally 100% wound closure, interruptin A at 5 and 10 μM (29.82-77.96% wound closure), and interruptin B at 1 μM (27.51% wound closure) showed significantly higher percentages of wound closure than the control (22.29-74.47% wound closure) at the time of 12 and 24 h. These indicated that interruptins A and B could accelerate the migration of HDF in the first 24 h of wound period. In the other hand, interruptin C slightly delayed HDF migration at the time of 24 h, nevertheless at the time of 36 h, its wound healing efficacy was equal to interruptins A and B by achieving wound closure. In HEK, the migration of interruptins-treated cells was monitored within 24 h (Table 4.20 and Figures 4.18 and 4.19). Interruptin C of all tested concentrations at 12 h not only expressed the best wound healing ability among tested substances with 70.23-76.78% wound closure but also significantly better than the control (53.07% wound closure). Interruptin A at dosages of 1 and 5 μM displayed 52.91-61.34% wound closure greater than control (46.48 %wound closure) at 12 h. This action revealed that interruptin A at concentrations of 1 and 5 μM could stimulate HEK migration in the first 12 h of wound healing. On the contrary, interruptin A at 10 μM and interruptin B at all tested concentrations delayed HEK migration. This effect was due to the cytotoxicity of interruptins A and B on HEK cell. The obtained results suggested that interruptins A-C possessed moderate wound healing activity by potentiating human skin cell migration. However, the wound healing efficacy of interruptins A-C relied on cell type, dosage of compounds as well as time of treatment. This study firstly discovered the bioactivity of interruptin C that facilitated epidermal cell, HEK, migration.

Table 4.19 The effect of interruptins A-C on HDF cell migration.

Compounds	Time (h)	% Wound closure			
		Control	**1 µM**	**5 µM**	**10 µM**
Interruptin A	0	0.00±4.87	0.00±4.87	0.00±4.87	0.00±4.87
	12	22.50±4.81	18.06±0.98	29.82±1.47$^{\#}$	26.52±2.55
	24	71.45±2.19	73.07±2.49	75.63±2.47*	77.96±2.04$^{\#}$
	36	100.00±0.00	100.00±0.00	100.00±0.00	100.00±0.00
Interruptin B	0	0.00±1.62	0.00±1.62	0.00±1.62	0.00±1.62
	12	22.29±1.58	27.51±3.87*	25.12±1.26	23.71±2.53
	24	74.47±0.26	77.06±2.31	75.89±1.12	75.36±3.34
	36	100.00±0.00	100.00±0.00	100.00±0.00	100.00±0.00
Interruptin C	0	0.00±3.02	0.00±3.02	0.00±3.02	0.00±3.02
	12	27.48±1.41	24.78±2.37	26.28±4.39	25.28±1.40
	24	76.40±1.81	72.84±1.79*	71.68±2.38*	72.68±1.52*
	36	100.00±0.00	100.00±0.00	100.00±0.00	100.00±0.00

Values are expressed as mean ± SD (n=3). $^{*}P < 0.05$ and $^{\#}P < 0.01$ compared to the control (0 µM) within the same time.

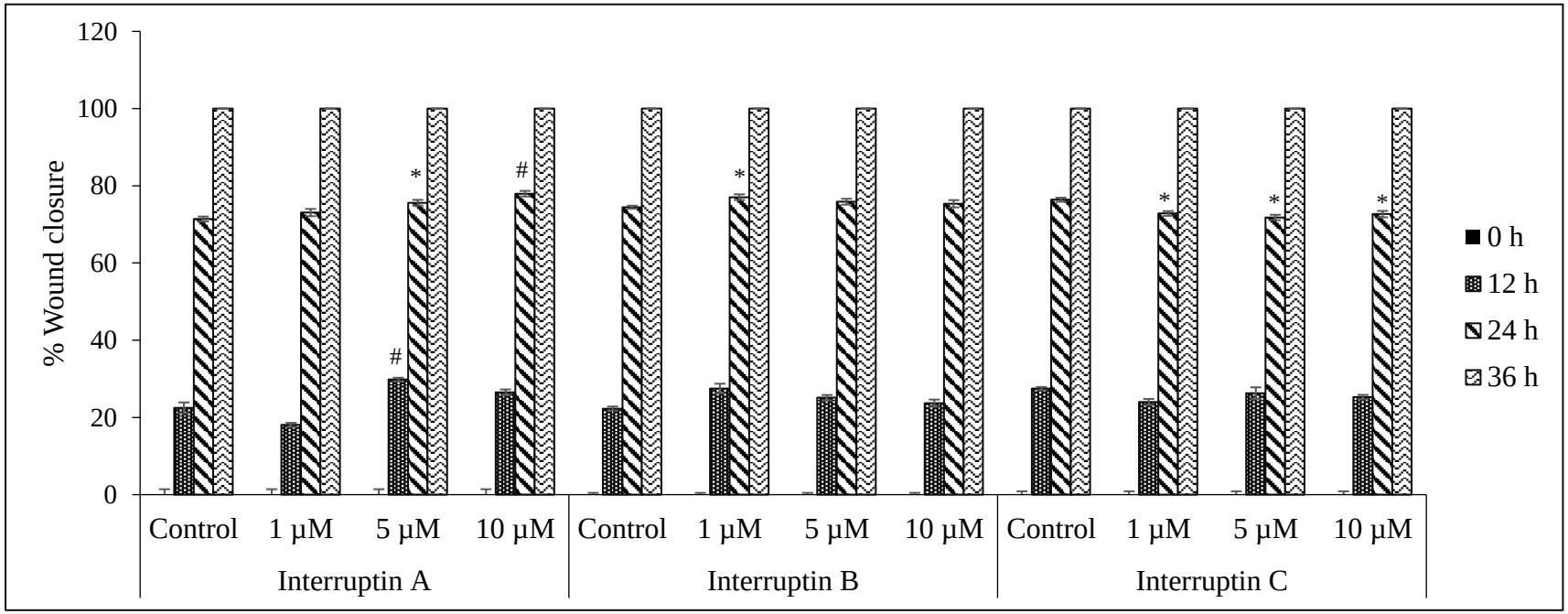

Figure 4.16 Effect of interruptins A-C on HDF cell migration. Percentage of wound close was mornitored within 36 h. $^{*}P$ <0.05 and $^{\#}P$ < 0.01 compared to the control (0 µM) within the same time

Time (h)	**Control** (0 μM)	**Interruptin A** (5μM)	**Interruptin B** (1μM)	**Interruptin C** (5μM)
0	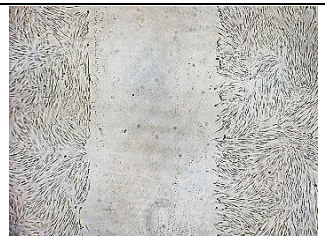	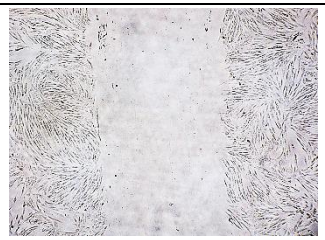	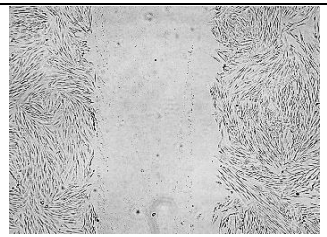	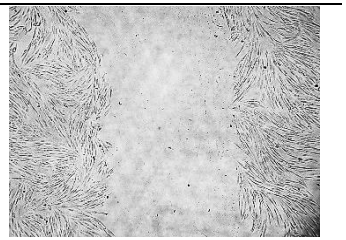
12	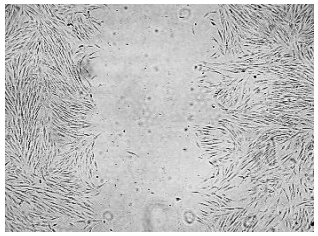	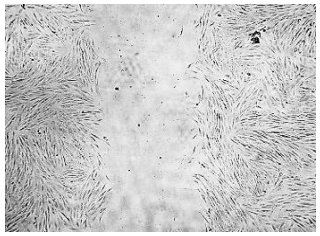	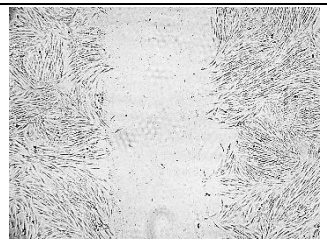	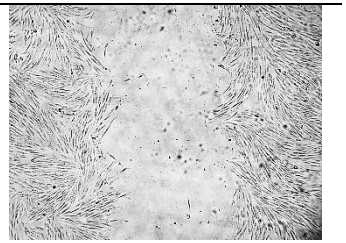
24	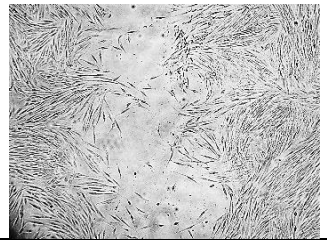	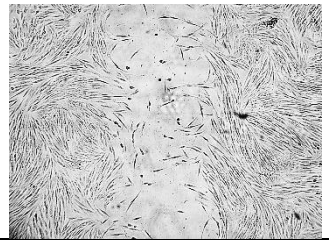	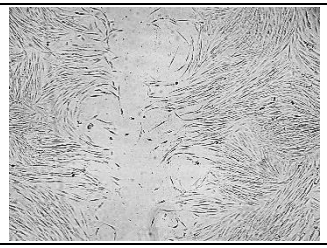	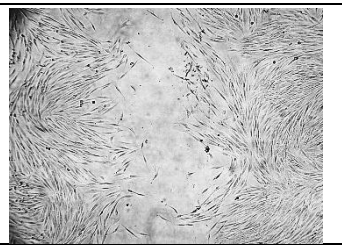
36	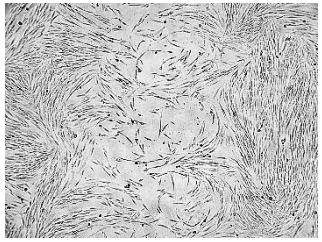	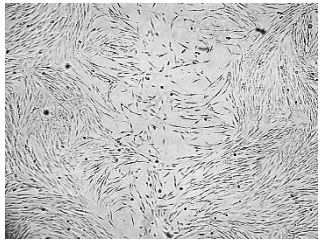	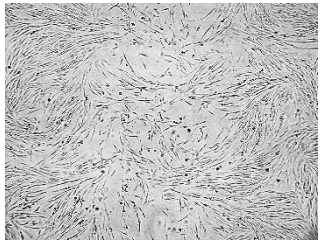	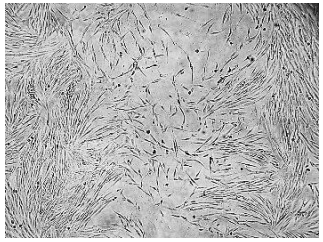

Figure 4.17 The photograps of HDF cell migration. Wound area was photographed every 12 h by inverted microscope over 36 h.

Table 4.20 The effect of interruptins A-C on HEK cell migration.

Compounds	**Time**	**% Wound closure**			
	(h)	**Control**	**1 µM**	**5 µM**	**10 µM**
Interruptin A	0	0.00±2.58	0.00±2.58	0.00±2.58	0.00±2.58
	12	46.68±3.64	61.34±3.11$^{\#}$	52.91±0.81$^{\#}$	41.52±1.39*
	24	100.00±0.00	100.00±0.00	100.00±0.00	100.00±0.00
Interruptin B	0	0.00±2.58	0.00±2.58	0.00±2.58	0.00±0.74
	12	46.68±3.64	39.01±1.49$^{\#}$	38.43±4.55$^{\#}$	23.15±1.19$^{\#}$
	24	100.00±0.00	100.00±0.00	93.71±10.89	53.97±4.00
Interruptin C	0	0.00±2.61	0.00±2.61	0.00±2.61	0.00±2.61
	12	53.07±0.97	76.78±3.44$^{\#}$	70.23±1.46$^{\#}$	71.38±3.15$^{\#}$
	24	100.00±0.00	100.00±0.00	100.00±0.00	100.00±0.00

Values are expressed as mean ± SD (n=3). $^{*}P < 0.05$ and $^{\#}P < 0.01$ compared to the control (0 µM) within the same time.

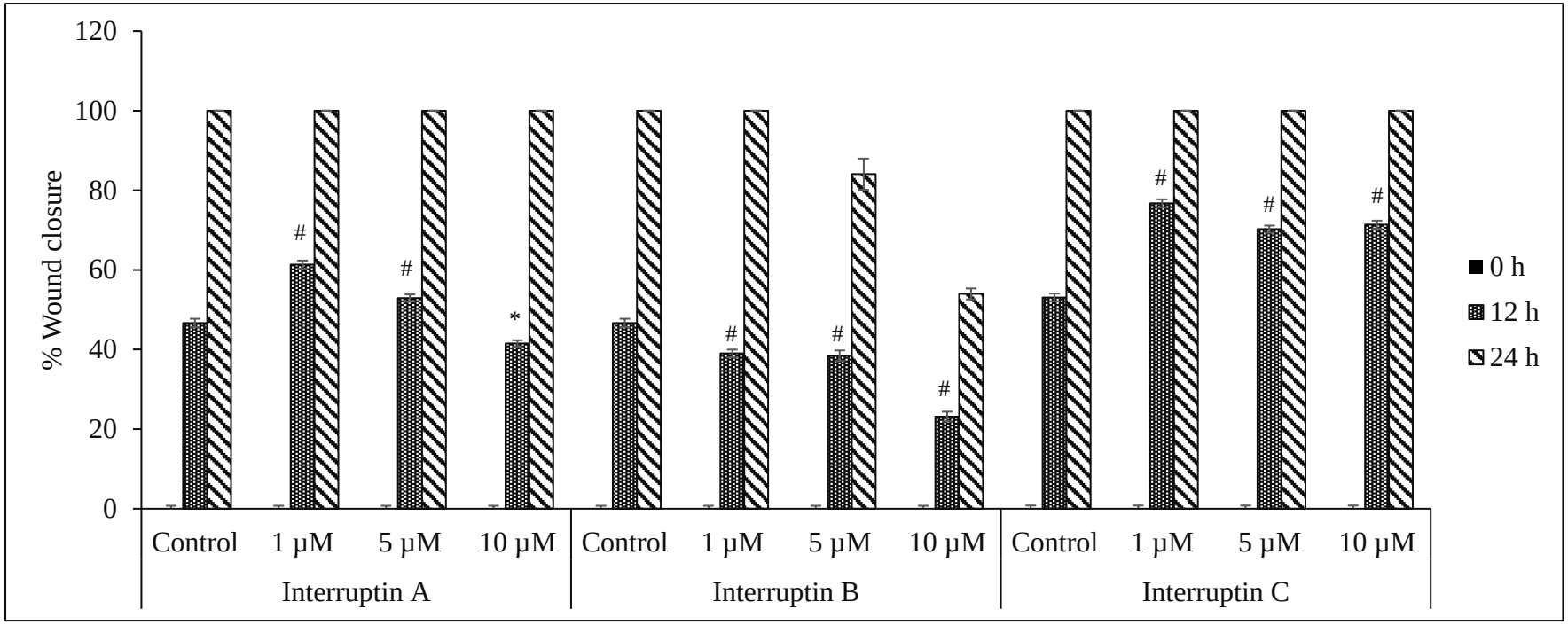

Figure 4.18 Effect of interruptins A-C on HEK cell migration. Percentage of wound close was mornitored within 24 h. $^{*}P < 0.05$ and $^{\#}P < 0.01$ compared to the control (0 µM) within the same time.

Time (h)	**Control** (0 μM)	**Interruptin A** (1μM)	**Interruptin B** (1μM)	**Interruptin C** (1μM)
0	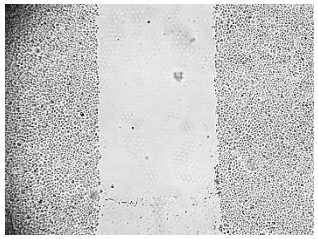	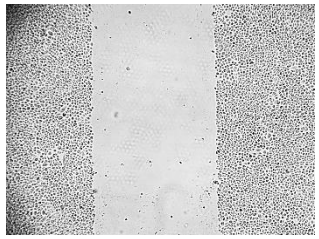	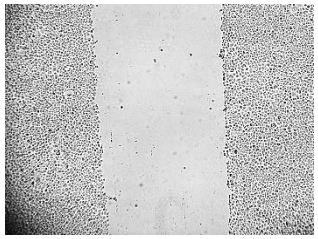	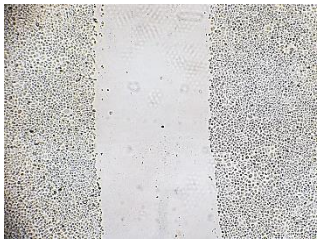
12	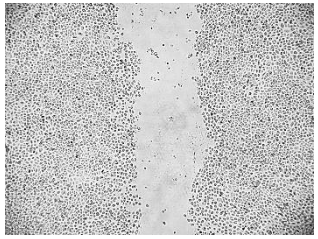	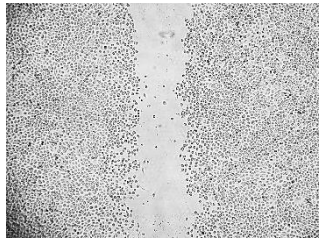	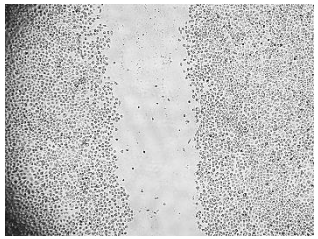	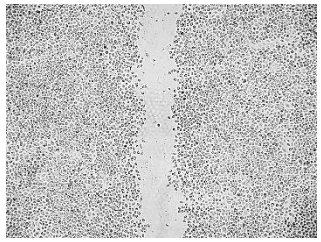
24	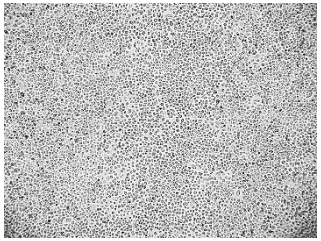	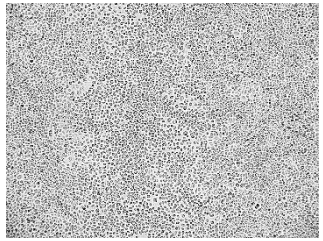	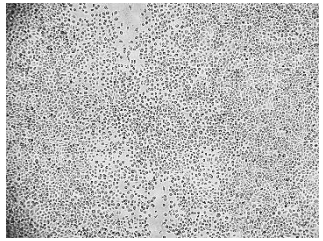	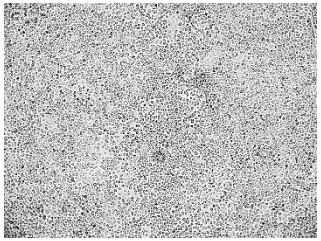

Figure 4.19 The photograps of HEK cell migration. Wound area was photographed every 12 h by inverted microscope over 24 h.

4.8 Anti-*P. acnes* activity of interruptins

P. acnes is a skin flora that can cause acne vulgaris. Its infection also leads to skin oxidative stress and inflammation. However, the treatment of acne has been facing the problem of bacterial drug resistance (46). Therefore, finding new effective anti-acne agents is still challenging. The antibacterial efficacy against *P. acnes* of interruptins A-C is presented in Table 4.21. Interruptin A was an effective inhibitory and bactericidal substance (MIC/MBC of 1.95/7.81 µg/mL) compared to other interruptins tested. The obtained result was consistent with the previous report that interruptin A exhibited the most potent antibacterial against Gram-positive skin infectious bacteria, including methicillin-sensitive *S. aureus* (MSSA), methicillin-resistant *S. aureus* (MRSA), *S. epidermidis* and *B. subtilis* with MIC/MBC values of 4/32, 4/8, 2/16 and 16/64 µg/mL, respectively, compared with vancomycin (MIC/MBC of 1/4 µg/mL, except *S. epidermidis* with MIC/MBC of 2/4 µg/mL), while interruptin B and C were not active (17). Previously published studies suggested that the potential antibacterial activity of coumarin compounds is involved with the existence of the OH functional group at position 7 together with its lipophilic property, and planar molecular structure that enhance the ability to penetrate the bacterial cell membrane (186-188). Moreover, the presence of a single bond and absence of substitution in the propionyl chain at 2'-carbon of interruptin A may be essential for the antibacterial efficacy (17).

Table 4.21 Anti *P. acnes* activity of interruptins A-C.

Samples	**MIC** (µg/mL)	**MBC (**µg/mL)
Interruptin A	1.95	7.81
Interruptin B	>250	>250
Interruptin C	>250	>250
Clindamycin	0.24	0.49

MBC, minimum inhibitory concentration; MIC, minimum bactericidal concentration.

4.9 High performance liquid chromatography method validation

The analytical procedure for measuring active ingredients in herb extracts is very important because the suitable method can reduce the errors that will occur during measurement. Since HPLC method for purity analysis of interruptins A-C had been reported but the performances of the method were not validated yet (17). Herein, the effectiveness of the method was ensured by validation following the ICH guideline (119,133).

4.9.1 HPLC condition

The optimal chromatographic condition for simultaneous quantitation of interruptins A-C content in *C. terminans* extract was accomplished by HPLC method using a reverse phase C18 column. Interruptins A, B, and C were successfully separated simultaneously using the mobile phase of methanol and 1% acetic acid in the ratio of 85:15 (v/v) with a flow rate of 1 mL/min in the mode of isocratic. The signals of interruptins A-C on HPLC chromatograms were monitored at 290 nm. The interruptins A, B and C were eluted at 17, 20, and 13 minutes, respectively (Figure 4.18).

4.9.2 Method validation

The performance parameters of method validation including linearity, range, specificity, LOD, LOQ, accuracy, and precision are shown in Table 4.22. For linearity and range, the calibration curves were conducted by measuring six different concentrations of standard solution in the range of 6.25-200 µg/mL for interruptins A and C and in the range of 12.5-400 µg/mL for interruptin B. All calibration curves displayed the linearities over their evaluated ranges with coefficient of determination (R^2) more than 0.999.

Table 4.22 Validation parameters of interruptins A-C using HPLC.

Parameters	**Interruptin A**	**Interruptin B**	**Interruptin C**
Linear Equation[a]	Y = 60390X - 252341	Y = 11353X- 112091	Y= 535009X - 10292
coefficients of determination	0.9996	0.9996	0.9997
Range (µg/mL)	6.25-200	12.5-400	6.25-200
%RSD of retention time	0.48	0.54	0.34
UV Absorption pattern (λmax) (nm)			
Standard	283, 340	331	286, 336
Sample	283, 339	330	284, 336
LOD (µg/mL)	0.81	3.13	0.20
LOQ (µg/mL)	1.63	6.25	0.46
Accuracy (% Recovery)			
10 µg/mL	91.30 ± 0.56	100.42 ± 1.46	100.51 ± 0.18
50 µg/mL	94.30 ± 2.88	106.49 ± 0.53	107.84 ± 0.75
100 µg/mL	99.45 ± 1.32	100.82 ± 0.61	105.05 ± 1.09
Precision(%RSD)			
Intra-day (*n=6*)	0.16	0.83	0.30
Inter-day (*n=3*)	0.92	0.44	1.18

[a] Y is peak area; X is interruptin concentration, LOD and LOQ are limit of detection and limit of quantification, respectively

For specificity, the variance of retention times and the homogeneity of UV absorption pattern were assessed. The % RSD of retention times of the three interruptins were less than 1%. Additionally, the UV absorption spectra of each interruptin in sample and standards were identical (Figure 4.18). Thus, the result indicated that this system was highly specific for analysis of interruptins A-C.

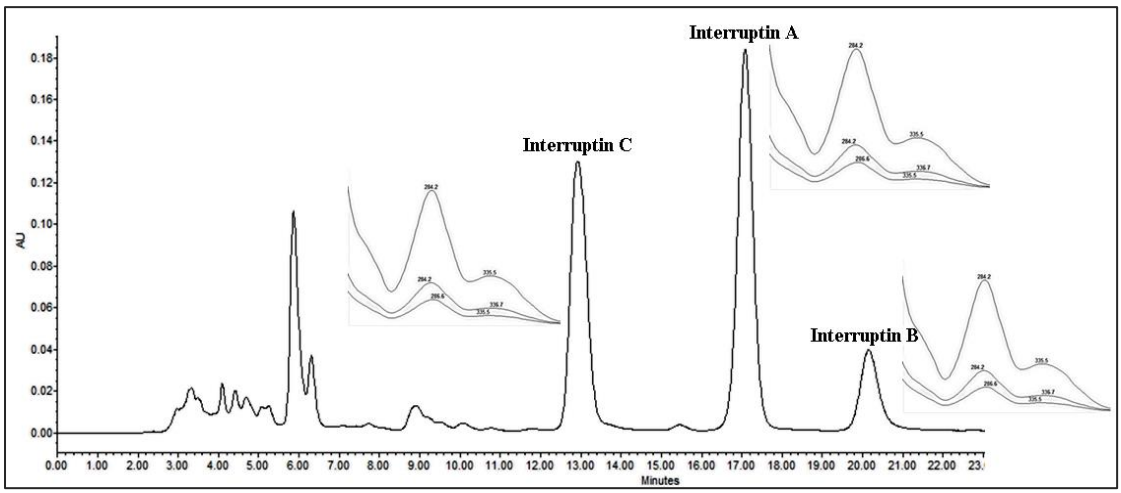

Figure 4.20 HPLC chromatogram of ethyl acetate extract of *C. terminans* and the UV absorption pattern of interruptins A-C

The LOD of the HPLC method for analysis of interruptins A-C was a range of 0.20-3.13 µg/mL, while LOQ were within 0.46-6.25 µg/mL. According to very low limitation values, it reflexed that tested system was sensitive to detect interruptins A-C.

The accuracy of the procedure was obtained from % recovery of spiked standards. The % recoveries of three spiked concentrations (10, 50 and 100 µg/mL) of each interruptin were within the range of 91-107% which was fit to the requirement of ICH guidelines (100 ± 10%). The data suggested that the analysis method was accurate for measuring interruptins A-C in a wide range of concentration.

The precision of HPLC method for monitoring of three compounds was normally displayed by % RSD of intra- and inter-day analysis. The precision value of intra-day was less than 1%, while inter-day precision was less than 2%. This parameter was consistent with ICH requirement. The data, therefore, recommended that this method was highly precise for analysis of interruptins A-C.

Conclusively, the results showed that the validation parameters of HPLC method were congruent with ICH guideline with efficient specificity, sensitivity, accuracy as well as precision. This suggested that this validated HPLC model was suitable to use as a standard method for simultaneous analysis interruptins A, B, and C content in plant crude extract.

4.10 Preparation of isopropanol extract of *C. terminans* (CE) and interruptins-rich *C. terminans* extract (IRCE)

As the limitation of using insufficient isolated interruptins, herein, the *C. terminans* crude extract containing a high content of interruptins was prepared. Although hexane was the best solvent for extraction of interruptins, it was introduced as a toxic organic solvent (189). Recently, green extraction or extraction with non-toxic solvent are widely interested for plant extraction. According to our preliminary study, interruptins A-C extraction using isopropanol with reflux or ultrasonication exhibited good efficacy. Therefore, isopropanol was chosen for preparation of *C. terminans extract* (CE), based on non-toxic property and its available to use in skin application (189-191). The prepared extract was then subjected to quantify interruptins contents using the validated HPLC (Table 4.23).

Subsequently, the interruptins-rich *C. terminans* extract (IRCE) was prepared from CE by precipitation with isopropanol and water. The impurity in solution was removed, while the precipitate was subjected to quantitate interruptins A-C contents and considered as IRCE. As shown in Table 4.23, the interruptins A, B and C contents in IRCE were increased to 2.17, 2.64, and 2.07-times, respectively, when compared to CE. This data revealed that simple precipitation technique could be used as a method for enrichment of interruptins A-C contents in *C. terminans* extract. However, this procedure still provided some undesirable pigments that caused dark green extract.

Table 4.23 Yield of CE and IRCE and interruptin A-C contents in extracts.

Sample	% yield of crude extract	Content in extract (mg/g)		
		Interruptin A	**Interruptin B**	**Interruptin C**
CE	4.69	5.37±0.09	1.03±0.05	4.34±0.35
IRCE	2.05	11.65±0.66*	2.72±0.24*	9.00±2.58*

Values are expressed as mean ± SD (n=3). *$P < 0.01$ compared to its content in CE. CE, isopropanol extract of *C. terminans*; IRCE, interruptins-rich *C. terminans* extract.

4.11 Bioactivity study of CE and IRCE

According to the results of intracellular ROS scavenging and anti-inflammatory studies, it suggested that interruptins A and B were potent antioxidants and anti-inflammatory agents and prepared IRCE demonstrated more than 2-times rich interruptins A-B compared to CE. The intracellular ROS scavenging efficacy and anti-inflammatory potential of CE and IRCE were consequently evaluated.

4.11.1 Effect of CE and IRCE on cell viability of human skin cells

Since isolated interruptins revealed diverse effects on cell viability depend on cell types (section 4.3), so the effect on cell viability of CE and IRCE was determined before the latter bioactivity evaluation and shown in Table 24. As a result, no cytotoxicity (82.33-99.45% cell viability) to HDF was observed after treatment with CE and IRCE. However, prepared IRCE seemed to be less toxic than original CE, this may be due to diminished impurities in IRCE. On the other hand, the highest dose of CE at 80 μg/mL exhibited weak cytotoxic to HEK (80-60% cell viability), and 20-80 μg/mL of IRCE showed weak to modulate cytotoxicity to HEK (60-40% cell viability). These probably owing to the effect of high interruptins A and B contents in extracts that consistent with the effect of isolated interruptins A and B on HEK which caused cell death when increasing concentration.

Table 4.24 Effect of CE and IRCE on human skin cell viability.

Concentration (μg/mL)	% Cell viability			
	HDF		HEK	
	CE	IRCE	CE	IRCE
0	100.00±0.85	100.00±0.85	100.00±1.01	100.00±1.01
10	90.27±3.54	94.93±1.23	90.92±1.43	81.35±1.01
20	88.49±2.67	99.45±1.64	89.39±2.43	77.66±0.71*
40	83.29±0.47	93.97±0.63	84.18±1.09	68.94±0.51*
80	82.33±3.19	95.62±1.32	67.24±1.75*	55.24±1.75*

Values are expressed as mean ± SD (n=3). * defined toxicity of prepared extracts. CE, isopropanol extract of *C. terminans*; IRCE, interruptins-rich *C. terminans* extract.

4.11.2 Intracellular ROS scavenging activity of CE and IRCE in human skin cells

According to the intracellular ROS scavenging potential of isolated interruptins, the ROS scavenging efficacy of CE and IRCE was also studied in human skin cells. As a result in HDF (Figure 4.19), all tested concentrations of both CE and IRCE scavenged ROS in the cells by suppressing fluorescence signal of DCF in a concentration-dependent fashion. The scavenging efficacy of CE and IRCE was counted as 6.48-66.25% and 36.98-82.73% ROS scavenging, respectively (Table 4.25). While only the highest concentration of 80 μg/mL CE and 40-80 μg/mL IRCE could slightly decrease fluorescence intensity of DCF in HEK cells that counted for 11.66-29.45% ROS scavenging. Regarding the result of ROS scavenging activity of isolated interruptins on HEK, interruptins A and B presented better scavenging ability when their concentrations were increased. Therefore, the ROS scavenging efficacy of CE and IRCE may be due to the increasing of interruptins A and B contents in the extracts. In addition, the % ROS scavenging of IRCE was greater than CE at the same concentration in both cells. This action perhaps accompanied by the higher portion of interruptins in IRCE than CE. This result also indicated that interruptin compounds were active ingredients of CE and IRCE for antioxidant activity. Moreover, the ROS scavenging

capacity of IRCE was comparable to isolated interruptins A and B although interruptin contents in IRCE (0.23-0.93 μg/mL for interruptin A and 0.05-0.21 μg/mL for interruptin B) were much lower when compared to active concentration of isolated interruptins A (0.40-8.00 μg/mL, equal to 1-20 μM) and B (0.40-7.96 μg/mL, equal to 1-20 μM). This result implied that the ROS suppressive ability of IRCE probably caused by synergistic action of interruptins A and B.

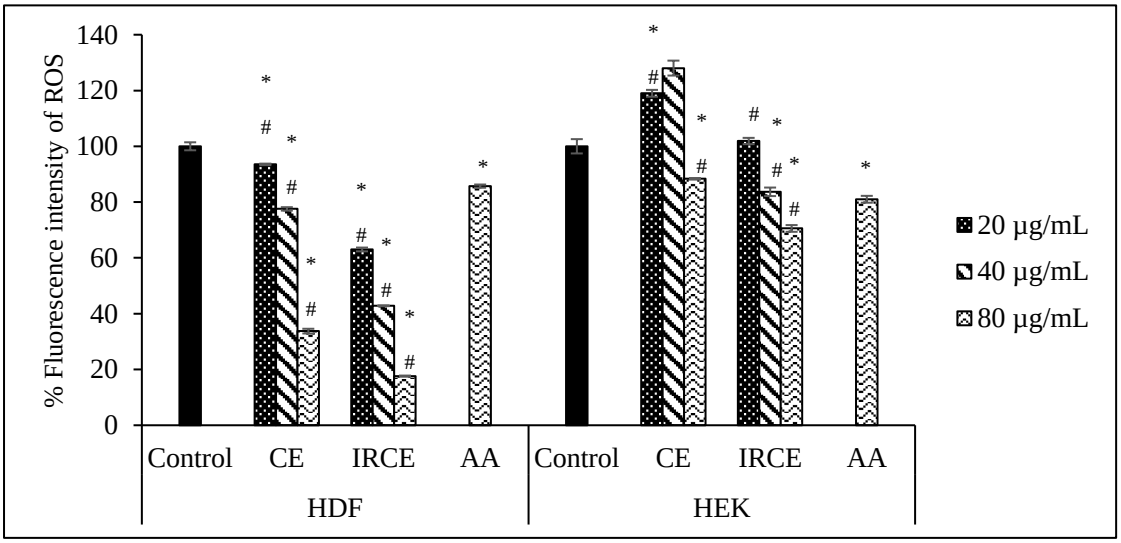

Figure 4.21 Percentage of fluorescence intensity of ROS in human skin cells treated with CE and IRCE determined by DCF-DA using flow cytometry. *, $^{\#}P < 0.01$ compared to the control (0 μg/mL) and ascorbic acid (AA, 80 μg/mL), respectively. CE, isopropanol extract of *C. terminans*; IRCE, interruptins-rich *C. terminans* extract.

Table 4.25 Percentage of ROS scavenging of CE and IRCE in human skin cells.

Concentration (μg/mL)	% ROS scavenging		
	CE	**IRCE**	**Ascorbic acid**
in HDF			
Control	0.00±1.43	0.00±1.43	0.00±1.43
20	6.48±0.27*,#	36.98±0.68*,#	
40	22.44±0.61*,#	57.18±0.13*,#	
80	66.25±0.84*,#	82.73±0.18*,#	14.28±0.57*
in HEK			
Control	0.00±2.56	0.00±2.56	0.00±2.56
20	-19.00±1.23*,#	-1.89±1.13#	
40	-28.04±2.68*,#	16.32±1.53*,#	
80	11.66±0.27*,#	29.45±1.20*,#	19.00±1.23*

Values are expressed as mean ± SD (n=3). *, #$P < 0.01$ compared to the control (0 μg/mL) and ascorbic acid (80 μg/mL), respectively. CE, isopropanol extract of *C. terminans*; IRCE, interruptins-rich *C. terminans* extract.

4.11.3 Anti-inflammatory activity of CE and IRCE

The previously obtained data (section 4.6.2) revealed that interruptins A and B possessed anti-inflammation by against NO production from macrophage cell. Hence, anti-inflammatory property of CE and IRCE was extended by evaluating inhibition efficacy on NO release in LPS-stimulated RAW 264.7 cells. The result showed that either CE or IRCE within tested concentrations dose-dependently suppressed NO production without cytotoxicity by providing cell viability more than 90% (cell viability >80 % are non-toxicity (150,151)) (Table 4.27). Interestingly, IRCE not only exhibited 2.37 times stronger inhibitory effect on NO release with IC_{50} of 6.96 μg/mL (contained 0.081 μg/mL and 0.019 μg/mL of interruptins A and B, respectively) than CE with IC_{50} of 16.41 μg/mL (contained 0.088 μg/mL and 0.017 μg/mL of interruptins A and B, respectively), but also demonstrated comparable result to standard drug indomethacin with IC_{50} of 4.24 μg/mL (Table 4.26). In regard to the interruptins

A and B contents in IRCE which 2-folds higher than in CE. This indicated that the better NO production inhibitory ability of IRCE was attributed to the higher of interruptins contents. According to the result of NO production inhibition of isolated interruptins on RAW 264.7 cells, interruptins A and B exhibited potent NO release suppression abilities with IC_{50} values as low as 12.18 μM (equal to 5.12 μg/mL) and 0.81 μM (equal to 0.32 μg/mL), respectively. However, the effective concentration of CE and IRCE on NO production inhibition contained much lower interruptins A and B contents when compared to effective dosage of isolated interruptins A and B. To the best of our knowledge, the result suggested that the potent NO inhibitory efficacy of CE and IRCE against LPS-stimulated RAW cell may possibly from the synergistic action of interruptins A and B.

Table 4.26 NO production inhibitory effect of CE and IRCE in RAW264.7 cells**.**

Compounds	**IC_{50}** (μg/mL)
CE	16.41
IRCE	6.96
Indomethacin	4.24

Table 4.27 Effect of CE and IRCE on RAW264.7 cell viability.

Concentration	**% Cell viability**		**Concentration**	**% Cell viability**
(μg/mL)	**CE**	**IRCE**	(μg/mL)	**Indomethacin**
Control	100.00±2.28	100.00±2.28	Control	100.00±2.28
5	92.70±2.27	95.06±2.81	1.79	97.57±0.49
10	94.84±2.87	94.35±3.39	3.38	97.99±4.43
20	95.55±4.89	99.35±2.48	7.16	99.87±1.17
40	97.36±1.60	98.19±2.85	10.73	98.32±0.95

Values are expressed as mean ± SD (n=3). No cytotoxicity was observed.

4.12 The stability of CE and IRCE

At present, stability study of interruptins has not been reported yet. This is the first report on stability of interruptins A and B in crude extracts. Since interruptins A and B exhibited diverse bioactivities such as antioxidation and anti-inflammation, they were therefore selected as markers for stability assessment of CE and IRCE. The contents of interruptins A and B in CE and IRCE that kept under various conditions including light protection and light exposure condition, cold and room temperature, as well as accelerated condition were monitored one-month interval throughout 3 months using validated HPLC method.

The effect of light on the stability of CE and IRCE was examined under two circumstances, including light-protected and light-exposed conditions under room temperature (30 ± 2°C) during a period of 3 months. It was found that the color and physical appearances of CE and IRCE were not changed in the light-protected situation, but the slightly increased of viscosity was observed under light-exposed condition. The contents of interruptins A and B in CE and IRCE under light-protection after examination period were 106.28% and 81.47% remaining, and 81.47% and 80.79% remaining, respectively. Under the light-exposed situation, interruptin A contents of CE and IRCE were over 89% remaining, while interruptin B contents of both CE and IRCE were less than 80% since month-2 with 63.93% and 71.02%, respectively (Table 4.28). These results indicated that CE and IRCE were stable when stored by protecting from light but not stable by loss of interruptin B quantity when was kept without light protection.

The thermostability of CE and IRCE were examined under two different temperatures, 4 ± 2°C and 30 ± 2°C, with light protection within 3 months. The results exerted that there were no changes in color and physical appearances of CE and IRCE during study period. The overall interruptins A and B contents in CE and IRCE were in the range of 80.79-106.28% remaining. However, remained interruptin B levels in either CE or IRCE that kept at 4 ± 2°C were slightly higher than that in 30 ± 2°C. The obtained data revealed that CE and IRCE were stable when were stored in room

temperature. Additionally, better stability was obtained when the extracts were maintained in cool condition.

Moreover, a stability test of CE and IRCE on the accelerated condition was carried out in a stability chamber at 40°C with a relative humidity of 75% over three months. The physical appearances and color of both extracts were also unchanged. Interruptin A contents in CE and IRCE at month-3 were similar with 83.98% and 81.08% remaining, respectively. On the contrary, the remaining levels of interruptin B in CE and IRCE were markedly decreased by approximately 36% since month-1 and continually diminished more than 50% at month-2 (Table 4.29). This finding implied that CE and IRCE could not store at room temperature for a long period although they were contained in well-closed container and protected from light. (145,146).

Table 4.28 Effect of light and temperature on CE and IRCE stability.

Extracts	**Time** (month)	**% Remaining (**compared to month 0)					
		Light-protected, 30 ± 2°C		**Light-exposed, 30 ± 2°C**		**Light-protected, 4 ± 2°C**	
		Interruptin A	**Interruptin B**	**Interruptin A**	**Interruptin B**	**Interruptin A**	**Interruptin B**
CE	0	100.00±4.42	100.00±3.59	100.00±4.42	100.00±3.59	100.00±4.42	100.00±3.59
	1	97.82±2.45	88.51±1.19	98.50±1.87	91.43±9.92	93.91±1.75	83.72±3.80
	2	101.97±3.45	82.20±3.26	92.63±2.72	60.64±3.94*	99.40±0.72	82.41±1.91
	3	106.28±1.86	81.47±4.45	89.53±0.50	63.93±1.23*	102.41±0.50	88.61±4.39
IRCE	0	100.00±4.59	100.00±7.32	100.00±4.59	100.00±7.32	100.00±4.59	100.00±7.32
	1	89.27±3.83	76.46±0.84*	92.19±0.92	82.05±2.88	91.43±1.30	85.61±1.21
	2	96.84±1.45	84.68±3.87	92.11±0.38	71.03±0.94*	94.35±2.57	78.04±6.33*
	3	98.85±1.38	80.79±2.07	91.85±042	71.02±0.57*	98.40±0.53	84.68±1.07

Values are expressed as mean ± SD (n=3). * indicated unstability (less than 80% remaining) when compared to month-0.

Table 4.29 Effect of accelerated condition on CE and IRCE stability.

Extracts	**Time** (month)	**% Remaining** (compared with time 0)	
		Interruptin A	**Interruptin B**
CE	0	100.00±4.42	100.00±3.59
	1	92.40±3.49	63.88±12.56 *
	2	89.99±1.05	33.00±1.25 *
	3	83.98±0.42	28.88±2.10 *
IRCE	0	100.00±4.59	100.00±7.32
	1	89.62±1.43	64.20±4.46 *
	2	87.02±1.45	40.53±2.09 *
	3	81.08±0.29	35.22±1.50 *

Values are expressed as mean ± SD (n=3). * indicated unstability (less than 80% remaining) when compared to month-0.

CHAPTER 5

CONCLUSION

1. The three natural occurring coumarin derivatives, interruptins A, B and C, were isolated from *Cyclosorus terminans* with 0.20-0.84% w/w of its crude extract. Interruptin A was found as a major compound as 0.84% w/w.

2. All isolated interruptins at 1-20 μM were innoxious to HDF by providing cell viability of 95.72-101.49%. Similarly, interruptins A and C exhibited no toxic to HEK with 82.54-106.63% cell viability, whereas interruptin B at high concentrations 10-20 μM was considered to modulate cytotoxic to HEK cells (42.79-67.80% cell viability).

3. Interruptins A and B were indicated as active substances of *C. terminans* in response to antioxidative and anti-photooxidative activity.

Interruptin A acted as the most potent proton radical scavenger determined by DPPH assay and the best electron transferring compound evaluated by FRAP assay with IC_{50} of 21.79 μM and antioxidant value of 682.45±16.31 mmol/L ascorbic acid/mol interruptin A, respectively. When tested on skin cells, 1-20 μM interruptins A and B demonstrated as potent ROS scavengers in HDF by dramatical reduction of ROS signal as 37.76-56.24% and 42.77-76.98% ROS scavenging, respectively, compared with the control without treatment. Whereas only minor ROS scavenging effect was observed (25.06% and 57.48% ROS scavenging) when examined in HEK with high tested concentration (20 μM). Moreover, these two substances were found to stimulate cellular transcriptional and translational responses of antioxidant enzymes, including SOD1, SOD2, CAT and GPx.

Interruptin A and B (5-20 μM) could suppress UVA-induced ROS formation in the HDF cells with 20.72-53.74% and 44.80-79.26% ROS scavenging, respectively, and diminish UVB-induced ROS formation by 10.29-56.89% and 52.73-81.52% ROS scavenging, respectively. Moreover, they also exhibited as potent anti-photooxidative compounds in HEK by eliminating intracellular ROS under UVA radiation as 37.65-62.47% and 40.37-78.40% ROS scavenging, respectively, and

scavenging UVB-generated ROS with 16.66-50.40% and 12.39-68.90 % ROS scavenging, respectively.

4. Interruptins A and B were also proved as anti-inflammatory agents by scavenging NO radical and reducing NO production in LPS-stimulated RAW264.7 cells. Among them, interruptin B was the most effective for quenching of NO radical and decreasing NO release with IC_{50} values as low as 67.68 μM and 0.81 μM, respectively. Their mechanism was suggested to involve *iNOS* mRNA down-regulation which probably due to up-regulation of *PPAR-γ* mRNA expression.

5. Interruptins A-C at low concentrations of 1-5 μM moderlately accelerated the migration HDF (27.51-29.82% wound closure) and HEK (52.91-76.78% wound closure) at the time of 12 h.

6. Among the three isolated interruptins, only interruptin A was an effective inhibitory and bactericidal substance against *Propionibacterium acnes* with MIC and MBC of 1.95 and 7.81 μg/mL, respectively.

7. The interruptins-rich *C. terminans* extract (IRCE) prepared by a simple precipitation technique using non-toxic solvents, isopropanol and water, provided 2.07-2.64 times interruptins A-C content higher than its initial extract (CE).

All tested concentrations (10-80 μg/mL) of IRCE did not toxic to HDF, whereas weak to moderate cytotoxicity to HEK was observed at 20-80 μg/mL IRCE. Nevertheless, IRCE demonstrated 1.25-5.71 folds more powerful intracellular ROS scavenging activity in human skin cells and exhibited 2.37 folds stronger inhibitory effect on NO release from LPS-stimulated RAW 264.7 cells with IC_{50} of 6.96 μg/mL than CE (IC_{50} of 16.41 μg/mL).

The IRCE extract that was stored at room temperature with light protection displayed good stability over 3-months, however, extract storage in cool condition provided better stability.

8. The high performance liquid chromatography (HPLC) with photodiode array detector was successfully validated for synchronous quantitation of interruptins A, B and C in a single injection. The HPLC condition was achieved by using a reverse-phase C18 analytical column, methanol/1% aqueous acetic acid (85:15, v/v), 1 mL/min flow rate. The validated HPLC method showed congruent validation

parameters required by International Conference of Harmonization (ICH) with linearity ($R^2 \geq 0.999$), range (typically 6.25–200 µg/mL), specificity, accuracy (100±10%), precision (intra-day <1%, inter-day <2%), LOD of 0.20-3.13 µg/mL and LOQ of 0.46-6.25 µg/mL.

Regarding the novel discovery from this study, it certainly indicates that interruptins A-C from *C. terminans* and its rich extract have a promising potential as natural antioxidants, anti-inflammatory as well as antibacterial substances and encourages the application of edible vegetable lower plant *C. terminans* for further pharmaceutical or cosmeceutical developments.

References

1. Toyoda M, Morohashi M. Pathogenesis of acne. Med Electron Microsc. 2001;34(1):29-40.
2. Shah H, Mahajan SR. Photoaging: New insights into its stimulators, complications, biochemical changes and therapeutic interventions. Biomed Aging Pathol. 2013;3(3):161-9.
3. Yoshikawa T, Naito Y. What is oxidative stress? Jpn Med Assoc J. 2002;45(7):271-6.
4. Valko M, Leibfritz D, Moncol J, Cronin MT, Mazur M, Telser J. Free radicals and antioxidants in normal physiological functions and human disease. Int J Biochem Cell Biol. 2007;39(1):44-84.
5. Matés JM, Pérez-Gómez C, De Castro IN. Antioxidant enzymes and human diseases. Clin Biochem. 1999;32(8):595-603.
6. Mates JM. Effects of antioxidant enzymes in the molecular control of reactive oxygen species toxicology. Toxicology. 2000;153(1-3):83-104.
7. Tie C, Golomb C, Taylor JR, Streilein JW. Suppressive and enhancing effects of ultraviolet B radiation on expression of contact hypersensitivity in man. J Invest Dermatol. 1995;104(1):18-22.
8. Roméro-Graillet C, Aberdam E, Biagoli N, Massabni W, Ortonne JP, Ballotti R. Ultraviolet B radiation acts through the nitric oxide and cGMP signal transduction pathway to stimulate melanogenesis in human melanocytes. J Biol Chem. 1996;271(45):28052-6.
9. Gęgotek A, Biernacki M, Ambrożewicz E, Surażyński A, Wroński A, Skrzydlewska E. The cross-talk between electrophiles, antioxidant defence and the endocannabinoid system in fibroblasts and keratinocytes after UVA and UVB irradiation. J Dermatol Sci. 2016;81(2):107-17.
10. Staberg B, Wulf HC, Klemp P, Poulsen T, Brodthagen H. The carcinogenic effect of UVA irradiation. J Invest Dermatol. 1983;81(6):517-9.
11. Fuchs J, Huflejt ME, Rothfuss LM, Wilson DS, Carcamo G, Packer L. Acute effects of near ultraviolet and visible light on the cutaneous antioxidant defense system. Photochem Photobiol. 1989;50(6):739-44.

12. Shindo Y, Witt E, Packer L. Antioxidant defense mechanisms in murine epidermis and dermis and their responses to ultraviolet light. J Invest Dermatol. 1993;100(3):260-5.
13. Nakatsuji T, Kao MC, Fang JY, Zouboulis CC, Zhang L, Gallo RL, et al. Antimicrobial property of lauric acid against *Propionibacterium acnes*: its therapeutic potential for inflammatory acne vulgaris. J Invest Dermatol. 2009;129(10):2480-8.
14. Kumar V, Abbas AK, Fausto N, Robbins SL, Cotran RS, editors. Chapter 2-acute and chronic inflammation. In: Robbins and Cotran pathologic basis of disease. 7th ed. Philadephia: Elsevier Saunders; 2005. p. 48-87.
15. Tewtrakul S, Subhadhirasakul S. Effects of compounds from *Kaempferia parviflora* on nitric oxide, prostaglandin E2 and tumor necrosis factor-alpha productions in RAW264. 7 macrophage cells. J Ethnopharmacol. 2008;120(1):81-4.
16. Kaewkroek K, Wattanapiromsakul C, Matsuda H, Nakamura S, Tewtrakul S. Anti-inflammatory activity of compounds from *Kaempferia marginata* rhizomes. Songklanakarin J Sci Technol. 2017;39(1):91-9.
17. Kaewsuwan S, Yuenyongsawad S, Plubrukarn A, Kaewchoothong A, Raksawong A, Puttarak P, et al. Bioactive interruptins A and B from *Cyclosorus terminans*: antibacterial, anticancer, stem cell proliferation and ROS scavenging activities. Songklanakarin J Sci Technol. 2015;37(3):309-17.
18. Kaewsuwan S, Plubrukarn A, Utsintong M, Kim SH, Jeong JH, Cho JG, et al. Interruptin B induces brown adipocyte differentiation and glucose consumption in adipose-derived stem cells. Mol Med Rep. 2016;13(3):2078-86.
19. Lange RW, Germolec DR, Foley JF, Luster MI. Antioxidants attenuate anthralin-induced skin inflammation in BALB/c mice: role of specific proinflammatory cytokines. J Leukoc Biol. 1998;64(2):170-6.
20. Ibbotson SH, Moran MN, Kochevar IE, Nash JF. The effects of radicals compared with UVB as initiating species for the induction of chronic cutaneous photodamage. J Invest Dermatol. 1999;112(6):933-8.

21. Frederic HM, editor. Chapter 5 The integumentary system. In: Fundamentals of anatomy & physiology. 7th ed. San Francisco: Pearson Benjamin Cummings; 2006. p. 153-178.
22. Elaine N, Katja H, editors. Chapter 5 The integumentary system. In: Human anatomy & physiology. 8th ed. San Francisco: Pearson Benjamin Cummings; 2010. p. 148-165.
23. Mckenzie RC, Sauder DN. The role of keratinocyte cytokines in inflammation and immunity. J Invest Dermatol. 1990;95(6):S105-7.
24. Forslind B. A domain mosaic model of the skin barrier. Acta Derm Venereol. 1994;74(1):1-6.
25. Zouboulis C, Adjaye J, Akamatsu H, Moe B, Niemann C. Human skin stem cells and the ageing process. Exp Gerontol. 2008;43(11):986-97.
26. Baglole CJ, Smith TJ, Foster D, Sime PJ, Feldon S, Phipps RP. Functional assessment of fibroblast heterogeneity by the cell-surface glycoprotein Thy-1. In: Chaponnier C, Desmouliere A, Gabbiani G, editors. Tissue Repair, Contraction and the Myofibroblast. Boston:Springer; 2006. p. 32-9.
27. Pathak MA, Stratton K. Free radicals in human skin before and after exposure to light. Arch Biochem Biophys. 1968;123(3):468-76.
28. Leonard SS, Harris GK, Shi X. Metal-induced oxidative stress and signal transduction. Free Radic Biol Med. 2004;37(12):1921-42.
29. Betteridge DJ. What is oxidative stress? Metabolism. 2000;49(2):3-8.
30. Lushchak VI. Free radicals, reactive oxygen species, oxidative stress and its classification. Chem Biol Interact. 2014;224:64-75.
31. Reuter S, Gupta SC, Chaturvedi MM, Aggarwal BB. Oxidative stress, inflammation, and cancer: how are they linked? Free Radic Biol Med. 2010;49(11):1603-16.
32. Holmström KM, Finkel T. Cellular mechanisms and physiological consequences of redox-dependent signalling. Nat Rev Mol Cell Biol. 2014;15(6):411-21.
33. Thannickal VJ, Fanburg BL. Reactive oxygen species in cell signaling. Am J Physiol-Lung Cell Mol Physiol. 2000;279(6):L1005-28.
34. Tyrrell RM, Keyse SM. New trends in photobiology the interaction of UVA radiation with cultured cells. J Photochem Photobiol B. 1990;4(4):349-61.

35. Tegos G, Dai T, Fuchs BB, Coleman JJ, Prates RA, Astrakas C, et al. Concepts and principles of photodynamic therapy as an alternative antifungal discovery platform. Front Microbiol. 2012;3:1-16.
36. Punnonen K, Jansén CT, Puntala A, Ahotupa M. Effects of in vitro UVA irradiation and PUVA treatment on membrane fatty acids and activities of antioxidant enzymes in human keratinocytes. J Invest Dermatol. 1991;96(2):255-9.
37. Shindo Y, Hashimoto T. Time course of changes in antioxidant enzymes in human skin fibroblasts after UVA irradiation. J Dermatol Sci. 1997;14(3):225-32.
38. Leccia MT, Yaar M, Allen N, Gleason M, Gilchrest BA. Solar simulated irradiation modulates gene expression and activity of antioxidant enzymes in cultured human dermal fibroblasts. Exp Dermatol. 2001;10(4):272-9.
39. Moysan A, Marquis I, Gaboriau F, Santus R, Dubertret L, Morlière P. Ultraviolet A-induced lipid peroxidation and antioxidant defense systems in cultured human skin fibroblasts. J Invest Dermatol. 1993;100(5):692-8.
40. Perez S, Sergent O, Morel P, Chevanne M, Dubos MP, Cillard P, et al. Kinetics of lipid peroxidation induced by UV beta rays in human keratinocyte and fibroblast cultures. Comptes Rendus Séances Société Biol Ses Fil. 1995;189(3):453-65.
41. Arakane K, Ryu A, Hayashi C, Masunaga T, Shinmoto K, Mashiko S, et al. Singlet Oxygen (1Δg) generation from coproporphyrin in *Propionibacterium acnes* on irradiation. Biochem Biophys Res Commun. 1996;223(3):578-82.
42. Masaki H. Role of antioxidants in the skin: anti-aging effects. J Dermatol Sci. 2010;58(2):85-90.
43. Dreno B, Poli F. Epidemiology of acne. Dermatology. 2003;206(1):7-10.
44. Graham GM, Farrar MD, Cruse-Sawyer JE, Holland KT, Ingham E. Proinflammatory cytokine production by human keratinocytes stimulated with *Propionibacterium acnes* and *P. acnes* GroEL. Br J Dermatol. 2004;150(3):421-8.
45. Leyden JJ. A review of the use of combination therapies for the treatment of acne vulgaris. J Am Acad Dermatol. 2003;49(3):S200-10.

46. Tsai TH, Tsai TH, Wu WH, Tseng JTP, Tsai PJ. In vitro antimicrobial and anti-inflammatory effects of herbs against *Propionibacterium acnes*. Food Chem. 2010;119(3):964-8.
47. Chiba K, Kawakami K, Sone T, Onoue M. Characteristics of skin wrinkling and dermal changes induced by repeated application of squalene monohydroperoxide to hairless mouse skin. Skin Pharmacol Physiol. 2003;16(4):242-51.
48. Niwa Y, Sumi H, Kawahira K, Terashima T, Nakamura T, Akamatsu H. Protein oxidative damage in the stratum corneum: evidence for a link between environmental oxidants and the changing prevalence and nature of atopic dermatitis in Japan. Br J Dermatol. 2003;149(2):248-54.
49. Fujita H, Hirao T, Takahashi M. A simple and non-invasive visualization for assessment of carbonylated protein in the stratum corneum. Skin Res Technol. 2007;13(1):84-90.
50. Kobayashi Y, Iwai I, Akutsu N, Hirao T. Increased carbonyl protein levels in the stratum corneum of the face during winter. Int J Cosmet Sci. 2008;30(1):35-40.
51. Masaki H. Role of antioxidants in the skin: anti-aging effects. J Dermatol Sci. 2010;58(2):85-90.
52. Pelle E, Mammone T, Maes D, Frenkel K. Keratinocytes act as a source of reactive oxygen species by transferring hydrogen peroxide to melanocytes. J Invest Dermatol. 2005;124(4):793-7.
53. Roméro-Graillet C, Aberdam E, Clément M, Ortonne JP, Ballotti R. Nitric oxide produced by ultraviolet-irradiated keratinocytes stimulates melanogenesis. J Clin Invest. 1997;99(4):635-42.
54. Sasaki M, Horikoshi T, Uchiwa H, Miyachi Y. Up-regulation of tyrosinase gene by nitric oxide in human melanocytes. Pigment Cell Res. 2000;13(4):248-52.
55. Schallreuter KU, Wazir U, Kothari S, Gibbons NC, Moore J, Wood JM. Human phenylalanine hydroxylase is activated by H2O2: a novel mechanism for increasing the L-tyrosine supply for melanogenesis in melanocytes. Biochem Biophys Res Commun. 2004;322(1):88-92.
56. Ohuchida M, Sasaguri Y, Morimatsu M, Nagase H, Yagi K. Effect of linoleic acid hydroperoxide on production of matrix metalloproteinases by human skin fibroblasts. Biochem Int. 1991;25(3):447-52.

57. Scharffetter-Kochanek K, Wlaschek M, Briviba K, Sies H. Singlet oxygen induces collagenase expression in human skin fibroblasts. FEBS Lett. 1993;331(3):304-6.
58. Shin MH, Rhie G, Kim YK, Park CH, Cho KH, Kim KH, et al. H_2O_2 accumulation by catalase reduction changes MAP kinase signaling in aged human skin in vivo. J Gen Intern Med. 2005;20(5):221-9.
59. Tanaka H, Okada T, Konishi H, Tsuji T. The effect of reactive oxygen species on the biosynthesis of collagen and glycosaminoglycans in cultured human dermal fibroblasts. Arch Dermatol Res. 1993;285(6):352-5.
60. Ahn SM, Yoon HY, Lee BG, Park KC, Chung JH, Moon CH, et al. Fructose-1, 6-diphosphate attenuates prostaglandin E_2 production and cyclo-oxygenase-2 expression in UVB-irradiated HaCaT keratinocytes. Br J Pharmacol. 2002;137(4):497-503.
61. Warren JB. Nitric oxide and human skin blood flow responses to acetylcholine and ultraviolet light. FASEB J. 1994;8(2):247-51.
62. Rhodes LE, Gledhill K, Masoodi M, Haylett AK, Brownrigg M, Thody AJ, et al. The sunburn response in human skin is characterized by sequential eicosanoid profiles that may mediate its early and late phases. FASEB J. 2009;23(11):3947-56.
63. Sies H, Stahl W, Sundquist AR. Antioxidant functions of vitamins: vitamins E and C, beta-carotene, and other carotenoids. Ann N Y Acad Sci. 1992;669(1):7-20.
64. Velioglu YS, Mazza G, Gao L, Oomah BD. Antioxidant activity and total phenolics in selected fruits, vegetables, and grain products. J Agric Food Chem. 1998;46(10):4113-7.
65. Trachootham D, Alexandre J, Huang P. Targeting cancer cells by ROS-mediated mechanisms: a radical therapeutic approach? Nat Rev Drug Discov. 2009;8:579-91.
66. Zelko IN, Mariani TJ, Folz RJ. Superoxide dismutase multigene family: a comparison of the CuZn-SOD (SOD1), Mn-SOD (SOD2), and EC-SOD (SOD3) gene structures, evolution, and expression. Free Radic Biol Med. 2002;33(3):337-49.

67. Winterbourn CC. Toxicity of iron and hydrogen peroxide: the Fenton reaction. Toxicol Lett. 1995;82:969-74.
68. Lei XG, Cheng WH, McClung JP. Metabolic regulation and function of glutathione peroxidase-1. Annu Rev Nutr. 2007;27:41-61.
69. Myllylä R, Majamaa K, Günzler V, Hanauske-Abel HM, Kivirikko KI. Ascorbate is consumed stoichiometrically in the uncoupled reactions catalyzed by prolyl 4-hydroxylase and lysyl hydroxylase. J Biol Chem. 1984;259(9):5403-5.
70. Herrera E, Barbas C. Vitamin E: action, metabolism and perspectives. J Physiol Biochem. 2001;57(1):43-56.
71. Halliwell B. Drug antioxidant effects. Drugs. 1991;42(4):569-605.
72. Kusumawati I, Indrayanto G. Natural antioxidants in cosmetics. Studies in natural products chemistry. 2013;40:485-505.
73. Carocho M, Morales P, Ferreira IC. Natural food additives: Quo vadis? Trends Food Sci Technol. 2015;45(2):284-95.
74. Carocho M, Ferreira IC. A review on antioxidants, prooxidants and related controversy: natural and synthetic compounds, screening and analysis methodologies and future perspectives. Food Chem Toxicol. 2013;51:15-25.
75. Pokorny J. Are natural antioxidants better-and safer-than synthetic antioxidants? Eur J Lipid Sci Technol. 2007;109(6):629-2.
76. Liu D, Sheng J, Li Z, Qi H, Sun Y, Duan Y, et al. Antioxidant activity of polysaccharide fractions extracted from *Athyrium multidentatum* (Doll.) Ching. Int J Biol Macromol. 2013;56:1-5.
77. Lai HY, Lim YY, Tan SP. Antioxidative, tyrosinase inhibiting and antibacterial activities of leaf extracts from medicinal ferns. Biosci Biotechnol Biochem. 2009;73(6):1362-6.
78. Chen J, Lei Y, Liu Y, Xiong C, Fu W, Ruan J. Extract of *Cyclosorus acuminatus* attenuates diabetic nephropathy in mice via modifying peroxisome proliferators activated receptor signalling pathway. Food Chem. 2011;128(3):659-66.
79. Li X, Zhou A, Han Y. Anti-oxidation and anti-microorganism activities of purification polysaccharide from *Lygodium japonicum* in vitro. Carbohydr Polym. 2006;66(1):34-42.

80. Chen YH, Chang FR, Lin YJ, Wang L, Chen JF, Wu YC, et al. Identification of phenolic antioxidants from Sword Brake fern (*Pteris ensiformis* Burm.). Food Chem. 2007;105(1):48-56.
81. Chai TT, Panirchellvum E, Ong HC, Wong FC. Phenolic contents and antioxidant properties of *Stenochlaena palustris*, an edible medicinal fern. Bot Stud. 2012;53(4):439-46.
82. Gomes A de J, Lunardi CN, Gonzalez S, Tedesco AC. The antioxidant action of *Polypodium leucotomos* extract and kojic acid: reactions with reactive oxygen species. Braz J Med Biol Res. 2001;34(11):1487-94.
83. Philips N, Smith J, Keller T, Gonzalez S. Predominant effects of *Polypodium leucotomos* on membrane integrity, lipid peroxidation, and expression of elastin and matrixmetalloproteinase-1 in ultraviolet radiation exposed fibroblasts, and keratinocytes. J Dermatol Sci. 2003;32(1):1-9.
84. Issa AY, Volate SR, Wargovich MJ. The role of phytochemicals in inhibition of cancer and inflammation: new directions and perspectives. J Food Compos Anal. 2006;19(5):405-19.
85. Kumar V, Abbas A, Aster J, editors. Chapter 3-inflammation and repair. In: Robbins and Cotran pathologic basis of disease. 9th ed. philadelphia, PA: Elsevier /Saunders; 2015. p. 69-112.
86. Kim HP, Son KH, Chang HW, Kang SS. Anti-inflammatory plant flavonoids and cellular action mechanisms. J Pharmacol Sci. 2004;96(3):229-45.
87. Bertolini A, Ottani A, Sandrini M. Dual acting anti-inflammatory drugs: a reappraisal. Pharmacol Res. 2001;44(6):437-50.
88. Rocha PN, Plumb TJ, Coffman TM. Eicosanoids: lipid mediators of inflammation in transplantation. Springer Semin Immunopathol. 2003;25(2):215-27.
89. Vane JR, Bakhle YS, Botting RM. Cyclooxygenases 1 and 2. Annu Rev Pharmacol Toxicol. 1998;38(1):97-120.
90. Vane JR, Botting RM. Anti-inflammatory drugs and their mechanism of action. Inflamm Res. 1998;47(2):78-87.
91. Morita I. Distinct functions of COX-1 and COX-2. Prostaglandins Other Lipid Mediat. 2002;68:165-75.

92. Charlier C, Michaux C. Dual inhibition of cyclooxygenase-2 (COX-2) and 5-lipoxygenase (5-LOX) as a new strategy to provide safer non-steroidal anti-inflammatory drugs. Eur J Med Chem. 2003;38(7-8):645-59.
93. Turini ME, DuBois RN. Cyclooxygenase-2: a therapeutic target. Annu Rev Med. 2002;53(1):35-57.
94. Fiorucci S, Meli R, Bucci M, Cirino G. Dual inhibitors of cyclooxygenase and 5-lipoxygenase. A new avenue in anti-inflammatory therapy? Biochem Pharmacol. 2001;62(11):1433-8.
95. Surh YJ, Chun KS, Cha HH, Han SS, Keum YS, Park KK, et al. Molecular mechanisms underlying chemopreventive activities of anti-inflammatory phytochemicals: down-regulation of COX-2 and iNOS through suppression of NF-κB activation. Mutat Res Mol Mech Mutagen. 2001;480:243-68.
96. Lappas M, Permezel M, Georgiou HM, Rice GE. Nuclear factor kappa B regulation of proinflammatory cytokines in human gestational tissues in vitro. Biol Reprod. 2002;67(2):668-73.
97. Nathan C, Xie QW. Regulation of biosynthesis of nitric oxide. J Biol Chem. 1994;269(19):13725-8.
98. Knowles RG, Moncada S. Nitric oxide synthases in mammals. Biochem J. 1994;298(Pt 2):249-58.
99. Guzik T, Korbut R, Adamek-Guzik T. Nitric oxide and superoxide in inflammation. J Physiol Pharmacol. 2003;54(4):469-87.
100. Muntané J, De la Mata M. Nitric oxide and cancer. World J Hepatol. 2010;2(9):337-44.
101. Wang Q, Kuang H, Su Y, Sun Y, Feng J, Guo R, et al. Naturally derived anti-inflammatory compounds from Chinese medicinal plants. J Ethnopharmacol. 2013;146(1):9-39.
102. Shaikh RU, Pund MM, Gacche RN. Evaluation of anti-inflammatory activity of selected medicinal plants used in Indian traditional medication system in vitro as well as in vivo. J Tradit Complement Med. 2016;6(4):355-61.
103. Tseng CC, Wolfe MM. Nonsteroidal anti-inflammatory drugs. Med Clin North Am. 2000;84(5):1329-44.

104. Aygün D, Kaplan S, Odaci E, Onger ME, Altunkaynak ME. Toxicity of non-steroidal anti-inflammatory drugs: a review of melatonin and diclofenac sodium association. Histol Histopathol. 2012;27(4):417-36.
105. Nonato FR, Barros TAA, Lucchese AM, Oliveira CEC, dos Santos RR, Soares MBP, et al. Antiinflammatory and antinociceptive activities of *Blechnum occidentale* L. extract. J Ethnopharmacol. 2009;125(1):102-7.
106. Kaewkroek K, Wattanapiromsakul C, Tewtrakul S. Anti-inflammatory mechanisms of compounds from *Curcuma mangga* rhizomes using RAW264. 7 macrophage cells. Nat Prod Commun. 2010;5(10):1547-50.
107. Anuja GI, Latha PG, Suja SR, Shyamal S, Shine VJ, Sini S, et al. Anti-inflammatory and analgesic properties of *Drynaria quercifolia* (L.) J. Smith. J Ethnopharmacol. 2010;132(2):456-60.
108. Tewtrakul S, Subhadhirasakul S. Effects of compounds from *Kaempferia parviflora* on nitric oxide, prostaglandin E_2 and tumor necrosis factor-alpha productions in RAW264. 7 macrophage cells. J Ethnopharmacol. 2008;120(1):81-4.
109. Liang Q, Wu Q, Jiang J, Duan J, Wang C, Smith MD, et al. Characterization of Sparstolonin B, a Chinese herb-derived compound as a selective Toll-like receptor antagonist with potent anti-inflammatory properties. J Biol Chem. 2011;286(30):26470-9.
110. Abiodun OO, Rodríguez-Nogales A, Algieri F, Gomez-Caravaca AM, Segura-Carretero A, Utrilla MP, et al. Antiinflammatory and immunomodulatory activity of an ethanolic extract from the stem bark of *Terminalia catappa* L.(Combretaceae): In vitro and in vivo evidences. J Ethnopharmacol. 2016;192:309-19.
111. Tagawa M, Iwatsuki K. Thelypteridaceae. In: Smitinand T, Larsen K, editors. Flora of Thailand, Volume 3, part 3 Pteridophytes. Bangkok; Royal Forest Department. 1988. p. 393-435.
112. Quadri-Spinelli T, Heilmann J, Rali T, Sticher O. Bioactive coumarin derivatives from the fern *Cyclosorus interruptus*. Planta Med. 2000;66(08):728-33.

113. Borges BG, da Rocha VD, Medina-Remon A, von Poser G, Maria Lamuela-Raventos R, Lucia Eifler-Lima V, et al. The antioxidant activity of coumarins and flavonoids. Mini Rev Med Chem. 2013;13(3):318-34.
114. Hoult JRS, Paya M. Pharmacological and biochemical actions of simple coumarins: natural products with therapeutic potential. Gen Pharmacol Vasc Syst. 1996;27(4):713-22.
115. Thuong PT, Hung TM, Ngoc TM, Ha DT, Min BS, Kwack SJ, et al. Antioxidant activities of coumarins from Korean medicinal plants and their structure-activity relationships. Phytother Res. 2010;24(1):101-6.
116. Emami S, Dadashpour S. Current developments of coumarin-based anti-cancer agents in medicinal chemistry. Eur J Med Chem. 2015;102:611-30.
117. Kurdelas RR, Lima B, Tapia A, Egly FG, Gonzalez SM, Rodríguez MV, et al. Antifungal activity of extracts and prenylated coumarins isolated from *Baccharis darwinii* Hook & Arn.(Asteraceae). Molecules. 2010;15(7):4898-907.
118. Kaewsuwan S, Sung JH, inventors. Compositions comprising the extract of *Cyclosorus terminans* or the compounds derived therefrom for improving or inhibiting obesity and lowering level of glucose in blood. Korean patent 10-2014-0003090. 2014.
119. Panichayupakaranant P. Quality Control and Standardisation of Herbal Medicines. Songkhla: Neopoint Creative & Studio; 2011.
120. Panichayupakaranant P. Active constituent-rich Herbal extracts for development of phytomedicine. Songklanagarind Med J. 2017;35(3):187-93.
121. Panichayupakaranant P, Charoonratana T, Sirikatitham A. RP-HPLC analysis of rhinacanthins in *Rhinacanthus nasutus*: validation and application for the preparation of rhinacanthin high-yielding extract. J Chromatogr Sci. 2009;47(8):705-8.
122. Kaewchoothong A, Tewtrakul S, Panichayupakaranant P. Inhibitory effect of phenylbutanoid-rich *Zingiber cassumunar* extracts on nitric oxide production by murine macrophage-like RAW264. 7 cells. Phytother Res. 2012;26(12):1789-92.
123. Sakunpak A, Sirikatitham A, Panichayupakaranant P. Preparation of anthraquinone high-yielding *Senna alata* extract and its stability. Pharm Biol. 2009;47(3):236-41.

124. Nirmal NP, Panichayupakaranant P. Anti-*Propionibacterium acnes* assay-guided purification of brazilin and preparation of brazilin rich extract from *Caesalpinia sappan* heartwood. Pharm Biol. 2014;52(9):1204-7.
125. Liu B, Dong B, Yuan X, Kuang Q, Zhao Q, Yang M, et al. Enrichment and separation of chlorogenic acid from the extract of *Eupatorium adenophorum* Spreng by macroporous resin. J Chromatogr B. 2016;1008:58-64.
126. Panichayupakaranant P, Itsuriya A, Sirikatitham A. Preparation method and stability of ellagic acid-rich pomegranate fruit peel extract. Pharm Biol. 2010;48(2):201-5.
127. Zou Y, Lu Y, Wei D. Antioxidant activity of a flavonoid-rich extract of *Hypericum perforatum* L. in vitro. J Agric Food Chem. 2004;52(16):5032-9.
128. Puttarak P, Panichayupakaranant P. A new method for preparing pentacyclic triterpene rich *Centella asiatica* extracts. Nat Prod Res. 2013;27(7):684-6.
129. Kaewbumrung S, Panichayupakaranant P. Antibacterial activity of plumbagin derivative-rich *Plumbago indica* root extracts and chemical stability. Nat Prod Res. 2014;28(11):835-7.
130. Panichayupakaranant P, Sakunpak A, Sakunphueak A. Quantitative HPLC determination and extraction of anthraquinones in *Senna alata* leaves. J Chromatogr Sci. 2009;47(3):197-200.
131. Panichayupakarananta P, Issuriya A, Sirikatitham A, Wang W. Antioxidant assay-guided purification and LC determination of ellagic acid in pomegranate peel. J Chromatogr Sci. 2010;48(6):456-9.
132. Kaewbumrung S, Panichayupakaranant P. Isolation of three antibacterial naphthoquinones from *Plumbago indica* roots and development of a validated quantitative HPLC analytical method. Nat Prod Res. 2012;26(21):2020-3.
133. ICH harmonized tripartite guideline. Validation of analytical procedures: text and methodology Q2 (R1). ICH. 2005.
134. Swartz ME, Krull IS. Handbook of Analytical Validation. USA: CRC Press; 2012.
135. Bahuguna A, Khan I, Bajpai VK, Kang SC. MTT assay to evaluate the cytotoxic potential of a drug. Bangladesh J Pharmacol. 2017;12(2):115-8

136. Eruslanov E, Kusmartsev S. Identification of ROS using oxidized DCFDA and flow-cytometry. Method Mol Biol. 2010;594:57-72.
137. Rachpirom M, Ovatlarnporn C, Thengyai S, Sontimuang C, Puttarak P. Dipeptidyl peptidase-IV (DPP-IV) inhibitory activity, antioxidant property and phytochemical composition studies of herbal constituents of Thai folk anti-diabetes remedy. Walailak J Sci Technol WJST. 2016;13(10):803-14.
138. Limmongkon A, Janhom P, Amthong A, Kawpanuk M, Nopprang P, Poohadsuan J, et al. Antioxidant activity, total phenolic, and resveratrol content in five cultivars of peanut sprouts. Asian Pac J Trop Biomed. 2017;7(4):332-8.
139. Wikipedia. Real-time PCR [Internet]. 2019 [cited 2019 Mar 10]. Available from: https://en.wikipedia.org/wiki/Real-time_polymerase_chain_reaction.
140. Boora F, Chirisa E, Mukanganyama S. Evaluation of nitrite radical scavenging properties of selected Zimbabwean plant extracts and their phytoconstituents. J Food Process. 2014;2014:1-7.
141. Premprasert C, Tewtrakul S, Wungsintaweekul J. Plaunol A from *Croton stellatopilosus* inhibits inducible nitric oxide synthase and cyclooxygenase-2 in macrophage RAW264. 7 cells. Nat Prod Commun. 2018;13(7):799-802.
142. Sae-wong C, Tansakul P, Tewtrakul S. Anti-inflammatory mechanism of *Kaempferia parviflora* in murine macrophage cells (RAW 264.7) and in experimental animals. J Ethnopharmacol. 2009;124(3):576-80.
143. Masternak MM, Al-Regaiey K, Bonkowski MS, Panici J, Sun L, Wang J, et al. Divergent effects of caloric restriction on gene expression in normal and long-lived mice. J Gerontol A Biol Sci Med Sci. 2004;59(8):B784-8.
144. CLSI. Methods for dilution antimicrobial susceptibility tests on bacteria that grow aerobically; approved standard-ninth edition. CLSI document M07-A9. Wayne, PA: Clinical and Laboratory Standards Institute; 2012.
145. Puttarak P, Charoonratana T, Panichayupakaranant P. Antimicrobial activity and stability of rhinacanthins-rich *Rhinacanthus nasutus* extract. Phytomedicine. 2010;17(5):323-7.
146. World Health Organization. Stability testing of active pharmaceutical ingredients and finished pharmaceutical products. WHO Tech Rep Ser. 2009;953:87-123.

147. Orth HCJ, Rentel C, Schmidt PC. Isolation, purity analysis and stability of hyperforin as a standard material from *Hypericum perforatum* L. J Pharm Pharmacol. 1999;51(2):193-200.
148. Taylor EW, Qian MG, Dollinger GD. Simultaneous on-line characterization of small organic molecules derived from combinatorial libraries for identity, quantity, and purity by reversed-phase HPLC with chemiluminescent nitrogen, UV, and mass spectrometric detection. Anal Chem. 1998;70(16):3339-47.
149. Zhou T, Zhu Z, Wang C, Fan G, Peng J, Chai Y, et al. On-line purity monitoring in high-speed counter-current chromatography: Application of HSCCC-HPLC-DAD for the preparation of 5-HMF, neomangiferin and mangiferin from *Anemarrhena asphodeloides* Bunge. J Pharm Biomed Anal. 2007;44(1):96-100.
150. ISO 10993-5. Biological evaluation of medical devices–Part 5: tests for in vitro cytotoxicity. ISO. 2009.
151. López-García J, Lehockỳ M, Humpolíček P, Sáha P. HaCaT keratinocytes response on antimicrobial atelocollagen substrates: extent of cytotoxicity, cell viability and proliferation. J Funct Biomater. 2014;5(2):43-57.
152. Chen S, Chen H, Tian J, Wang Y, Xing L, Wang J. Chemical modification, antioxidant and α-amylase inhibitory activities of corn silk polysaccharides. Carbohydr Polym. 2013;98(1):428-37.
153. Singh A, Dutta PK, Kumar H, Kureel AK, Rai AK. Synthesis of chitin-glucan-aldehyde-quercetin conjugate and evaluation of anticancer and antioxidant activities. Carbohydr Polym. 2018;193:99-107.
154. Shimada K, Fujikawa K, Yahara K, Nakamura T. Antioxidative properties of xanthan on the autoxidation of soybean oil in cyclodextrin emulsion. J Agric Food Chem. 1992;40(6):945-8.
155. Mathew S, Abraham TE. In vitro antioxidant activity and scavenging effects of *Cinnamomum verum* leaf extract assayed by different methodologies. Food Chem Toxicol. 2006;44(2):198-206.
156. Efferth T, Kuete V. Cameroonian medicinal plants: pharmacology and derived natural products. Front Pharmacol. 2010;1(123):1-19.
157. Kadhum AAH, Al-Amiery AA, Musa AY, Mohamad AB. The antioxidant activity of new coumarin derivatives. Int J Mol Sci. 2011;12(9):5747-61.

158. Zou C, Du Y, Li Y, Yang J, Feng T, Zhang L, et al. Preparation of lacquer polysaccharide sulfates and their antioxidant activity in vitro. Carbohydr Polym. 2008;73(2):322-31.
159. Ekanayake MS, Jensen JM, Proksch E, Aschauer H, Schmook FP, Meingassner JG. Expression of epidermal keratins and the cornified envelope protein involucrin is influenced by permeability barrier disruption. J Invest Dermatol. 1998;111(3):517-23.
160. Schäfer M, Werner S. The cornified envelope: a first line of defense against reactive oxygen species. J Invest Dermatol. 2011;131(7):1409-11.
161. Foti M, Piattelli M, Baratta MT, Ruberto G. Flavonoids, coumarins, and cinnamic acids as antioxidants in a micellar system. Structure-activity relationship. J Agric Food Chem. 1996;44(2):497-501.
162. Mathew S, Abraham TE. In vitro antioxidant activity and scavenging effects of *Cinnamomum verum* leaf extract assayed by different methodologies. Food Chem Toxicol. 2006;44(2):198-206.
163. Filipsky T, Riha M, Macakova K, Anzenbacherová E, Karlickova J, Mladenka P. Antioxidant effects of coumarins include direct radical scavenging, metal chelation and inhibition of ROS-producing enzymes. Curr Top Med Chem. 2015;15(5):415-31.
164. Ma Q. Role of Nrf2 in oxidative stress and toxicity. Annu Rev Pharmacol Toxicol. 2013;53:401-26.
165. Shindo Y, Witt E, Han D, Epstein W, Packer L. Enzymic and non-enzymic antioxidants in epidermis and dermis of human skin. J Invest Dermatol. 1994;102(1):122-4.
166. Ceriello A, Morocutti A, Mercuri F, Quagliaro L, Moro M, Damante G, et al. Defective intracellular antioxidant enzyme production in type 1 diabetic patients with nephropathy. Diabetes. 2000;49(12):2170-7.
167. Wassmann S, Wassmann K, Nickenig G. Modulation of oxidant and antioxidant enzyme expression and function in vascular cells. Hypertension. 2004;44(4):381-6.

168. Prince M, Li Y, Childers A, Itoh K, Yamamoto M, Kleiner HE. Comparison of citrus coumarins on carcinogen-detoxifying enzymes in Nrf2 knockout mice. Toxicol Lett. 2009;185(3):180-6.
169. Na HK, Kim EH, Jung JH, Lee HH, Hyun JW, Surh YJ. (-)-Epigallocatechin gallate induces Nrf2-mediated antioxidant enzyme expression via activation of PI3K and ERK in human mammary epithelial cells. Arch Biochem Biophys. 2008;476(2):171-7.
170. Briganti S, Picardo M. Antioxidant activity, lipid peroxidation and skin diseases. What's new. J Eur Acad Dermatol Venereol. 2003;17(6):663-9.
171. Milani P, Gagliardi S, Cova E, Cereda C. SOD1 transcriptional and posttranscriptional regulation and its potential implications in ALS. Neurol Res Int. 2011;2011:1-9.
172. Glorieux C, Zamocky M, Sandoval JM, Verrax J, Calderon PB. Regulation of catalase expression in healthy and cancerous cells. Free Radic Biol Med. 2015;87:84-97.
173. Tan M, Li S, Swaroop M, Guan K, Oberley LW, Sun Y. Transcriptional activation of the human glutathione peroxidase promoter by p53. J Biol Chem. 1999;274(17):12061-6.
174. Comhair SA, Erzurum SC. The regulation and role of extracellular glutathione peroxidase. Antioxid Redox Signal. 2005;7(1-2):72-9.
175. Ghosh B, Barbosa E, Singh I. Characterization of fibroblast cytoplasmic proteins that bind to the 3′ UTR of human catalse mRNA. Mol Cell Biochem. 2000;209(1-2):9-15.
176. Sampath D, Perez-Polo R. Regulation of antioxidant enzyme expression by NGF. Neurochem Res. 1997;22(4):351-62.
177. Haque R, Chun E, Howell JC, Sengupta T, Chen D, Kim H. MicroRNA-30b-mediated regulation of catalase expression in human ARPE-19 cells. PloS One. 2012;7(8):e42542. doi: 10.1371/journal.pone.0042542
178. Cao C, Leng Y, Liu X, Yi Y, Li P, Kufe D. Catalase is regulated by ubiquitination and proteosomal degradation. Role of the c-Abl and Arg tyrosine kinases. Biochemistry. 2003;42(35):10348-53.

179. Smith HL, Howland MC, Szmodis AW, Li Q, Daemen LL, Parikh AN, et al. Early stages of oxidative stress-induced membrane permeabilization: a neutron reflectometry study. J Am Chem Soc. 2009;131(10):3631-8.
180. Yeo SK, Liong MT. Effects and applications of sub-lethal ultrasound, electroporation and UV radiations in bioprocessing. Ann Microbiol. 2013;63(3):813-24.
181. Patel RM, Patel NJ. In vitro antioxidant activity of coumarin compounds by DPPH, super oxide and nitric oxide free radical scavenging methods. J Adv Pharm Educ Res. 2011;1:52-68.
182. Liang YC, Tsai SH, Tsai DC, Lin-Shiau SY, Lin JK. Suppression of inducible cyclooxygenase and nitric oxide synthase through activation of peroxisome proliferator-activated receptor-γ by flavonoids in mouse macrophages. FEBS Lett. 2001;496(1):12-8.
183. Ricote M, Li AC, Willson TM, Kelly CJ, Glass CK. The peroxisome proliferator-activated receptor-γ is a negative regulator of macrophage activation. Nature. 1998;391(6662):79-82
184. Li M, Pascual G, Glass CK. Peroxisome proliferator-activated receptor γ-dependent repression of the inducible nitric oxide synthase gene. Mol Cell Biol. 2000;20(13):4699-707.
185. Kim EJ, Kwon KJ, Park JY, Lee SH, Moon CH, Baik EJ. Effects of peroxisome proliferator-activated receptor agonists on LPS-induced neuronal death in mixed cortical neurons: associated with iNOS and COX-2. Brain Res. 2002;941(1-2):1-10.
186. Kayser O, Kolodziej H. Antibacterial activity of simple coumarins: structural requirements for biological activity. Z Für Naturforschung C. 1999;54(3-4):169-74.
187. de Souza SM, Delle MF, Smânia A. Antibacterial activity of coumarins. Z Fuer Naturforschung C. 2005;60(9-10):693-700.
188. Sardari S, Mori Y, Horita K, Micetich RG, Nishibe S, Daneshtalab M. Synthesis and antifungal activity of coumarins and angular furanocoumarins. Bioorg Med Chem. 1999;7(9):1933-40.

189. ICH harmonized guideline. Impurities: guideline for residual solvents. Q3C(R6). ICH. 2016.
190. Church AS, Witting MD. Laboratory testing in ethanol, methanol, ethylene glycol, and isopropanol toxicities. J Emerg Med. 1997;15(5):687-92.
191. World Health Organization. Guide to local production: WHO-recommended handrub formulations. WHO. 2010:1-9.

VITAE

Name Mr. Suriya Chaiwong

Student ID 5610730015

Educational Attainment

Degree	Name of Institution	Year of Graduation
Bachelor of Science (Biomedical Sciences) (2^{nd} class honors)	Naresuan University	2013
Bachelor of Law	Naresuan University	2013

Scholarship Awards during Enrolment

1. PSU-Ph. D. Scholarship (2013), Prince of Songkla University
2. Graduate School Dissertation Funding for Thesis (2015), Prince of Songkla University
3. Scholarship for Support Exchange Student and International Credit Transferred Through ASEAN Community (2015), Prince of Songkla University

List of Publications and Proceedings

1. **Chaiwong S**, Puttaruk P, Kaewsuwan S. Anti *Propionibacterium acnes* activity, HPLC method validation for simutaneous analysis and extraction of coumarins from the fern *Cyclosorus terminans*. Lat Am J Pharm 2018; 31(9):1791-7.
2. **Chaiwong S,** Puttarak P, Sretrirutchai S, Kaewsuwan S. In vitro anti-inflammatory and antioxidative activities of isolated interruptins from *Cyclosorus terminans*. Lat Am J Pham (Accepted May 23, 2019)
3. **Chaiwong S**, Sritrirutchai S, Wiriyakulops S. ROS scavenging effect of isolated interruptins from *Cyclosorus terminans*. In: Wangsintaweekul J, Kaewnoi S, editors. CDD 2016. Proceedings of the 4th Current Drug Development International Conference; 2016 June 1-3; Phuket, Thailand. Songkhla: Neo point; 2016. p. 155-6.

4. อนุสิทธิบัตรไทยเลขที่ 14778 เรื่องวิธีการวิเคราะห์ปริมาณสารอินเตอร์รับตินเอ บีและซีด้วยเทคนิคไฮเพอร์ฟอร์แมนซ์ลิควิดโครมาโตกราฟี ออกให้วันที่ 25 ธันวาคม 2561 โดยมีคณะผู้ประดิษฐ์ประกอบด้วย นางสาวสิรีวรรณ วิริยกุลโอภาศ นายภาณุพงศ์ พุทธรักษ์ และ**นายสุริยา ชัยวงค์**